5-2018

Point Kinetics-based Methods for Uranium Assay in Tagged Neutron Interrogation

Matthew Christopher Tweardy
University of Tennessee, mtweardy@vols.utk.edu

To the Graduate Council:

I am submitting herewith a dissertation written by Matthew Christopher Tweardy entitled "Point Kinetics-based Methods for Uranium Assay in Tagged Neutron Interrogation." I have examined the final electronic copy of this dissertation for form and content and recommend that it be accepted in partial fulfillment of the requirements for the degree of Doctor of Philosophy, with a major in Nuclear Engineering.

Jason P. Hayward, Major Professor

We have read this dissertation and recommend its acceptance:

Thomas Handler, Lawrence H. Heilbronn, Ronald E. Pevey

Accepted for the Council:

Dixie L. Thompson

Vice Provost and Dean of the Graduate School

(Original signatures are on file with official student records.)

Point Kinetics-based Methods for Uranium Assay in Tagged Neutron Interrogation

A Dissertation Presented for the

Doctor of Philosophy

Degree

The University of Tennessee, Knoxville

Matthew Christopher Tweardy

May 2018

Acknowledgements

While only one name ends up on the document, the process of taking a doctoral dissertation from concept to completion invariably involves the time, expertise, and support of countless others. I would like to first thank my advisor Jason Hayward who oversaw my work the entire time I was at the University of Tennessee. No matter how busy he was, he was always willing to sit down with me and talk through concepts, offer recommendations, or simply listen to me. He was the one who believed in me often more than I believed in myself, and I could not have completed this process without his unwavering support.

I would also like to thank Seth McConchie at Oak Ridge National Laboratory whose subject expertise started me off on the right foot and continued to be a source of invaluable assistance throughout the duration of this project. At the beginning of my work he provided me with relevant papers and codes so that I could quickly familiarize myself with this complex topic about which I knew very little. He assisted me with accessing a necessary computing cluster, provided me with data, and always made sure I was on the right track.

Matthew Blackston and Paul Hausladen generously offered their time, expertise, and measurement data to me. Our conversations gave me a crucial understanding of tagged neutron interrogation measurement systems. Fellow students Aaron Nowack, Micah Folsom, and Bonnie Canion, among others provided me technical and moral support when I needed it. Colleagues John Mattingly at North Carolina State University and Stephen Croft at Oak Ridge National Laboratory are also deserving of recognition for offering their technical expertise and for taking a continued interest in my work. I would also like to thank my doctoral committee members Ron Pevey, Lawrence Heilbronn, and Thomas Handler for graciously agreeing to supervise my dissertation.

Abstract

Enrichment assay of large (>1 kg) uranium objects is a necessary capability for nuclear safeguards and nuclear security applications. While passive gamma ray measurements are traditionally used, these methods may be unreliable for large inhomogeneous objects. Tagged neutron interrogation (TNI) of uranium using a time-tagged external D-T neutron source allows for transmission imaging as well as fission site imaging of neutron single and double coincidences. This work develops four point kinetics-based methods of estimating enrichment from a theoretical TNI measurement. These methods expand upon traditional point kinetics models in an effort to describe the fission chain propagation of TNI measurements of bare uranium metal while retaining enough simplicity to invert them and assay enrichment. The methods focus on each of the enrichment-sensitive parameters within the point kinetics model—source-object coupling, chain-starting multiplicity, and neutron multiplication. The accuracy and sensitivities of each method are evaluated using a combination of Monte Carlo simulation data and data from TNI measurements. A study on how the coincidence response and neutron multiplication are affected by physical characteristics of large uranium objects informs what specific information needs to be known a priori or from neutron imaging to successfully assay enrichment using point kinetics-based methods.

Table of Contents

List of Tables

List of Figures

Nomenclature

This is not an exhaustive list of the acronyms and symbols used in this work, but rather a reference for acronyms and symbols that are not repeatedly defined each time they are used.

Acronyms

AmLi americium–lithium

API associated particle imaging

APNIS Advanced Portable Neutron Imaging System

AWCC Active Well Coincidence Counter

D-T deuterium-tritium

DU depleted uranium

HEU highly-enriched uranium

NMDC Nuclear Materials Detection & Characterization Group

NMIS Nuclear Materials Identification System

ORNL Oak Ridge National Laboratory

PGF probability generating function

TNI tagged neutron interrogation

TOF time-of-flight

Point Kinetics Symbols

Φ_n nth reduced-factorial moment of the emitted fission chain multiplicity distribution

$\Phi_{1,t}$ component of Φ_1 due to transmitted source neutrons

$\Phi_{1,f}$ component of Φ_1 due to fission chain neutrons

ν_{in} nth reduced-factorial moment of the induced-fission prompt-neutron multiplicity distribution

ν_{sn} nth reduced-factorial moment of the chain-starting prompt-neutron multiplicity distribution

N_{ind} largest number of neutrons emitted by a fission-neutron-induced fission

N_{cs} largest number of neutrons emitted by a a fission-chain-starting interaction

M_T total neutron multiplication

M_L leakage neutron multiplication

p_c probability of a fission neutron being captured without multiplication

p_f probability of a fission neutron inducing further fission

Other Symbols

N_A Avogadro's number

ρ mass density

Σ_R removal macroscopic cross section

ε total detection efficiency

Chapter 1

Introduction

Nondestructive assay and characterization of uranium has several applications in the fields of nuclear materials control and accountability (NMC&A), nuclear security, nuclear safeguards, and nuclear nonproliferation, among others. Typical assay characteristics of interest include enrichment, neutron self-multiplication, and fissile mass. Due to the low spontaneous fission rate of uranium isotopes, active interrogation methods are commonly used to induce a measurable signal for uranium assay. Tagged neutron interrogation (TNI) techniques can perform transmission and fission-site imaging of uranium metal [6]. These techniques use an associated particle imaging (API) deuterium-tritium (D-T) neutron generator system to interrogate an object with 14.1 MeV neutrons that are time and directionally-tagged. An array of detectors opposite the D-T generator records neutron detections in list mode. Using source-correlated neutron coincidences, the locations of induced fissions can be reconstructed [7]. While imaging the geometry and location of uranium is important, the ability to assay the fissile mass and/or enrichment of an interrogated uranium object would greatly improve the capability of these TNI systems, particularly for NMC&A applications.

TNI systems have recently been developed to image large fissionable objects [7]. Using time-of-flight (TOF) techniques, TNI can record the single, double, and possibly triple prompt-neutron coincidences that are a result of induced fission within the interrogated object [7]. Traditionally, coincidence counting has employed the point kinetics model to relate the detected neutron multiplicities to characteristics of the material, such as neutron self-multiplication and equivalent mass [8]. While large fissionable objects violate the

assumptions inherent to the point kinetics model, this research aims to begin incorporating imaging data from TNI measurements and an understanding of the fission chain propagation process to correct for the effects of these violations. This research explores if leveraging TNI capabilities allows for previous point kinetics-based techniques of passive and active coincidence/multiplicity counting to be adapted in order to estimate assay characteristics of interest (neutron self-multiplication, fissile mass, and enrichment) of bare uranium metal measured with TNI methods when uranium reference objects are not available for calibration purposes. A new point kinetics model that is appropriate for TNI of bare uranium metal is developed. Several methods based on this model are analyzed for accuracy and sensitivity using Monte Carlo simulation data as well as measurement data from TNI systems.

Chapter 2 is a literature review of prior work that is relevant to the goals of this research. It begins by describing the development of the point kinetics model theory and how probability theory can be used to describe the propagation of fission chains in deeply subcritical systems. It then traces the implementation of the point kinetics model in both passive and active assay systems as well as the work surrounding evaluating and correcting for the systematic biases introduced by the limiting assumptions of the point kinetics model. Tagged neutron interrogation systems and current uranium enrichment assay methods are also outlined.

Chapter 3 introduces the D-T model, which is a general point kinetics model developed to account for the coupling between the D-T neutron source and the uranium object in a TNI measurement. Two point kinetics assumptions are evaluated using Monte Carlo simulations of bare uranium objects under D-T neutron interrogation in an effort to determine how appropriate a point kinetics model is for this use case. The D-T model serves as a basis for the development of several methods that estimate enrichment from theoretical TNI measurements. Each of these methods modifies the D-T model, whether it be in the definitions of certain parameters or an extension of the model to account for other chain-starting interactions.

Chapter 4 describes a robust suite of Monte Carlo simulation analysis tools that have been developed to evaluate the potential of these methods along with the systematic biases inherent to each of them. A study on the optimal number of Monte Carlo histories for

these simulations is performed in the interest of optimizing simulation accuracy and limited computing resources. Data from over 49 000 Monte Carlo simulations are evaluated in order to determine how each point kinetics-based assay method performs over a wide range of uranium masses, enrichments, geometries, and source direction profiles.

In addition to the Monte Carlo-generated input data, data from two measurement systems, a low-resolution system and a comparatively higher-resolution system, are used to evaluate how well some of the point kinetics-based methods can estimate enrichment from real-life TNI measurements. These measurements are described in chapter 5. The process of correcting the measurement data for detection efficiencies so that values for emitted fission chain singles, doubles, etc. can be fed into the point kinetics-based methods is discussed, along with the inherent statistical and systematic uncertainties.

Chapter 6 describes the first two point kinetics-based methods of uranium assay. Denoted coupling-based methods, both the DT-f method and the DT-f-n2n method attempt to estimate uranium enrichment from the source-object coupling, which is described in terms of enrichment using transmission physics equations. The DT-f method is unique in that it assumes all chain-starting interactions are induced fission on ^{235}U or ^{238}U in order to easily estimate multiplication from emitted doubles per single, which is needed to estimate enrichment. The effects of this assumption are evaluated, leading to the formulation of the DT-f-n2n method. This method extends the DT-f method by introducing a second coupling term to account for fission chains initiated by (n,2n) interactions, in addition to those initiated by 14.1 MeV induced fission. The ratio of these couplings, known as the beta ratio, is purely a function of enrichment and is thus used for enrichment estimation. This increases the number of unknowns in the point kinetics equations, so either transmitted singles or emitted fission chain triples are needed along with emitted fission chain singles and doubles. Two software-based strategies are used to solve this more complex system of nonlinear equations.

Chapter 7 introduces a version of the D-T model where all chain-starting interactions are considered and uses this assumption to estimate enrichment from emitted fission chain doubles after estimating multiplication from transmitted and emitted fission chain singles. Data from Monte Carlo simulations are used to evaluate the method's uncertainty sensitivity.

While the goal of this research is to develop point kinetics-based methods that can back-out enrichment from emitted multiplicities, several other physical factors also contribute to the emitted multiplicities, such as total uranium mass, geometry, and source-object coupling. Chapter 8 describes a comprehensive study which quantifies the sensitivity of emitted doubles per single and leakage multiplication to these physical parameters using data from Monte Carlo simulations.

Chapter 9 describes the hybrid method—a method based on the D-T model that combines precomputed Monte Carlo information about the relationships between leakage multiplication, uranium mass, and enrichment with emitted fission chain multiplicity inputs to yield more physical results when inverting point kinetics equations. The hybrid method relies on TNI measurements to provide accurate inputs about the uranium mass and geometry of the measured object. A sensitivity study on how the hybrid method responds to biases in inputs of uranium mass, geometry, emitted doubles per single, and source profile is performed. Data from Monte Carlo simulations as well as experimental measurements are used to evaluate the hybrid method's potential. Chapter 10 provides concluding thoughts and suggestions for future work.

Chapter 2

Theory and Background

2.1 Point Kinetics Model Theory

Portions of section 2.1 have been previously published under the title "A Point Kinetics Model for Estimating Neutron Multiplication of Bare Uranium Metal in Tagged Neutron Measurements," by M. C. Tweardy, S. McConchie, and J. P. Hayward, in *IEEE Transactions in Nuclear Science* [9] © 2017 IEEE, and have been adapted for this work.

In neutron coincidence and multiplicity assay, the distribution of the number of neutrons (multiplicity) emitted from a fissile sample is measured and interpreted in terms of known properties of the detector system and physical properties of the sample. First-principle analytic equations, derived for a point-like object, express the expected emitted neutron multiplicities in terms of nuclear data and model parameters that correspond to some physical property of interest. These equations can be inverted, allowing for the estimation of unknown model parameters from measured neutron multiplicities calculated from experimental pulse trains [10]. This point kinetics model is based on the following fundamental assumptions about the detection system and neutron interactions within a fissile sample [10]:

1. The object has a point geometry. All neutrons born within the object are born at a single points with a single energy and induce fission with uniform probability p_f. They are also detected with uniform absolute detection efficiency ε.

2. Induced fissions occur at the same time as the event initiating the fission chain (superfission concept in [11]).

3. All neutrons either induce prompt fission or escape the object. Delayed neutrons and neutron absorption without multiplication are negligible.

4. Neutrons do not scatter in the detector and return to the object.

5. No dead-time losses of neutron signals occur in the detector.

These assumptions simplify the mathematics to a point where closed form expressions of emitted neutron multiplicities are easily derived, at the cost of introducing systematic error in all but the simplest theoretical cases. Consequently, experimental methods have been developed to reduce or account for this systematic error [12]. Typically, only the first two or three neutron multiplicities are measurable, allowing for only two or three unknown model parameters to be solved for. Therefore, methods of reducing the number of unknown model parameters, such as incorporating sample imaging, have the potential to considerably improve the capabilities of neutron coincidence measurements.

Hage and Cifarelli [13] as well as Böhnel [11] derived expressions for the expected emitted neutron multiplicity distribution from a theoretical fission chain using the point kinetics model. Böhnel's method of using probability generating functions (PGFs) in the point kinetics model is used in this work, and some intermediate steps are presented in this section. The PGF $h_{sn}(y)$ describes a fission chain emitted from a point-like object when only a single neutron initiates the chain and is given by the recursion

$$h_{sn}(y) = (1 - p_f)y + p_f \sum_{\nu=0}^{N_{ind}} P_\nu^{ind} (h_{sn}(y))^\nu, \tag{2.1}$$

where p_f is the probability that a single neutron induces further fission and y is a dummy variable. The summation term is the PGF for the induced-fission prompt-neutron multiplicity. Each induced fission produces ν neutrons (up to a maximum of N_{ind}) with probability P_ν^{ind}, each of which further propagates the fission chain with PGF $h_{sn}(y)$.

This result, known as the Böhnel equation, is incorporated into the PGF $h_{mn}(y)$ that describes the emitted neutron distribution from a general chain-starting event:

$$h_{mn}(y) = \sum_{\nu=0}^{N_{cs}} P_{\nu}^{cs} (h_{sn}(y))^{\nu}, \tag{2.2}$$

where the summation term describes the prompt-neutron multiplicity of the chain-starting event which emits ν (up to a maximum of N_{cs}) with probability P_{ν}^{cs}. The mn subscript denotes the case where a fission chain is initiated by an event producing multiple neutrons, instead of a single neutron as in eq. (2.1). It is interesting to note that eq. (2.2) is a degenerate form of eq. (2.1) when the chain-starting event is taken to be the same induced-fission interaction.

The probabilities and the reduced-factorial moments of the fission chain multiplicity distribution can be calculated from a general PGF $h(y)$. The probability P_n that n neutrons in the fission chain will be emitted is calculated using

$$P_n = \frac{1}{n!} \frac{\partial^n}{\partial y^n} \Big(h(y) \Big) \Big|_{y=0}, \tag{2.3}$$

and the nth reduced-factorial moment of the fission chain multiplicity distribution (hereafter referred to as the fission chain moment) Φ_n is calculated using

$$\Phi_n = \frac{1}{n!} \frac{\partial^n}{\partial y^n} \Big(h(y) \Big) \Big|_{y=1}. \tag{2.4}$$

The rationale behind preferring moments over probabilities for describing the multiplicity distribution is largely historical. In the initial development of neutron coincidence counting, analog signal processing did not have the capability to store list-mode data. Thus, a shift register circuit was used to record the reduced-factorial moments of the detected neutron coincidence distribution [14]. Modern digital signal processing and faster neutron detectors have enabled the acquisition of list-mode data.

The first three fission chain moments of the PGF $h_{mn}(y)$ from eq. (2.2) are calculated by applying eq. (2.4):

$$\Phi_1 = \left(M_T - \frac{M_T - 1}{\nu_{i1}}\right)\nu_{s1}, \tag{2.5}$$

$$\Phi_2 = \left(M_T - \frac{M_T - 1}{\nu_{i1}}\right)^2 \left[\nu_{s2} + \nu_{i2}\nu_{s1}\frac{M_T - 1}{\nu_{i1}}\right], \tag{2.6}$$

$$\Phi_3 = \left(M_T - \frac{M_T - 1}{\nu_{i1}}\right)^3 \left[\nu_{s3} + \left(2\nu_{i2}\nu_{s2} + \nu_{i3}\nu_{s1}\right)\frac{M_T - 1}{\nu_{i1}} + 2\left(\nu_{i2}\right)^2\nu_{s1}\left(\frac{M_T - 1}{\nu_{i1}}\right)^2\right]. \tag{2.7}$$

The quantity ν_{in} is the nth reduced-factorial moment of the induced-fission prompt-neutron multiplicity distribution. Generally,

$$\nu_{in} = \sum_{\nu=0}^{N_{ind}} \frac{\nu!}{n!(\nu - n)!} P_\nu^{ind}, \tag{2.8}$$

where N_{ind} is the highest value of ν observed for the distribution described by the probabilities P_ν^{ind}. Similarly, ν_{sn} is the nth reduced-factorial moment of the chain-starting event prompt-neutron multiplicity distribution described by the probabilities P_ν^{cs}, with a maximum multiplicity of N_{cs}:

$$\nu_{sn} = \sum_{\nu=0}^{N_{cs}} \frac{\nu!}{n!(\nu - n)!} P_\nu^{cs}. \tag{2.9}$$

The total neutron multiplication M_T expresses the increase in neutron population arising from a single neutron in a subcritical multiplying sample. It is defined as the ratio of the number of neutrons produced in a sample to the number of neutrons produced by the chain-starting event within the sample. In the point kinetics model, it is related to the familiar effective multiplication factor k_{eff} as well as the probability of a fission neutron inducing further fission p_f:

$$M_T = \frac{1}{1 - k_{eff}} = \frac{1}{1 - p_f\nu_{i1}}. \tag{2.10}$$

Because coincidence measurements count the distribution of neutrons that are emitted or "leak out" of an object, much of the existing literature uses an alternate definition of multiplication for simplicity. Leakage multiplication M_L is defined as the ratio of the number of neutrons escaping a sample to the initial number of neutrons produced by the chain-starting event within the sample. It accounts for the probability of neutron capture without multiplication p_c:

$$M_L = \frac{1 - p_f - p_c}{1 - p_f \nu_{i1}} = (1 - p_f - p_c) M_T, \tag{2.11}$$

where the term $(1 - p_f - p_c)$ can be interpreted as the probability that a neutron born within the object escapes the object and is available for detection.

The point kinetics model assumption that neutron absorption without multiplication is negligible (i.e. $p_c \approx 0$) allows for the following equalities [15]:

$$M_L \approx \left(M_T - \frac{M_T - 1}{\nu_{i1}} \right), \tag{2.12}$$

$$\frac{M_L - 1}{\nu_{i1} - 1} \approx p_f M_T = \frac{M_T - 1}{\nu_{i1}}. \tag{2.13}$$

The appropriateness and consequences of this point kinetics model assumption is evaluated for TNI of bare uranium metal in section 3.1.1.

Using the approximation in eq. (2.12), eqs. (2.5) to (2.7) can also be written in terms of leakage multiplication:

$$\Phi_1 = M_L \nu_{s1}, \tag{2.14}$$

$$\Phi_2 = M_L^2 \left[\nu_{s2} + \nu_{i2} \nu_{s1} \left(\frac{M_L - 1}{\nu_{i1} - 1} \right) \right], \tag{2.15}$$

$$\Phi_3 = M_L^3 \left[\nu_{s3} + (2\nu_{i2}\nu_{s2} + \nu_{i3}\nu_{s1}) \left(\frac{M_L - 1}{\nu_{i1} - 1} \right) + 2 (\nu_{i2})^2 \nu_{s1} \left(\frac{M_L - 1}{\nu_{i1} - 1} \right)^2 \right]. \tag{2.16}$$

2.2 Point Kinetics Model Applications

2.2.1 Passive Assay

The initial development of the point kinetics model focused chiefly on fission chains initiated by either spontaneous fission or (α,n) reactions in plutonium [11–13]. The point kinetics model equations for passive coincidence and multiplicity counting use the concept of an effective ^{240}Pu mass m_{240} [11]. This assumes that isotopic information is known before a measurement via "gamma-ray spectroscopy, mass spectroscopy, or other facility information" [12]. The total mass of plutonium can then be calculated from the effective ^{240}Pu mass based on knowledge of the effective neutron yield for chain-starting events (spontaneous fission in this case) for each plutonium isotope. The fission chain initiation rate F is solved for using the point kinetics model equations. Effective ^{240}Pu mass is then calculated using the following equation:

$$m_{240} = \frac{F}{473 \text{ fissions/s-g}}. \tag{2.17}$$

Passive assay techniques, however, are not suitable for expedient assay of uranium. Unlike plutonium, uranium has a relatively low spontaneous fission neutron yield. For example, one International Atomic Energy Agency (IAEA) significant quantity of uranium (25 kg) enriched to 20 percent ^{235}U will emit only 282 neutrons/second from spontaneous fission. Compare this to an IAEA significant quantity of plutonium (8 kg) which may emit on the order of 10^6 neutrons/second [1]. Table 2.1 shows that the spontaneous fission neutron emission rate for uranium isotopes is smaller than plutonium isotopes by nearly five orders of magnitude. While passive uranium assay is technically feasible, it is not currently used by the IAEA for nondestructive assay applications [16]. Consequently, assay of neutron self-multiplication and uranium mass is typically performed using active interrogation techniques.

Table 2.1: Neutron emission rates from spontaneous fission of selected isotopes important to nuclear safeguards [1]

Isotope	Neutron Emission Rate (n/s-g)
^{240}Pu	1020
^{238}Pu	2500
^{235}U	0.0003
^{238}U	0.0011

2.2.2 Active Assay

Americium–lithium (AmLi) sources have commonly been used as the active source in uranium assay systems, such as the Active Well Coincidence Counter (AWCC) [8].

The point kinetics model applied to active uranium assay is similar to that of passive plutonium assay. One key difference is the nuclear multiplicity distributions used in the point kinetics equations, defined by probabilities P_ν^{ind} and P_ν^{cs}. The multiplicity distribution for a fission energy neutron inducing fission P_ν^{ind} is based on a 2 MeV neutron inducing fission on ^{235}U [17]. The multiplicity distribution for a chain-starting event P_ν^{cs} depends on the interrogation source used. In the case of the AWCC, this is based on an AmLi neutron spectrum inducing fission on ^{235}U [17]. The AmLi neutron source emits neutrons with an average energy of 0.3 MeV [18]. The threshold energy for induced fission in ^{238}U is approximately 1 MeV, so the quantity of ^{238}U has little effect on the fission chain initiation rate. It can however, contribute to multiplication.

Because AmLi source neutrons cannot be distinguished from fission neutrons in the AWCC, they are a source of background in the singles rate that must be accounted for. In addition to AmLi source neutrons, contributions by passive background neutrons and scattered AmLi source neutrons also contribute to the background in the singles rate [8]. For this reason, using doubles and triples for AWCC uranium mass assay has traditionally produced more accurate results [8]. If neutron leakage multiplication is known or can be assumed, only the doubles rate is necessary to estimate ^{235}U mass [8]. Using a combination of doubles and triples rates allows for calculation of leakage multiplication independent of ^{235}U mass. The calculated multiplication can then be plugged back in to estimate ^{235}U mass.

In a method developed by Ensslin *et al.*, calibrations using known samples that are of similar geometry and composition as the measurement sample are performed to generate a calibration curve that associates the induced fission rate calculated from point kinetics equations and measured doubles or triples rates to ^{235}U mass [8]. The relationship between the fission chain initiation rate F and the ^{235}U mass m_{235} is calculated using the following equation:

$$F = Cm_{235}Y, \tag{2.18}$$

where Y is the output of the AmLi source in neutrons/second and C is the coupling term. This coupling essentially depends upon the solid angle between the AmLi source and the measurement object as well as the neutron multiplication of the measurement object. Measurements of uranium oxide samples in [19] show that using triples and doubles can improve the ^{235}U mass assay root-mean-square error from 9.1 percent to 4.4 percent.

In most active well counters, high density polyethylene is used to slow the fission neutrons down to thermal energies for absorption by ^{3}He detectors. Neutrons slowed to epithermal energies can scatter back into the sample cavity and initiate fission chains within the sample object. The point kinetics model assumption that all fissions occur at a single point is often violated due to this effect because epithermal neutrons initiate fission chains mostly on the outer edge of the sample object. This is in comparison to AmLi neutrons which, at an average energy of 0.3 MeV, tend to initiate fission chains homogeneously in the sample [20]. If calibration measurements with known standards of similar geometry to the measurement object are used to determine the source coupling, as in the Ensslin *et al.* method, this point kinetics model violation does not bias the analysis. However, if it is desirable to not require known standards, this effect can produce systematic bias, which can be difficult to quantify.

A method for active interrogation of uranium using an AmLi source was developed by Goddard [20]. The measurements used boron-carbide filters around the uranium sample to prevent epithermal neutrons from inducing fission in the sample [20]. This allows for the source coupling to be expressed entirely in terms of factors that can be calculated using measurement calibration and nuclear data. The relationship between the fission chain initiation rate and the effective ^{235}U mass m_{235} is calculated using the following equation:

$$m_{235} = \frac{F M_{235}}{\phi_{Li} \sigma_{f\_Li} N_A}, \tag{2.19}$$

where ϕ_{Li} is the AmLi source neutron flux through the sample, σ_{f_Li} is the microscopic induced-fission cross section for AmLi source neutrons on ^{235}U, M_{235} is the molar mass of ^{235}U, and N_A is Avogadro's number [20]. This method assumes that leakage multiplication is equal to 1.0 and that fission chains are initiated homogeneously within the uranium object

by AmLi neutrons. Both of these assumptions are shown to be appropriate for the 212.5 gram uranium oxide samples evaluated by Goddard [20].

The point kinetics model has also been used in assay techniques that do not use AmLi sources in a well counter. A technique known as delayed neutron re-interrogation uses a pulsed D-T neutron generator to induce fission in a uranium sample, which results in delayed-neutron-precursor fission products [21]. Delayed neutrons are emitted randomly in time with respect to the initial induced fission. The D-T neutron generator is repeatedly pulsed until a steady-state source of delayed neutrons is achieved. After each pulse, neutron coincidences are counted using moderated ^{3}He tubes. This steady-state source of delayed neutrons mimics a spontaneous fission source within the uranium sample so that point kinetics techniques developed for passive plutonium assay can be used. A combination of the Feynman reduced variance method [22] and point kinetics models allows for leakage multiplication M_L to be estimated from doubles per single and triples per single rates. The amount of ^{235}U mass can then be estimated from singles S using the calculated value of M_L if a calibration curve relating mass to S/M_L^2 is generated using known standards of chemical and geometric form similar to that of the interrogated sample. This method was able to estimate total multiplication to within less than 5 percent of Monte Carlo-simulated values for a series of HEU metal spheres ranging from 0.592 kg to 13.722 kg [21]. While the accuracy of this assay is good enough for most applications, this technique suffers from the same disadvantage of AWCC techniques in that it requires known calibration standards similar to the interrogated sample in order to perform a meaningful assay.

2.3 Corrections to the Point Kinetics Model

While the point kinetics model is useful in that it simplifies the neutron fission chain propagation so that quantities of interest such as plutonium mass and neutron multiplication can be calculated from coincidence and multiplicity measurements, the assumptions required for this simplicity can result in sometimes significant systematic biases. Previous work has focused on correcting for the biases introduced by two of these assumptions for the passive assay of plutonium mass—the assumption that neutrons from (α,n) interactions are the

same energy as those produced by the spontaneous fission of ^{240}Pu and the assumption that a fission neutron has the same probability of inducing further fission no matter where it was born in the fissionable sample. While the passive assay of plutonium samples and TNI of uranium samples have many differences, a review of the methods that correct for the violation of these point kinetics model assumptions is useful. Results in this research suggest that both of these assumptions are violated and introduce significant systematic biases in TNI of uranium samples. While the goal of this research is to avoid the need for corrections based on calibration measurements or Monte Carlo results in favor of incorporating imaging and elemental identification data available from TNI methods, the prior work summarized in sections 2.3.1 and 2.3.2 can serve as a guideline for applying corrections to the point kinetics model equations for TNI applications.

2.3.1 Point Geometry Assumption

The assumption that all fissions occur at a single point within a plutonium sample implies that all neutrons born within the sample have the same multiplication. However, neutrons born at the edge of a sample will be less likely to induce further fission and will have lower multiplication than neutrons born in the center of the sample. The bias introduced by this assumption has been shown to result in the underestimation of effective ^{240}Pu mass and an overestimation of leakage multiplication and the alpha value (the ratio of (α,n) neutrons to spontaneous fission neutrons) [23, 24]. The magnitudes of this bias in effective mass estimation varies with composition, sample geometry, and total mass.

The shape of the multiplication distribution has been evaluated using Monte Carlo simulations in several studies [3, 23–26]. Most of these studies have focused on cylindrical geometries of plutonium metal, which tend to have higher multiplication than oxides. In the point kinetics model, the singles, doubles, and triples rates are functions of the leakage multiplication raised to various integer powers M_L^n, up to fifth order. The traditional point kinetics model accomplishes this by raising the average leakage multiplication to the nth power, $\langle M_L \rangle^n$. This treatment underestimates the average of the squared leakage multiplication $\langle M_L^2 \rangle$, as is shown by the second-order example in fig. 2.1. This is also the case for higher orders of leakage multiplication, resulting in the point kinetics

model underestimating doubles and triples. The result of inverting these equations is an underestimate of effective ^{240}Pu mass.

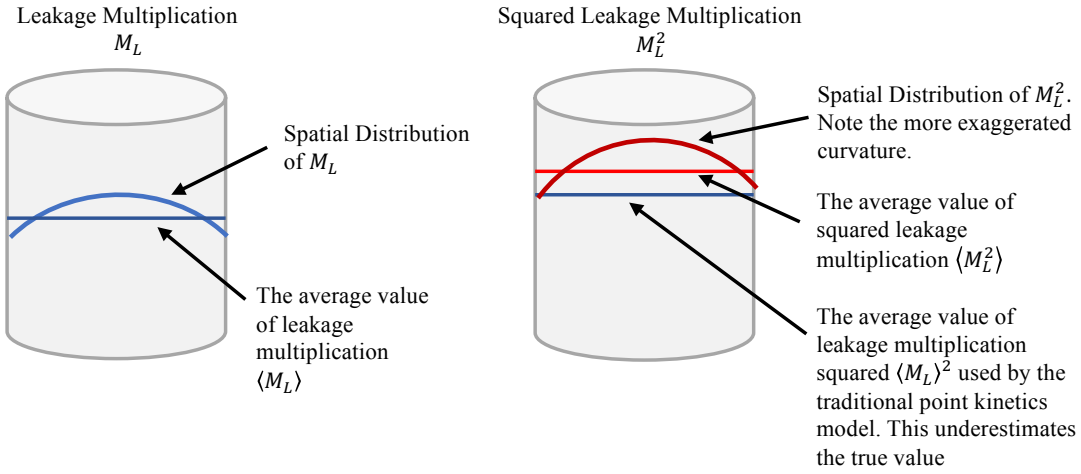

Figure 2.1: The effect of the spatial distribution of leakage multiplication on the average value of squared leakage multiplication. This has been adapted from a similar figure in [3].

The Weighted Point Model (WPM) developed by Krick and colleagues implemented a physics-based correction to the systematic bias introduced by the spatial multiplication distribution for passive assay of impure plutonium metals [24, 27]. Prior to the WPM, the negative mass biases in kg-size plutonium metal samples had been corrected for using calibration measurements and Monte Carlo simulations of samples with a known effective mass [23]. However, this only corrected for the bias in effective mass and not the multiplication or alpha value. The WPM used different weighting parameters for the spontaneous fission and (α,n) contributions for both the doubles and triples equations, amounting to four weighting factors in total. The WPM used Monte Carlo simulations to calculate each of these weighting factors and correlate them to leakage multiplication for plutonium samples of varying mass, geometry, and impurity composition. From these simulations, a curve was fit to express the weighting factors in terms of multiplication. The simulations showed these fits to be independent of sample geometry. Using these fits on a test set of plutonium samples, Monte Carlo simulations demonstrated that estimating leakage multiplication, alpha, and effective ^{240}Pu mass all improved using the WPM [24]. Because the WPM, like the standard point kinetics model, assumed that (α,n) and spontaneous

fission neutrons have the same energy, Krick and colleagues also observed a systematic bias in effective ^{240}Pu mass using the WPM for (α,n) energies outside of the 1–2 MeV range [24]. The ideal samples that were used to calculate the weighting factors in the WPM also do not extend perfectly to all scenarios. Small but measurable systematic biases were observed when assaying spherical geometries, as the weighting factors were calculated with cylindrical geometries. Nonhomogeneous samples also exhibited large systematic biases.

Work by Croft *et al.* expanded upon the work by Krick and colleagues by offering a semi-physical description of the spatial dependence of multiplication [25]. The weighting factors, referred to as the reduced spatial moments g_n, are expressed as a ratio of nth-order leakage multiplication to the average leakage multiplication to the nth power [25]:

$$g_n = \frac{\langle M_L^n \rangle}{\langle M_L \rangle^n}. \tag{2.20}$$

The point kinetics model equations are rewritten so that each occurrence of nth-order leakage multiplication M_L^n is accompanied by the corresponding nth-order reduced spatial moment. The $\langle M_L^n \rangle$ terms are calculated as a volume-weighted average of the spatially-dependent leakage multiplication $\langle M_L^n(\mathbf{r}) \rangle$. Monte Carlo simulations were used to calculate several values for $\langle M_L^n(\mathbf{r}) \rangle$ by changing the location of the source of spontaneous fission neutrons. While this approach to the WPM did not evaluate its method as rigorously on simulations and measurement data (as was done by Krick and colleagues), it represents a new physical explanation for the spatial dependence of leakage multiplication, namely that a volume-weighted average is an appropriate approach for implementing a spatial correction. This is intuitive because the probability of induced fission for a fission neutron is a function of the plutonium mass it must travel through, which is equivalent to volume for homogeneous samples. In the case of TNI of uranium, this correction may not be as straightforward as the spatial distribution of chain-starting interactions is not only a function of mass or volume like it is for spontaneous fission of plutonium.

The Spatial Multiplication Model (SMM) developed by Hauck and Henzl expanded upon the work of Croft *et al.* by attempting to describe the radial extent of the spatial distribution of leakage multiplication with an additional parameter in the point kinetics

model equations [3]. The average nth-order leakage multiplication $\langle M_L^n(\mathbf{r})\rangle$ is then described by a curve function with two parameters—an amplitude value M_A and a period value M_R. Several different curve functions were evaluated, but the best fitting functions were the cosine and Bessel functions. These choices followed from the reactor physics description of neutron flux within a cylindrical volume [28]. In order to solve for the now four unknown variables (effective ^{240}Pu mass, alpha, M_A, and M_R), Hauck and Henzl tried two different approaches. The first approach used the detected quad rates to solve for all four variables. The second approach attempted to relate M_R and M_L so that only singles, doubles, and triples rates were necessary to invert the SMM point kinetics equations. They used Monte Carlo simulations of ideal plutonium metal cylinders of varying dimensions with no (α,n) contribution to determine the relationship between M_R and M_L. Using this relationship and singles, doubles, and triples rates from simulation, they demonstrated that the SMM could improve the estimate of the effective ^{240}Pu mass for higher multiplication plutonium metal samples, up to about M_L of 2.5. The SMM represents an improvement over the WPM because it does not require Monte Carlo simulations of all detector-object configurations to correct for the spatial distribution of multiplication. Work is ongoing to implement these functional corrections into thermal neutron multiplicity counter software [29].

2.3.2 Single Energy Assumption

While the spatial distribution of multiplication is typically the largest source of systematic bias in the passive assay of high-multiplication plutonium samples, many of the approaches discussed in the previous section assume that (α,n) and spontaneous fission neutrons have the same energy. The validity of this assumption is largely dependent upon the type of impurities within the plutonium sample.

In passive plutonium assay, fission chains can be initiated by either the spontaneous fission of ^{240}Pu or an (α,n) interaction on an impurity within the sample. This is most common with plutonium oxide samples. The traditional point kinetics model assumes that the neutrons resulting from both of these sources have the same energy. This implies that neutrons from both sources have the same probability of inducing further fission, that these fissions will have the same multiplicity distribution, and that they will have the same detection efficiency.

Krick, Langner, and Stewart observed that this assumption was producing systematic bias in plutonium mass assay and developed energy-dependent equations for the measured singles, doubles, and triples rates [30]. They defined new parameters within the existing point kinetics model equations that specified the detection efficiency, probability of a neutron inducing further fission, and the multiplicity of these fissions for neutrons produced by (α,n) interactions. They also developed a method of correlating the ratio of total counts between different detector rings in a given multiplicity counter to average (α,n) neutron energy. Using Monte Carlo simulations of measurements in different multiplicity counters, (α,n) neutron energy was correlated to a bias between the plutonium mass as calculated using traditional point kinetics equations and the plutonium mass as calculated using the energy-dependent equations. These calibrations were then applied to measurements where (α,n) neutron energy was first estimated from the ring ratio and then a bias correction was applied. This method was shown to nearly eliminate all energy dependence in the assay bias.

Santi *et al.* expanded on Krick, Langner, and Stewart's work by deriving equations for quads and pents that account for the detection efficiency and induced fission multiplicity and probability for (α,n) neutrons [29]. They also accounted for nonzero probability of parasitic neutron capture in their equations.

Santi and Geist combined the energy-dependent corrections with the WPM and developed different point kinetics model equations [31]. While they employed all of the corrections from the WPM, the only energy dependence they added into the equations was for the multiplicity of fissions induced by (α,n) neutrons. This separate multiplicity parameter was calculated using a ring ratio technique similar to the one described in [30] that also used quadruple coincidences. They still assumed that (α,n) neutrons and neutrons from ^{240}Pu spontaneous fission had the same probability of inducing further fission and the same detection efficiency. Implementing energy-dependent corrections into the WPM was shown to improve assay bias by 20–40 percent for Monte Carlo-simulated measurements. However, quads are difficult to measure in real measurements with any degree of certainty. While this combination of energy and geometry-based corrections has not yet been evaluated for real plutonium measurements, it can serve as a guideline for combining these two types of corrections to the point kinetics model equations used in TNI applications.

2.4 Tagged Neutron Interrogation

TNI systems are defined by the ability to "tag" the time and/or position of a particle emitted from the interrogation source. This research focuses on systems that use an Associated Particle Imaging (API) deuterium-tritium (D-T) neutron generator system to interrogate samples with monoenergetic 14.1 MeV neutrons. The D-T neutron generator creates neutrons using the $d + t \rightarrow \alpha + n$ reaction. The alpha particle is emitted directly opposite the 14.1 MeV neutron and is detected by a pixelated array of alpha particle detectors. This allows for the direction of the emitted neutron to be inferred based upon the alpha detector in which its correlated alpha particle is detected. Mihalczo provides a good summary of three TNI systems that have been developed at Oak Ridge National Laboratory (ORNL): Nuclear Materials Identification System (NMIS), Fieldable Nuclear Materials Identification System (FNMIS), and Advanced Portable Neutron Imaging System (APNIS) [4].

The neutron detectors are typically plastic or liquid scintillators that operate on the timescale of fission chains (tens of nanoseconds) as opposed to ^{3}He-based systems that require moderation and a consequently longer time scale (microseconds). This makes it possible to correlate an alpha event in the API neutron generator to an event in a neutron detector.

By time-tagging the source neutrons, a time window is opened during which source and induced fission radiation is expected to arrive in the detector. This allows for differentiation between gamma ray signals, transmitted (uncollided) source neutrons, and neutrons due to fission chains using TOF analysis. An example of this TOF spectrum is shown in fig. 2.2. This differentiation allows for a significant reduction in the emitted fission chain singles background. The high singles background due to transmitted source neutrons is often what prevents other active interrogation methods from using the measured singles rates in their analysis [8].

The ability to identify the transmitted neutron signal allows for transmission image reconstruction to provide tomographs of measured items [6]. This allows for a two or three-dimensional image of the attenuation of source neutrons and, consequently, material identification based on the attenuation coefficient [4].

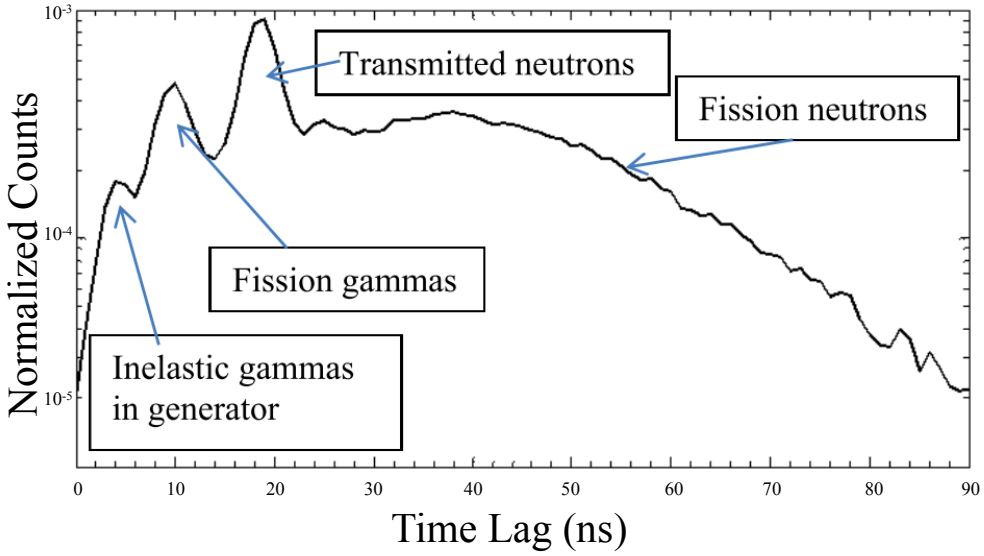

Figure 2.2: Example time response of a TNI system interrogating an enriched uranium object. "Time Lag" on the x-axis refers to the time between detection of the associated alpha particle from the D-T reaction and detection by the neutron detectors [4]. © 2017 IEEE

When performing a TNI measurement of uranium, transmission imaging can identify the location of uranium but it cannot give any information about the enrichment. This is because all uranium isotopes have similar total cross sections for 14.1 MeV neutrons. Work by Hausladen and others at ORNL has developed fission site imaging tomography techniques for TNI systems in order to differentiate uranium metal of varying enrichment [7]. This has shown to effectively differentiate DU from enriched uranium in reconstructed images. This differentiation is relative, however, and cannot be used to estimate an enrichment value from a tomographic reconstruction.

This research focuses on applications of the point kinetics model for a family of TNI systems, not a specific system. As TNI is an area of active research, the following assumptions for capabilities of a TNI system are used:

1. Fission site imaging, in combination with transmission imaging, can perfectly reconstruct the 3-D geometry of a bare uranium sample, identifying the physical boundaries of regions where the uranium is of higher enrichment.

2. The average source neutron path through a uranium object is known perfectly. This requires accurate calibration of the directional distribution of the D-T neutron source as well as any correction due to inelastic scatter of the source neutrons.

In some cases these are simplified assumptions that may not yet be true for current systems, but provide a theoretical basis for the application of point kinetics models.

2.5 Uranium Enrichment Assay Methods

This section surveys some of the methods that have been previously developed and/or are commonly used to perform nondestructive assay of uranium enrichment. Passive gamma ray methods are by and large the most popular for safeguards measurements, but may not be effective for large, inhomogeneous metal samples or samples that are heavily shielded with high-Z materials.

2.5.1 Passive Gamma Ray Spectrometry

Passive gamma ray methods focus on the 186 keV gamma ray emitted by ^{235}U α decay [32]. However, these methods are limited by the "infinite thickness criterion", which assumes that the uranium closest to the edge of the inspection volume is identical to that of the more interior material. This assumption is required because of the self-attenuating nature of uranium. For example, 2.0 mm of uranium metal attenuates more than 99 percent of 186 keV gamma rays [32]. These methods also rely on known calibration standards to correlate a gamma measurement response to an enrichment. Thus, these passive gamma ray methods for estimating uranium enrichment are susceptible to error when the uranium object under question is not homogeneously mixed, has a high-Z shielding, or known calibration standards are not available.

If the geometry and composition of the matrix is known, there are more advanced software solutions that can account for the effects of shielding and reduce the need for calibration standards. The In-Situ Object Counting Systems (ISOCS) is one such technology [33]. It allows the user to specify the geometry and composition of a container using a library of templates, and corrects for any attenuation effects based on precise factory characterization of the germanium detector and an extensive library of correction factors generated from precomputed Monte Carlo simulations. This technique is still susceptible to the main drawback of other gamma-based enrichment assay methods, that high-Z shielding, including self-shielding, can dramatically reduce the measurable signal.

2.5.2 Monte Carlo Methods for TNI

Mattingly *et al.* developed a method for verifying enrichment declarations for highly-enriched uranium (HEU) shipments to the Y-12 National Security Complex using NMIS [34]. A time-tagged ^{252}Cf source interrogated annular castings containing several kgs of HEU metal. The zeroth and first reduced-factorial moments of neutron and gamma ray time correlations with the ^{252}Cf source were measured and compared to Monte Carlo simulations to determine enrichment. A nonlinear calibration surface was able to predict both enrichment and uranium mass using the two moments. The method was first tested on a set of known

standards in order to implement empirical corrections before measuring the rest of the almost 500 inspection objects. While this method was able to estimate enrichment and uranium mass to within 5 percent of the declared value, this approach would not be applicable to situations where known standards are not available and/or calibrations based on Monte Carlo simulations are not desirable.

A master's thesis by Swift developed a method for estimating uranium enrichment based on results of TNI measurements of uranium metal [35]. Measurements of HEU surrounded by depleted uranium (DU) and polyethylene were simulated using MCNP-PoliMi [36]. The enrichment of the center HEU was considered unknown. Several simulations of varying enrichment were performed and the true enrichment was estimated by using the simulation that best matched the measured source-neutron TOF distribution. This method was able to predict enrichment to within 6 percent.

Recent work by Crye used a similar method as Swift to interpret measurements of HEU castings surrounded by DU [5]. This analysis assumed that the location of the HEU within the measurement matrix was unknown. Using the reconstructed transmission image and doubles image from NMIS measurements, the geometry could be inferred. Using this geometric information and coincidence measurement data from separate measurements of the same samples using a ^{252}Cf source, Monte Carlo simulations were used to match uranium enrichment to the source-neutron TOF distribution. When measuring an approximately 18 kg sample of HEU, this method was able to estimate an enrichment between 82 and 95 percent, depending on the amount of DU and polyethylene shielding.

The method of performing several Monte Carlo simulations to match TOF coincidence response to measurement is advantageous in that it does not require calibration measurements of known reference standards. It is one of the first methods that has accurately estimated uranium enrichment without the need for these standards. This capability was only made possible by leveraging the unique transmission and fission imaging capabilities of TNI measurement systems to determine the geometry of the matrix and spatial distribution of enriched uranium. In previous methods, this spatial distribution would have to be assumed homogeneous.

However, this method also has its drawbacks. It is not quick, as it requires a specialized analyst to create Monte Carlo simulations for each measurement and then run them to a desired level of accuracy. It is also dependent on the ability of the simulation software, in this case MCNP-PoliMi, to accurately model the detector response. It also may not be appropriate for treaty verification applications, as geometric details of nuclear arms are often highly classified.

2.5.3 Delayed Neutron Re-interrogation

A technique developed by Myers, Goulding, and Hollas presented a novel method of determining uranium enrichment for bulk samples using delayed neutrons [37]. This expanded upon prior research by Li [38] and Campbell [39] that showed delayed neutrons could be used to assay sub-gram uranium samples by demonstrating this capability for bulk samples. It is based on the delayed neutron re-interrogation technique that uses a pulsed D-T neutron generator to create a steady-state source of delayed neutrons within a uranium sample [21, 40]. Once a steady-state source of delayed neutrons has been achieved, the D-T neutron source is shut off and the delayed neutrons are counted using moderated ^{3}He tubes. The shape of this die-away curve is a sum of decaying exponentials which can be approximated by the six-group fast fission delayed neutron precursor model [41]. A best fit determination can estimate enrichment. In general, a die-away curve for a sample with higher enrichment will have a longer tail, as delayed neutrons are more likely to induce fission and extend the length of the fission chain. Measurements of uranium oxide and metal samples of around 1 kg uranium and varying enrichments were assayed. Measurements of the bare uranium metal samples overestimated DU samples by 1–5 percent ^{235}U by weight and underestimated HEU samples by 1–4 percent ^{235}U by weight depending on the die-away time used for fitting. Uncertainties of 1–4 percent ^{235}U by weight for the enrichment estimates of the metal samples were reported. The authors claim that no measurement standards are needed in order to perform this enrichment assay. However, at the time of this writing, this method has only shown preliminary proof-of-concept and needs to be further developed and evaluated.

While the delayed neutron re-interrogation method of enrichment assay is still in the early stages of development, it serves as a good goal in terms of the accuracy desirable for the point kinetics-based methods of enrichment assay developed by this dissertation.

2.6 List of Original Contributions

The following list summarizes the original research contributions that are presented in this work:

1. Development and validation of new point kinetics models that extend existing models to include external D-T neutron source coupling

2. Development of four methods to estimate uranium enrichment and neutron multiplication that leverage imaging and source-correlation capabilities of TNI systems

3. Sensitivity analysis and evaluation of new uranium enrichment and multiplication estimation methods using Monte Carlo simulations and TNI measurement data

4. Evaluation of several point kinetics model assumptions for uranium including the negligible parasitic capture assumption, chain-starting multiplicity isotopic sensitivity, and all neutrons born at a point assumption

5. Development of a robust Monte Carlo simulation and analysis suite to analyze point kinetics models

6. Evaluation of uncertainties in estimating emitted fission chain multiplicities from measured multiplicity data in TNI measurements

Chapter 3

D-T Model

Unlike passive coincidence and multiplicity measurements where each fission chain is assumed to be initiated by either a spontaneous fission of the fissionable material under assay or an (α,n) reaction in the matrix, active measurements initiate fission chains using an external source. In building a point kinetics model representing any kind of active interrogation, it is imperative to understand the coupling between the interrogation source and the object under interrogation. The D-T Model is a general expanded point kinetics model that has been designed to account for the source-object coupling, and serves as a basis for methods described in this work to estimate enrichment and neutron multiplication of large uranium objects under TNI.

In passive measurements, the spontaneous fission rate can be parameterized in terms of the fissionable material mass, typically an effective ^{240}Pu mass. In active measurements, however, the fission chain initiation rate is not as straightforward. It is a function of several factors, including the geometry of the source-object-detector system and the isotopic makeup of the interrogation object.

TNI measurement systems provide knowledge of the direction, relative time, and energy of the source neutron. This motivates coupling the fission chain PGF in eq. (2.2) to a new model parameter β that represents the fraction of emitted source neutrons that initiate fission chains in the uranium sample. Conversely, the fraction transmitted through the object is

$1-\beta$. The resulting D-T model PGF $h_f(y)$ is

$$h_f(y) = (1-\beta)y + \beta h_{mn}(y), \tag{3.1}$$

where y is a dummy variable and $h_{mn}(y)$ is defined in eq. (2.2).

By applying eq. (2.4) to eq. (3.1), the first two reduced-factorial fission chain moments Φ_1 and Φ_1 can be calculated:

$$\Phi_1 = (1-\beta) + \beta\left(M_T - \frac{M_T - 1}{\nu_{i1}}\right)\nu_{s1}, \tag{3.2}$$

$$\Phi_2 = \beta\left(M_T - \frac{M_T - 1}{\nu_{i1}}\right)^2\left[\nu_{s2} + \nu_{i2}\nu_{s1}\left(\frac{M_T - 1}{\nu_{i1}}\right)\right]. \tag{3.3}$$

In the D-T model, source neutrons that are transmitted through the object are technically considered fission chains with a multiplicity of one. However, a theoretical TNI measurement can distinguish the emitted singles rate due to transmitted source neutrons $\Phi_{1,t}$ from the emitted singles rate due to fission chain multiplication within the uranium object $\Phi_{1,f}$ based on TOF. The equation for the emitted singles rate [eq. (3.2)] can be split into two parts which can be independently measured:

$$\Phi_{1,t} = (1-\beta), \tag{3.4}$$

$$\Phi_{1,f} = \beta\left(M_T - \frac{M_T - 1}{\nu_{i1}}\right)\nu_{s1}. \tag{3.5}$$

A theoretical TNI measurement of a bare uranium object produces values for both components of the emitted singles rate ($\Phi_{1,t}$ and $\Phi_{1,f}$), as well as the emitted doubles rate Φ_2.

The convention used in this work is that the term "emitted fission chain singles" refers to $\Phi_{1,f}$ when discussing the D-T model or subsequent methods derived from it. Because all double (and larger) neutron coincidences can only come from source-neutron-induced fission chains, "emitted fission chain doubles" refers to Φ_2. There are no transmitted source neutron components of doubles or larger reduced-factorial moments.

Values for the ν_{sn} chain-starting multiplicity terms are highly dependent on the assumptions made about which nuclear reactions induced by a 14.1 MeV source neutron are considered chain-starting reactions. This is discussed in further detail in chapter 6.

The neutrons produced by 14.1 MeV source-neutron interactions in the uranium are referred to as "induced neutrons" and can either further propagate the fission chain via induced fission or escape. Neutrons produced by induced fission later in the fission chain are also considered "induced neutrons". Induced neutron interactions occur at fission neutron energies which can be modeled by a Watt spectrum. An average energy of 2 MeV is assumed for the emitted neutrons of induced fissions. Thus, values for the ν_{in} terms are calculated from the multiplicity distribution for 2 MeV induced fission on ^{235}U measured by Zucker and Holden [42]. At this energy, the multiplicity distribution is largely insensitive to uranium enrichment.

3.1 Evaluating Point Kinetics Model Assumptions

Monte Carlo simulations described in chapter 4 were used to evaluate the appropriateness of the traditionally applied point kinetics model assumptions listed in section 2.1 for 14.1 MeV TNI of bare uranium metal.

3.1.1 Negligible Parasitic Capture Assumption

The point kinetics framework combines the spatial, energy, isotopic, and directional variations in fission chain propagation into the single concept of average neutron multiplication. The increase in neutron population due to a single neutron is known as the total self-multiplication factor M_T. Another quantity of interest is the number of induced fissions per neutron $p_f M_T$, where p_f is the probability that an induced fission neutron induces further fission. However, a description of the neutron population that escapes from a fissionable sample and can be detected by an external detector, is necessary when applying the point kinetics model to a measurement scenario. In order to account for the neutron population increase due to fission and neutron population decrease due to parasitic capture, the leakage self-multiplication term M_L is often used. It is defined as the increase in the emitted neutron

population as a result of one additional neutron in the system. It can also be defined as the ratio of neutrons leaking out of a fissionable sample to the number of neutrons created by the chain-starting event:

$$M_L = (1 - p_f - p_c)M_T = \frac{(1 - p_f - p_c)}{1 - p_f\nu_{i1}}, \tag{3.6}$$

where ν_{i1} is the average number of neutrons produced by an induced fission and p_c is the probability that a neutron is parasitically captured.

In order to limit the dimensionality of the point kinetics model equations, it is commonly assumed that parasitic capture of neutrons within the fissionable object is negligible. In other words, the only neutron losses within the sample are from inducing fission. This allows for leakage self-multiplication M_L to remain a function of only one characteristic parameter, p_f. This assumption manifests itself when the $p_f M_T$ term, which appears in the point kinetics model equations, in expressed in terms of only M_L. The following assumption is used [15]:

$$p_f M_T \approx \frac{M_L - 1}{\nu_{i1} - 1} = M_T \left[p_f - \frac{p_c/p_f}{\nu_{i1} - 1} \right] \tag{3.7}$$

This approximation holds when $p_c/p_f \ll 1$.

Monte Carlo simulations were used to assess the validity of this assumption for a bare uranium metal object under active interrogation by 14.1 MeV neutrons. The results were compared to another Monte Carlo simulation of a passive assay of a weapons-grade plutonium sample. The physical characteristics of the plutonium were taken from [43]. Figure 3.1 shows that the assumption condition $p_c/p_f \ll 1$ for the uranium to be considerably worse compared to the passive plutonium simulation. The largest p_c/p_f ratios were seen in simulations with greater concentrations of ^{238}U.

This is largely explained by the difference in the macroscopic cross section ratios Σ_γ/Σ_f between ^{238}U and ^{235}U. Using fission-energy-averaged cross sections, this ratio is approximately 0.237 and 0.0785 for ^{238}U and ^{235}U, respectively [44]. However, the p_c/p_f ratios for DU (0.3 percent ^{235}U) simulations increased well beyond the ^{238}U Σ_γ/Σ_f ratio, with p_c/p_f increasing with total uranium mass. This is likely a result of a downscattering effect from inelastic scatter in ^{238}U. Neutrons born inside larger objects will undergo more

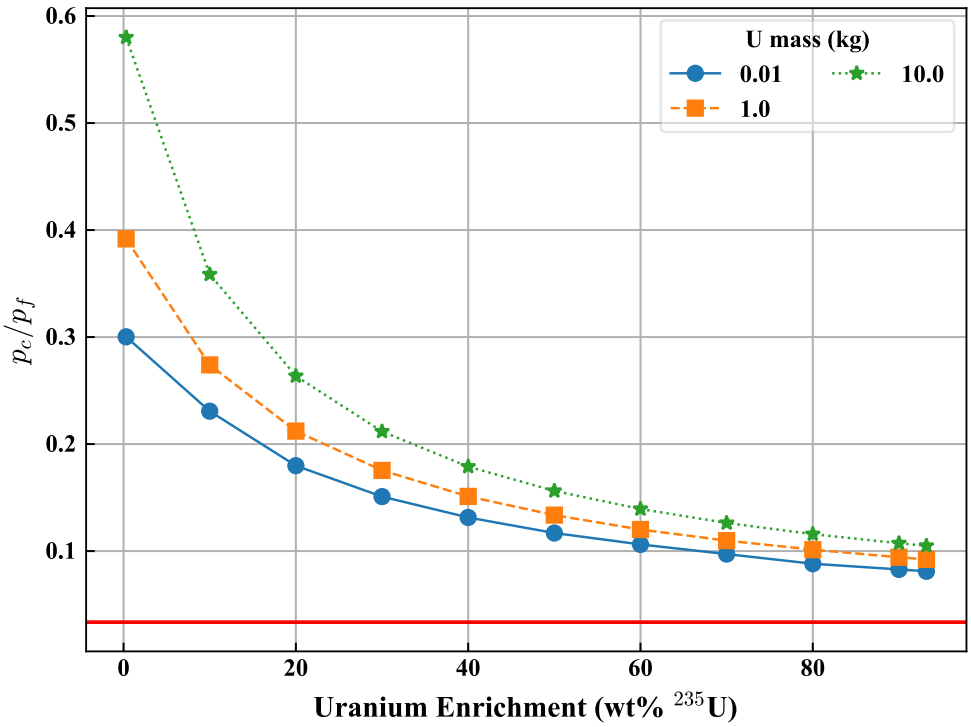

Figure 3.1: Monte Carlo estimates of the induced neutron capture-to-fission ratio for uranium. The solid red line represents the Monte Carlo estimate for a passive plutonium simulation.

scatters and lose more energy before removal compared to those born inside smaller objects, as shown in fig. 3.2.

While the point kinetics model assumption that $p_c/p_f \ll 1$ is obviously violated to varying degrees for uranium samples, it was determined that this violation ultimately resulted in very little systematic error when used to calculate emitted fission chain doubles. Figure 3.3 shows the percent difference between the Monte Carlo-estimated doubles and doubles calculated using the point kinetics model equation [eq. (3.8)] that incorporates the negligible-capture assumption.

$$\Phi_2 = \beta M_L^2 \left[\nu_{s2} + \nu_{i2}\nu_{s1} \left(\frac{M_L - 1}{\nu_{i1} - 1} \right) \right]. \tag{3.8}$$

Monte Carlo estimates for all parameters in eq. (3.8) are used to calculate the point kinetics estimate for doubles.

3.1.2 All Neutrons are Born at a Point

The violation of the point kinetics model assumption that all neutrons are born at a point has been shown to introduce significant bias in the assay of plutonium mass using passive coincidence and multiplicity counters, particularly for high-multiplication samples [23, 24]. This arises from the fact that neutrons born in the center of a fissionable sample have a different probability of inducing further fission than those born near the edge. Using active interrogation sources can exacerbate this effect because the first generation of fission-chain neutrons are born with some spatial distribution that is determined by the coupling between the source and the sample under interrogation.

Ensslin *et al.* note that "the assumption of constant fission probability only works for samples that are dilute or thin with respect to the neutron mean free path, such as oxides" [12] when performing passive assay on plutonium samples. For context, the largest mean free path for a neutron with Watt spectrum energies in uranium metal was calculated using cross sections from ENDF/B-VII.1 [2]. For pure ^{235}U, the largest mean free path is 3.125 cm, while it is 3.055 cm for pure ^{238}U. Thus, samples that have dimensions larger than 1 cm may be susceptible to violating this point kinetics assumption.

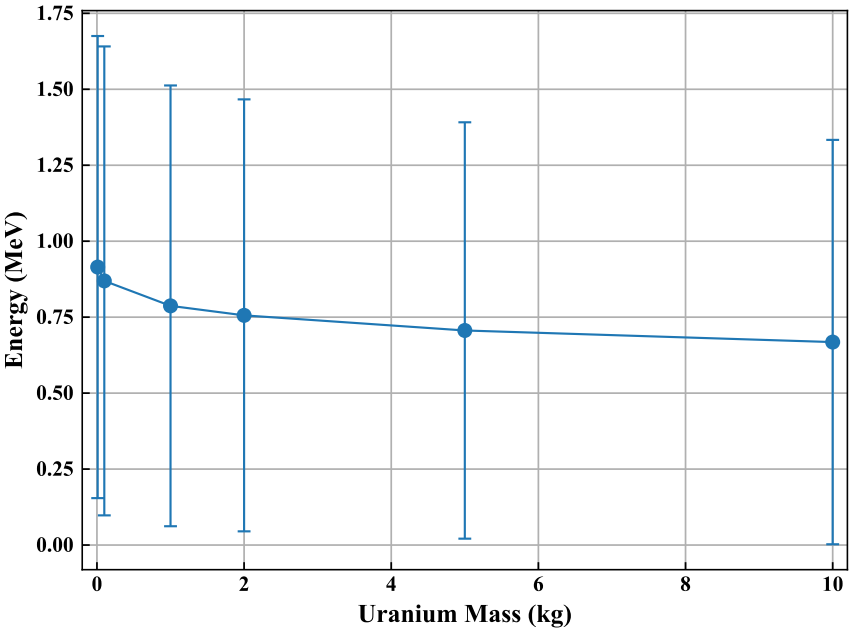

Figure 3.2: Energy of induced neutrons (generation ≥ 1) when undergoing a removal interaction [fission, capture, (n,xn)] versus total uranium mass for 50 percent ^{235}U case. Error bars are one standard deviation of the energy distribution as estimated by Monte Carlo. These distributions are highly non-Gaussian.

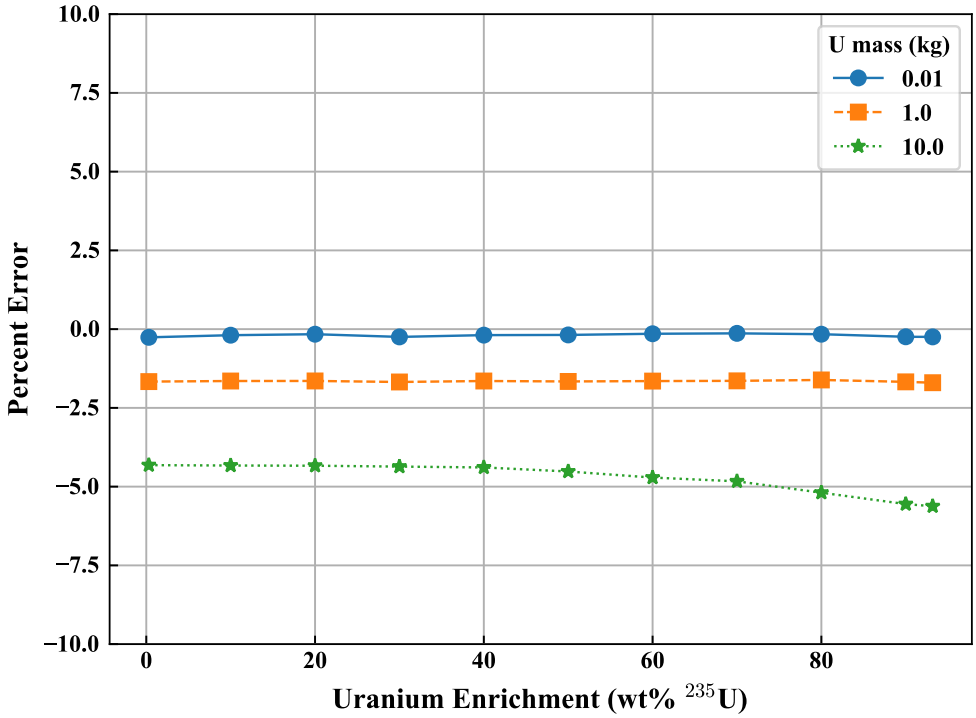

Figure 3.3: Percent error in emitted fission doubles due to negligible-capture assumption for a spherical geometry

Monte Carlo simulations were performed to evaluate the spatial distribution of chain-starting interactions. For low-multiplication samples, the neutrons born from chain-starting interactions represent the majority of the neutrons born during TNI. The simulations are described in further detail in chapter 4, with the 14.1 MeV source neutron directional distribution modeled off a central NMIS pixel and uranium objects of varying mass and enrichment. Chain-starting events include induced fission, (n,xn) and (n,γ) parasitic capture. These spatial distributions were not sensitive to enrichment. Results for a sphere with 90 percent enrichment are shown in fig. 3.4. They suggest that for a typical NMIS source pixel, the spatial distribution of chain-starting interactions begins to become heterogeneous for spherical uranium metal samples of 100 g and larger. These results do not show the spatial distribution in the z direction.

Figure 3.5 shows x-y spatial distributions for induced fissions for all fission-chain generations including the chain-starting interaction. These plots show that for the 1000 g and 10 000 g spheres, the fission spatial distributions are still biased towards the direction of the external source, whereas the smaller samples seem to have their fissions distributed evenly throughout the volume. This does not, however, imply that the point kinetics assumption that all neutrons are born at a point is a good assumption for these smaller samples. It does imply that an average position can be calculated analytically, opening the door to analytical corrections based on knowledge of the objects geometry similar to those developed for passive plutonium measurements by Croft *et al.* [25] and Hauck and Henzl [3].

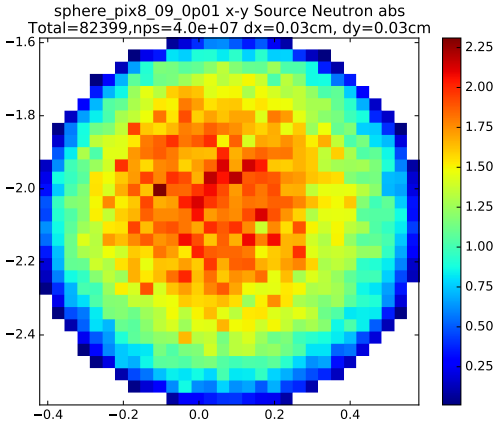

(a) 10 grams (0.503 cm radius)

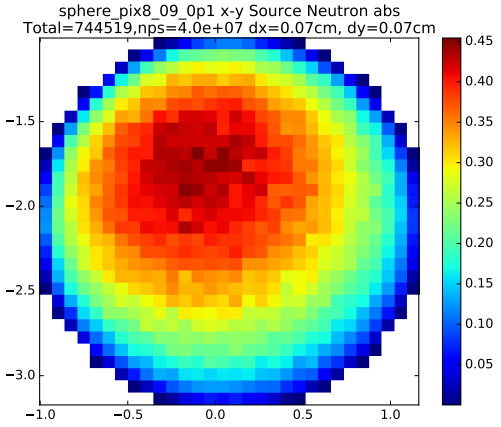

(b) 100 grams (1.084 cm radius)

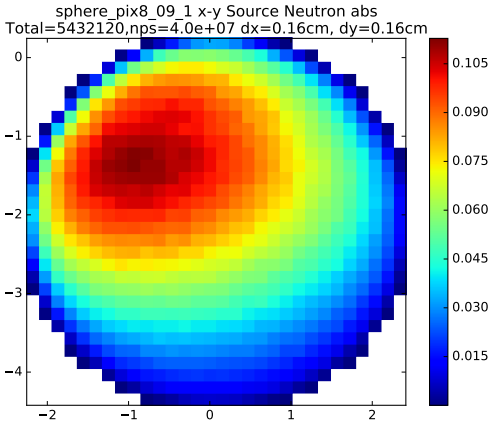

(c) 1000 grams (2.335 cm radius)

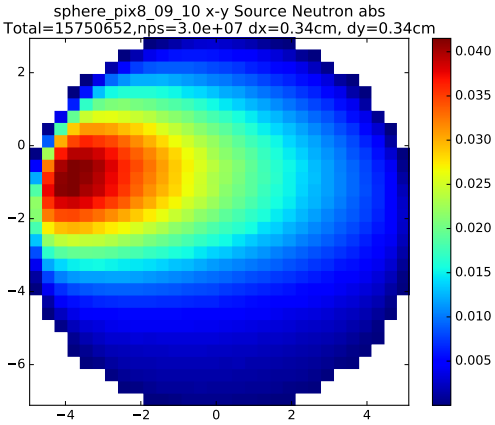

(d) 10 000 grams (5.031 cm radius)

Figure 3.4: 2-D spatial distribution of chain-starting interactions for a uranium metal sphere with 90 percent enrichment

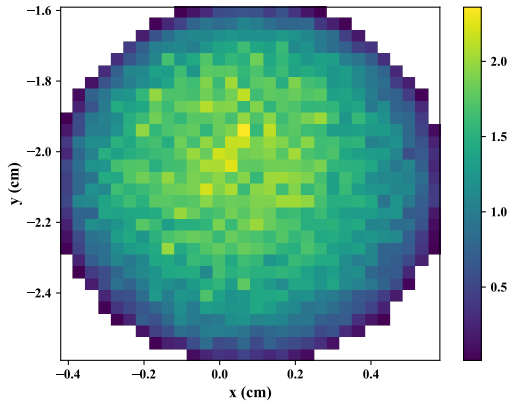

(a) 10 grams (0.503 cm radius)

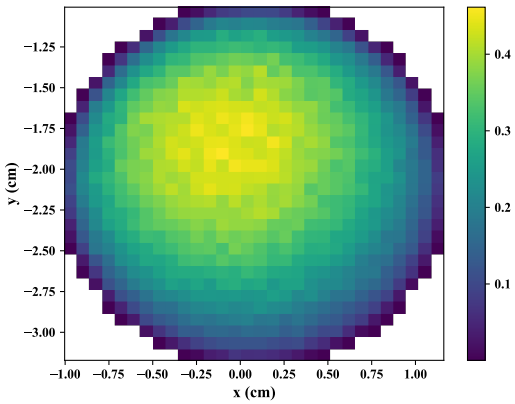

(b) 100 grams (1.084 cm radius)

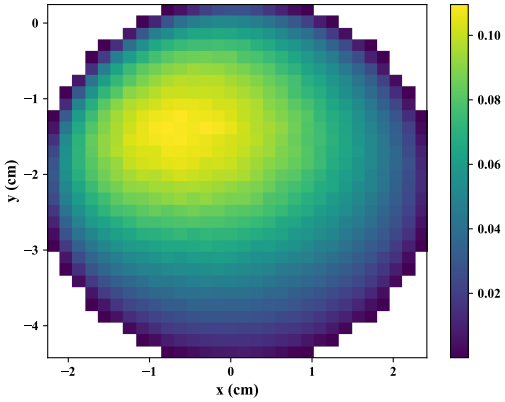

(c) 1000 grams (2.335 cm radius)

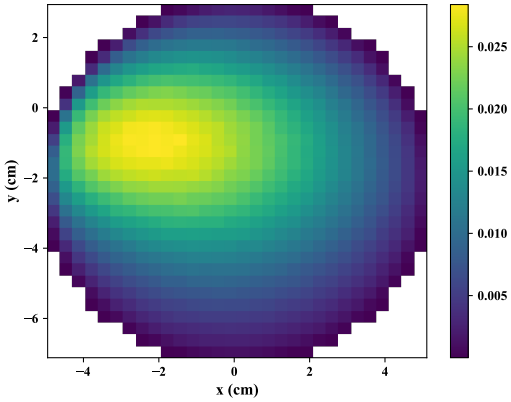

(d) 10 000 grams (5.031 cm radius)

Figure 3.5: 2-D spatial distribution of all induced fissions for a uranium metal sphere with 90 percent enrichment

Chapter 4

Monte Carlo Simulations

Due to the inherent difficulties of accessing uranium metal samples with varying kg-quantity masses, enrichments, and shapes, Monte Carlo simulations were used extensively to simulate neutron fission chain propagation in uranium metal under TNI. MCNPX-PoliMi v2.0.0 [45] was used due to its improved modeling of correlations between neutron energy and fission multiplicity modeling and convenient output files that track collisions and fission multiplicities.

4.1 MCPNX-PoliMi Simulation Suite

An extensive suite of scripts has been developed to automate the process of running MCNPX-PoliMi and parsing the output files. The simulations are typically performed on a 64-core machine owned by the Nuclear Materials Detection & Characterization group (NMDC) at ORNL. The suite accepts the following input parameters for simulation:

- Uranium mass
- Uranium enrichment, as a mass fraction of ^{235}U
- Object geometry—either annular casting, solid cylinder, solid sphere, or regular tetrahedron
- Type of 14.1 MeV neutron interrogation source: internal or external

  - Internal source: geometric center or distributed throughout the volume of the uranium object
  - External source: directional distribution based on the central alpha pixel of NMIS, a sum of all APNIS alpha pixels, or straight

The suite can parse the following characteristics from MCNPX-PoliMi output files:

- Probabilities and reduced-factorial moments of the emitted-neutron multiplicity distribution
- Total and leakage neutron multiplication
- Probabilities that a neutron will be captured, induce fission, undergo (n,2n), (n,3n), (n,4n) interactions. These probabilities are separated by "source" (14.1 MeV) neutrons and "induced" neutrons (neutrons produced by some multiplying reaction). These probabilities are further broken down by uranium isotope (^{235}U or ^{238}U).
- Fraction of source neutrons incident on an object, if the source is external to the object
- Average linear path length of source neutron through an object
- Ratio of induced neutron captures to fissions
- Reduced-factorial moments of the multiplicity of neutron interactions, separated by source neutrons and induced neutrons. These moments are further broken down into only fission reactions and all multiplying interactions [capture, (n,xn), etc.]
- Sphericity of the geometry, which is a measure of how spherical an object is [46]
- Statistical uncertainties associated with most of the above values
- A histogram of the neutron energy distribution for neutrons that undergo capture, fission, (n,2n), (n,3n), (n,4n), again separated by "source" and "induced" neutrons. The mean and standard deviation of these distributions are also recorded.

- The x-y-z locations of the all multiplying neutron-induced events by fission chain generation. These can be plotted in a two-dimensional (x-y) plane and can be broken down by type of interaction [fission, (n,2n), (n,3n), (n,4n), (n,γ)].

Additional simulation parsers have been developed to calculate the Euclidean distance and total distance that a 14.1 MeV neutron travels within uranium metal before it is captured and/or induces fission.

The uranium objects were assumed to only contain ^{235}U and ^{238}U and the simulations assumed perfect discrimination between emitted singles due to transmitted source neutrons and those due to source-initiated fission chains.

4.2 Simulations Performed

Throughout this research, several rounds of Monte Carlo simulations using the simulation suite described in section 4.1 have been performed to verify, validate, and assess the ability of the various point kinetics models to describe emitted multiplicities or assay physical parameters of a uranium sample. The initial set of Monte Carlo simulations were used to analyze methods in chapters 3, 6 and 7. Simulation results using masses from 0.01, 0.1, 1.0, 2.0, 5.0, and 10.0 kg of uranium metal are shown, although many more masses between these values were used. Uranium enrichments span from 0 percent to 100 percent ^{235}U by weight in steps of 10 percent. Geometries used include the annular casting, solid cylinder and solid sphere. Unless specifically stated in the results, the directional distribution of the 14.1 MeV source neutrons is modeled off of the central NMIS pixel, sometimes referred to as pixel 8.

Additional simulations were also performed to model the 17.915 kg uranium metal castings that were used in experiments by Crye [5], as well as the 17.1 kg casting used by Hausladen *et al.* [7]. The data from these experiments were used to evaluate various point kinetics-based methods developed in chapters 6 and 9. These experiments and how they were used in the context of this research are discussed further in chapter 5. The simulations allow for validation of MCNPX-PoliMi as well as the custom parsers. Aside from the size of the uranium sample, these simulations did not differ from the other simulations that were performed. No other matrix material, equipment, or detectors were modeled in an effort to

simplify the simulations and reduce systematic bias of the fission chain propagation process. The only exception to this are the simulations of the APNIS measurement used to estimate components of detection efficiency, which included a basic model of the neutron detector bank. These simulations are described further in section 5.2.

A second round of simulations was performed with increased fidelity on the input parameters. These simulations included all combinations of uranium masses from 1.0 to 7.0 kg in steps of 0.05 kg, enrichments from 0 percent to 100 percent ^{235}U by weight in steps of 2 percent, geometries including annular casting, solid cylinder, sphere, and regular tetrahedron, and both the straight and central NMIS pixel source direction profiles. This amounted to 49 370 total simulations. These simulations were used to perform the parametric studies in chapter 8 and to generate the lookup tables used by the hybrid method in chapter 9.

4.3 NPS Study

While the ability to use a 64-core machine greatly reduced the total time necessary to run all of these simulations, the scope of the simulations necessitated certain optimizations. A key optimization for a Monte Carlo simulation is determining an adequate number of histories to run (NPS). In the simulations performed for this study, one history is a single 14.1 MeV source neutron emitted external to the uranium assay object. This study was carried out using input parameters that span the space used in this research. All combinations of uranium enrichments of 0 percent, 50 percent, and 100 percent ^{235}U by weight, uranium masses of 0.1, 1, 10, and 17.915 kg, and annular casting, solid cylinder, and solid sphere geometries were used. This resulted in 45 simulations for each different NPS. The NPS values used were 2×10^4, 10^5, 10^6, and 10^7, for a total of 225 simulations. The most important values that these Monte Carlo simulations estimate are the emitted multiplicities and multiplication. So, the effect of NPS on the relative statistical uncertainty in the emitted fission chain singles, doubles, total multiplication, and leakage multiplication was analyzed. The simulation parsing software estimated a standard deviation and variance due to statistical uncertainty for each of these estimated values, which was used in the analysis.

The percent uncertainty of a Monte Carlo estimate $\hat{x}$ is defined as $100\frac{\sigma_{\hat{x}}}{\hat{x}}$ where $\sigma_{\hat{x}}$ is the statistical uncertainty of the estimate $\hat{x}$.

The results are shown in fig. 4.1. Ultimately, an NPS of 10^6, or one million D-T source neutrons, was chosen as an ideal value to use because it kept the majority of the estimates to within 1 percent statistical error.

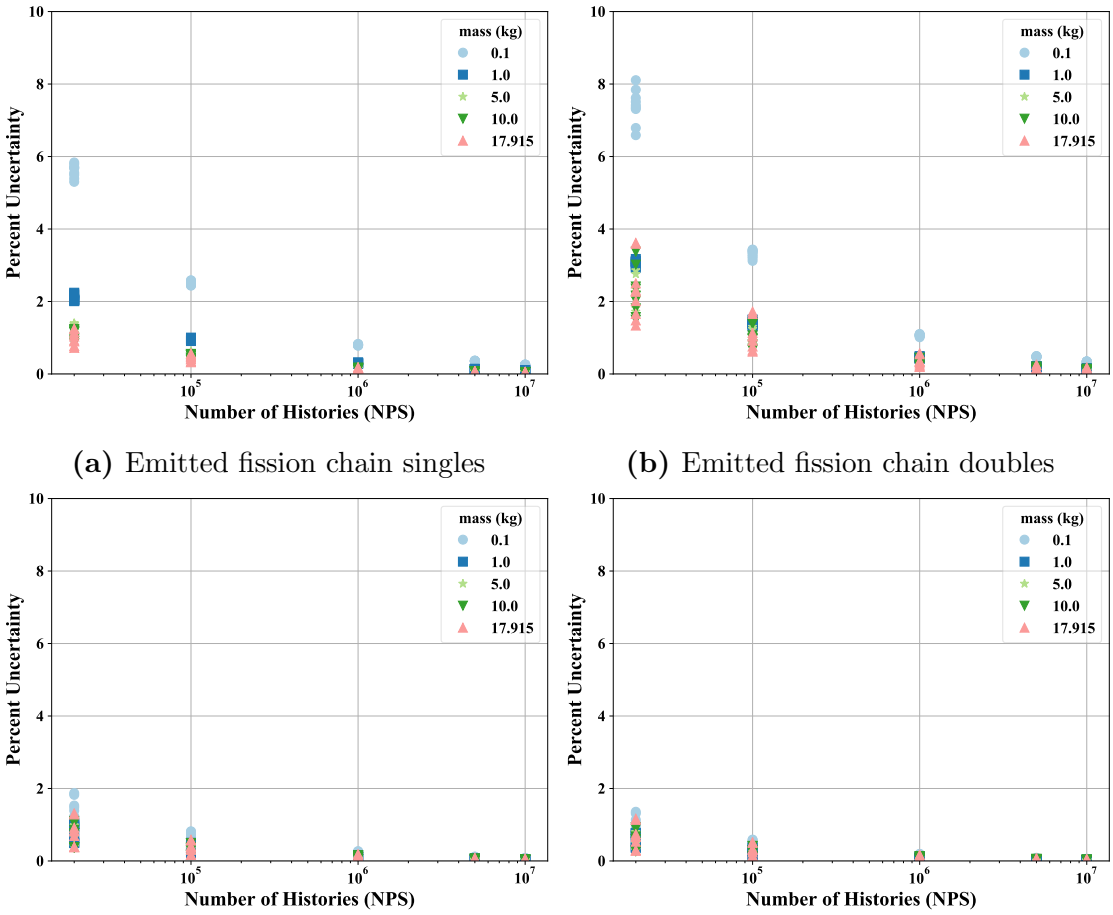

(a) Emitted fission chain singles

(b) Emitted fission chain doubles

(c) Total multiplication.

(d) Leakage multiplication

Figure 4.1: Percent uncertainty of Monte Carlo estimates versus number of histories

Chapter 5

Experimental Data

Data from two different measurements systems were used to evaluate the ability of the point kinetics models developed in this work to estimate neutron multiplication and enrichment of a bare uranium metal object. These two systems are the Nuclear Materials Identification System (NMIS) [4] and the Advanced Portable Neutron Imaging System (APNIS) [7], both developed at ORNL. This chapter describes these active interrogation imaging systems and the measurements of large uranium objects they perform, as well as the process for performing efficiency corrections to calculate emitted fission chain neutron singles and doubles from measured observables.

5.1 NMIS Measurement Data

The measurement setup for NMIS consists of an API neutron generator with 16 alpha detector pixels opposite an array of 32 plastic neutron scintillators in a fan beam arrangement, known as the transmission imaging detectors. These transmission imaging detectors are used to detect transmitted D-T source neutrons. Eight larger plastic neutron

scintillators were positioned above and below the transmission imaging detectors and are used to detect fission neutrons. Measurements performed by Crye using NMIS interrogated annular castings of HEU (93.19 percent ^{235}U by weight) and DU (0.3 percent ^{235}U by weight) uranium metal (ρ=18.75 g/cm^3) [5]. In addition to ^{235}U and ^{238}U, the castings also contained small amounts of ^{234}U and ^{233}U, which were found to have a negligible affect on the emitted multiplicities and neutron multiplication. The experimental setup is shown in fig. 5.1, and a more complete discussion of the experiment can be found in [5]. The emitted fission chain singles and doubles rates for each of the 16 alpha pixels, normalized per emitted D-T neutron in the direction of a given pixel, were estimated by correcting for total detection efficiency and dead-time losses [5]. The measured fission chain singles and doubles rates from the central alpha pixel (pixel 8) are typically used to represent the entire volume. While this does assume a certain chemical and isotopic homogeneity, the values for measured doubles per single per alpha event over all pixels where the casting is between the source and detectors appear to be relatively constant, as can be seen in fig. 5.2. Uncertainties are shown but they are so small that they are barely visible on the plot.

Emitted fission chain singles $\Phi_{1,f}$ and doubles rates Φ_2 are calculated from measured fission chain singles S and doubles D counts that are associated with a given alpha pixel that registers α counts in the alpha detector. Each count in the alpha detector corresponds to a single D-T source neutron emitted in that directional pixel. A correction for total neutron detection efficiency ε is also applied. The combination of systematic and statistical uncertainty in ε is denoted as σ_ε. The uncertainties associated with the estimates of the emitted fission chain singles and doubles rates $\Phi_{1,f}$ and Φ_2 are denoted as σ_1 and σ_2, respectively. Assuming gate fraction and dead-time corrections have already been applied to the measured singles and doubles counts,

$$\Phi_{1,f} = \frac{S}{\varepsilon\alpha}, \tag{5.1}$$

$$\Phi_2 = \frac{D}{\varepsilon^2\alpha}. \tag{5.2}$$

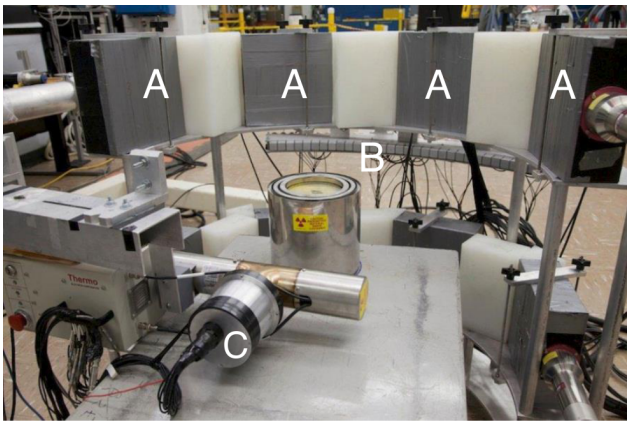

Figure 5.1: The experimental setup for NMIS measurements of uranium storage castings. The top four large plastic scintillators are marked by A, while B marks the smaller plastic scintillators used for tomographic imaging. The API neutron generator is marked by C [5]. © 2017 IEEE

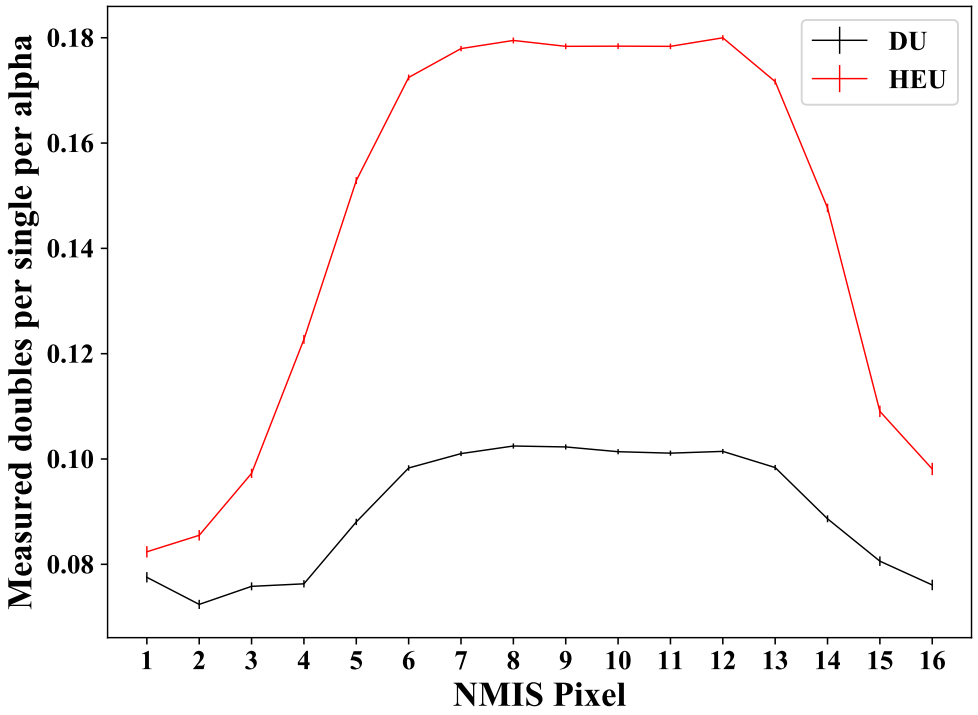

Figure 5.2: Alpha pixel profile for uranium casting measurements [5]

Propagating these uncertainties based on eqs. (5.1) and (5.2),

$$\sigma_1 = \Phi_{1,f}\sqrt{\left(\frac{\sigma_S^2}{S^2} + \frac{\sigma_\varepsilon^2}{\varepsilon^2}\right)}, \tag{5.3}$$

$$\sigma_2 = \Phi_2\sqrt{\left(\frac{\sigma_D^2}{D^2} + \frac{4\sigma_\varepsilon^2}{\varepsilon^2}\right)}. \tag{5.4}$$

The statistical uncertainties of the measured singles and doubles, denoted as σ_S and σ_D, respectively, are assumed to be the square root of the counts. While these are not Poisson-distributed random variables, this assumption is used as a conservative estimate. The number of alpha pixel counts is a fixed parameter of the measurement, so it has no uncertainty. While the detection efficiency will have both random and systematic sources of uncertainty, the nature of the systematic error is unknown and depends upon the geometry of the measurement. As a conservative estimate, the total uncertainty was assumed to be 10 percent of the calibrated value. In the case of the experiments performed by Crye, the total detection efficiency was estimated using ^{252}Cf calibration measurements [5].

$$\sigma_S = \sqrt{S}$$
$$\sigma_D = \sqrt{D}$$
$$\sigma_\varepsilon = 0.1\varepsilon$$

Substituting these values into eqs. (5.3) and (5.4) gives the equations used to estimate uncertainty of emitted fission chain singles and doubles rates from the measurements performed in [5]:

$$\sigma_1 = \Phi_{1,f}\sqrt{\left(\frac{1}{S} + \frac{1}{100}\right)}, \tag{5.5}$$

$$\sigma_2 = \Phi_2\sqrt{\left(\frac{1}{D} + \frac{1}{25}\right)}. \tag{5.6}$$

While the assumption of 10 percent relative uncertainty of the total detection efficiency is conservative, the assumed value of this parameter can have a significant effect on the uncertainty of the emitted multiplicities. For measurements with sufficient measurement times, such as those described in [5] where each alpha pixel has more than 10^7 alpha counts, the statistical uncertainty of the singles and doubles counts, which were assumed to be Poisson-distributed in the above equations, is negligible. The uncertainty in the total detection efficiency drives the uncertainty in the emitted multiplicities. As can be seen in fig. 5.3, the uncertainty in the emitted fission chain doubles per single can quickly get out of hand if there is not adequate uncertainty in the total detection efficiency.

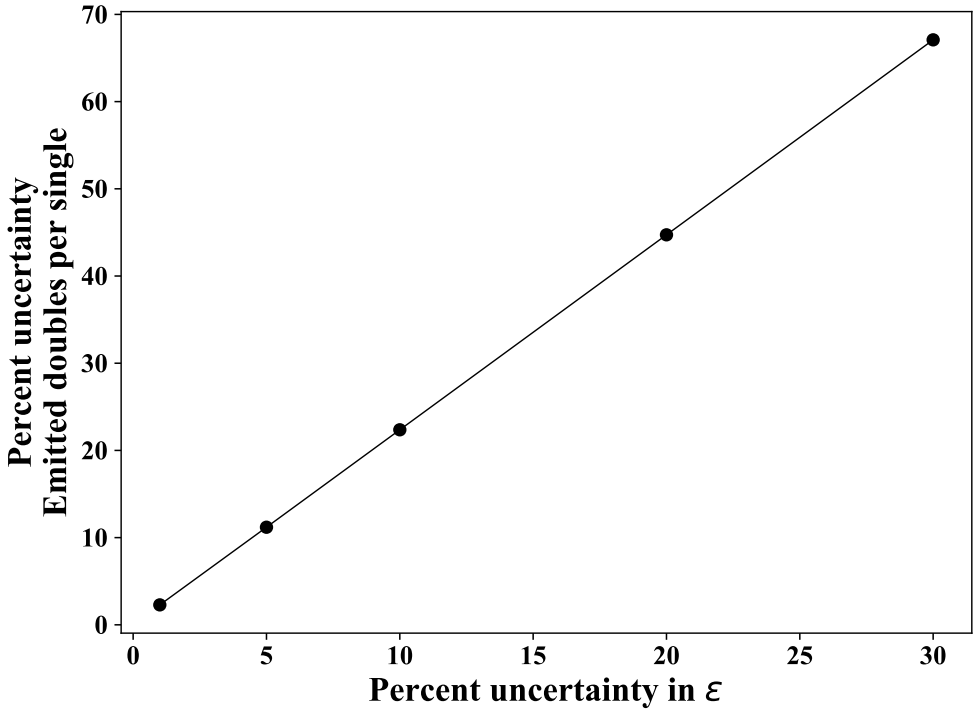

Figure 5.3: The effect of uncertainty in the total detection efficiency on the uncertainty of emitted fission chain doubles per single for an NMIS measurement

5.2 APNIS Measurement Data

The APNIS achieves higher imaging resolution than the NMIS by using 36 plastic scintillator neutron block detectors each with 100 pixels which are read by four photomultipliers. Electronics from a Siemens Inveon^{TM} preclinical system determine the position of interaction

and timestamp for each neutron interaction [47]. This results in 3600 total pixels. The detector array is curved in such a way that the center of each block detector is approximately 85 cm away from the API D-T neutron generator. A turnstile in between the neutron generator and detector array rotates the interrogation object in order to perform an imaging measurement. In the measurement considered in this work, an annular casting containing approximately 17 kg of DU is positioned adjacent to a polyethylene block on top of a steel box. The experimental setup is shown in fig. 5.4 and a more complete discussion of the setup can be found in [7].

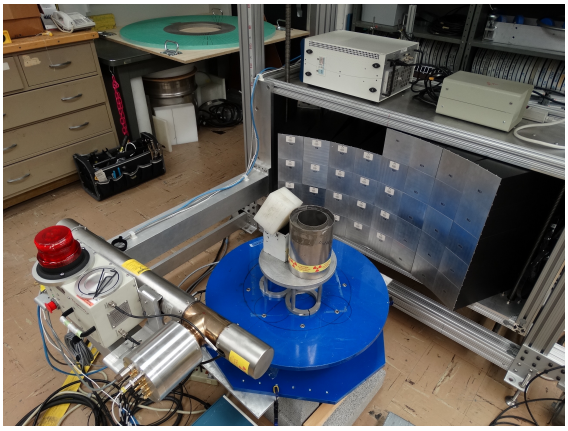

(a) Top-down

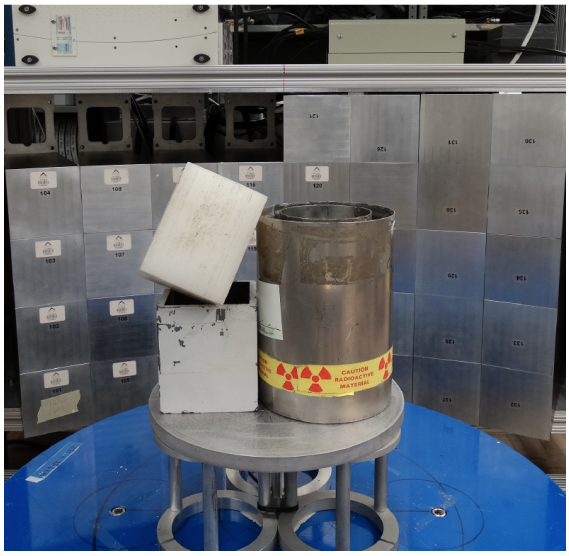

(b) D-T generator point of view

Figure 5.4: Views of the APNIS experiment

While the D-T generator emits 14.1 MeV neutrons isotropically, the alpha detectors only cover a limited solid angle which defines the directional profile of the D-T neutrons incident upon an interrogation object.

While the APNIS typically rotates the interrogation assembly using 36 angular projections, data from a single projection were used in this work. This orientation is shown in fig. 5.4b from the view of the neutron generator. Because the measurement data were to be used to evaluate relatively simplistic point kinetics models, this projection was chosen to minimize the amount of moderation of D-T and induced fission neutrons. The data include detected transmitted source neutron singles, fission chain singles, and fission chain

doubles normalized by the number of associated alpha particle detections for 80 pixels along the direction of the detector arc and 50 pixels in the vertical (floor to ceiling) direction. Dr. Matthew Blackston, who is part of the NMDC at ORNL, provided the data. In order to estimate emitted fission chain singles and doubles from these data, a significant amount of data processing and efficiency estimation and correction was applied. This began with determining the pixels that define the DU casting using the transmission, singles, and doubles projections. This was accomplished by simply plotting the data and estimating the bounding box by eye. Figure 5.5 shows the measured data with the bounding box superimposed. This

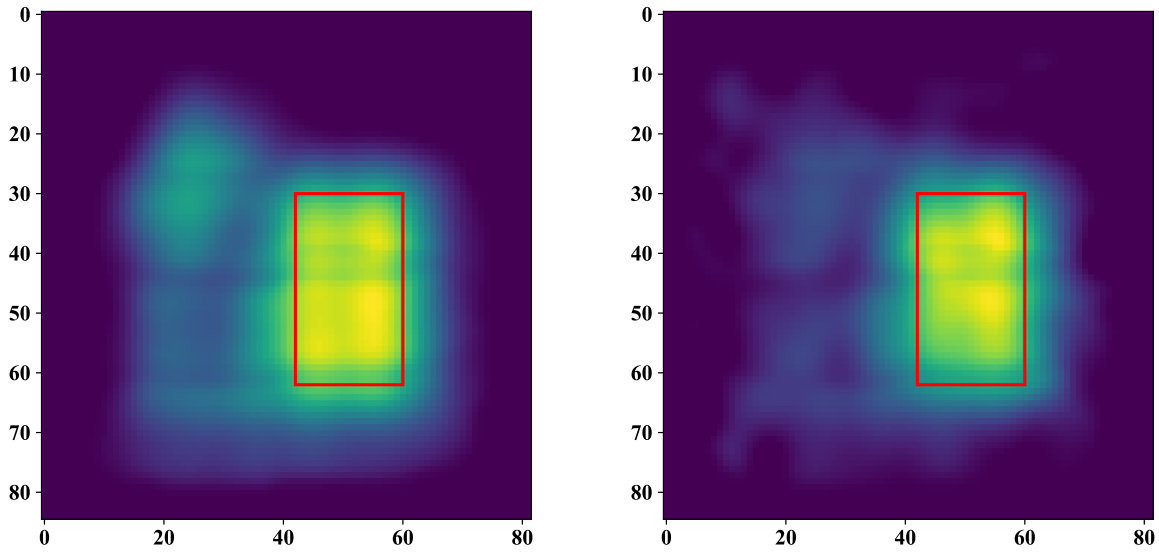

(a) Singles **(b)** Doubles

Figure 5.5: APNIS projection images

bounding box was used to estimate an average value of measured doubles per single $\frac{D_m}{S_m}$ for this subset of pixels by simply dividing the doubles data by the singles data and taking an average value for the pixels within the bounding box.

In order to get an estimate for the emitted fission chain doubles per single (referred to as simply "emitted doubles per single" for brevity) from measured doubles per single, corrections for both geometric and intrinsic efficiency must be applied. There are two components to intrinsic efficiency for detecting singles and doubles associated with an alpha detection within a fission window—the energy-dependent detection probability of a neutron inside the detector and the efficiency loss due to true fission neutron singles and doubles that

are detected outside of the finite fission window. In the APNIS measurement, the fission window is set to 25–45 nanoseconds relative to an alpha detection in the API D-T neutron generator.

Both of these components of intrinsic detection efficiency, as well as the geometric detection efficiency, are estimated using a Monte Carlo simulation in MCNPX-PoliMi. The simulation models the basic detector geometry but omits room geometries such as electronics boxes, stands, and room walls. The DU casting is modeled as containing only ^{235}U and ^{238}U and the steel box and polyethylene cube are omitted from the simulation geometry. Dr. Matthew Blackston provided data from a "flood measurement", which measures detections of source neutrons from the D-T generator without an interrogation object present. This allowed the directional profile of the D-T source to be generated for use in the Monte Carlo simulation. Custom parsing scripts tally the following attributes:

- $S_{emitted}$: The total number of fission chain neutrons emitted from the casting
- $D_{emitted}$: The total number of fission chain neutron doubles emitted from the casting
- $S_{incident}$: The total number of emitted fission chain neutrons emitted from the DU casting that are incident on the block detectors and able be detected. The criteria for "able to be detected by the block detectors" is if the neutron crosses half of the active volume of the block detector.
- $D_{incident}$: The total number of emitted fission chain neutron doubles emitted from the DU casting that are incident on the block detectors and able be detected
- $S_{detected}$: The total of all incident fission chain neutrons weighted by their energy-dependent intrinsic detection probability. These weights are determined by calibration data for neutron detection probability versus energy for the block detectors provided by Dr. Matthew Blackston.
- $D_{detected}$: The total of all incident fission chain neutron doubles weighted by their energy-dependent intrinsic detection probabilities

- $S_{FW detected}$: The total of all incident fission chain neutrons weighted by their energy-dependent intrinsic detection probability that are detected within the fission chain window

- $D_{FW detected}$: The total of all incident fission chain neutron doubles weighted by their energy-dependent intrinsic detection probability that are detected within the fission chain window

The geometric detection efficiency ε_g is estimated using eq. (5.7):

$$\varepsilon_g = \frac{S_{incident}}{S_{emitted}}. \tag{5.7}$$

Intrinsic efficiency is different for singles ε_{iS} and doubles ε_{iD}. They are estimated using eqs. (5.8) and (5.9):

$$\varepsilon_{iS} = \frac{S_{FW detected}}{S_{emitted}}, \tag{5.8}$$

$$\varepsilon_{iD} = \frac{D_{FW detected}}{D_{emitted}}. \tag{5.9}$$

If these efficiencies are known, the emitted doubles per single $\frac{\Phi_2}{\Phi_{1,f}}$ for the APNIS measurement can be estimated using eq. (5.10):

$$\frac{\Phi_2}{\Phi_{1,f}} = \frac{D_m \varepsilon_{iS}}{S_m \varepsilon_g \varepsilon_{iD}}. \tag{5.10}$$

The Monte Carlo simulation produced the following estimates for the efficiencies: $\varepsilon_g = 0.1027$, $\varepsilon_{iS} = 0.0422$, and $\varepsilon_{iD} = 0.0021$. According to the Monte Carlo simulation data, using the finite time window of 25–45 nanoseconds to identify neutrons from fission chains results in omitting approximately 16.4 percent of emitted fission chain singles and approximately 28.7 percent of emitted fission chain doubles.

Figure 5.6 shows the time distribution for detection of true fission neutrons from the Monte Carlo simulation. The red hatched area denotes those emitted fission chain neutrons that are detected within the 25–45 nanosecond "fission neutron" window. This gives a visual sense of the efficiency loss due to this finite time window.

The simulated energy distribution of fission neutrons incident on the detector differs significantly from a Watt spectrum that would be expected for fission neutrons. This is a result of downscattering by fission neutrons as they interact in the casting after being produced by an induced fission. This resulted in a significant amount of fission neutrons entering the detector below the detection energy threshold of approximately 2 MeV, which reduced detection efficiency. This can be seen in fig. 5.7, which shows a normalized histogram of neutron energy for neutrons incident on the block detectors superimposed on a few ^{238}U-induced-fission Watt-spectra probability density functions. These Watt spectra vary in the incident energy of the neutron inducing fission but are relatively similar. The ground truth energy distribution of fission neutrons inside the DU casting should be somewhere in between the Watt spectra. The calibrated detection probabilities versus energy as supplied by Dr. Matthew Blackston are plotted on the right axis in red.

In later APNIS post-processing, a downscatter correction is typically applied, but it was not applied to the data used in this research. This correction is approximate, complex, and relies on transmission reconstruction information [48]. Because it is not possible at the time of writing to apply this correction to the data used in this research, an alternate method of applying a downscatter correction is described below. This results in an additional set of intrinsic efficiencies that can be used to correct the measured data. This downscatter correction method is a modification on the Monte Carlo process for estimating intrinsic efficiencies described in the bulleted list above. When the detection probability contribution weight of a fission chain neutron is calculated (using the calibrated detection probability curve shown in red in fig. 5.7), the actual energy of the simulated neutron is not used, but is instead sampled from a Watt spectrum. Because the Watt spectra for induced fission vary depending on the energy of the incident neutron, which Watt spectrum is used is also sampled [49, 50]. Based on previous Monte Carlo simulations of the APNIS experiment, 72.6 percent of induced fissions are induced by source neutrons with an average energy of

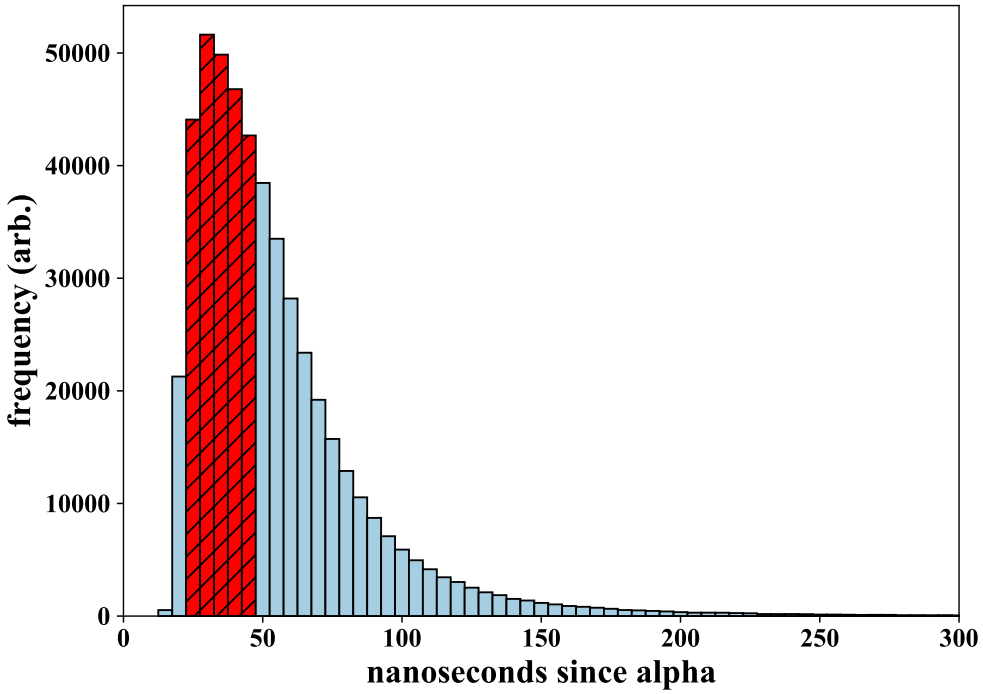

Figure 5.6: Time distribution of detected fission neutrons in APNIS Monte Carlo simulation

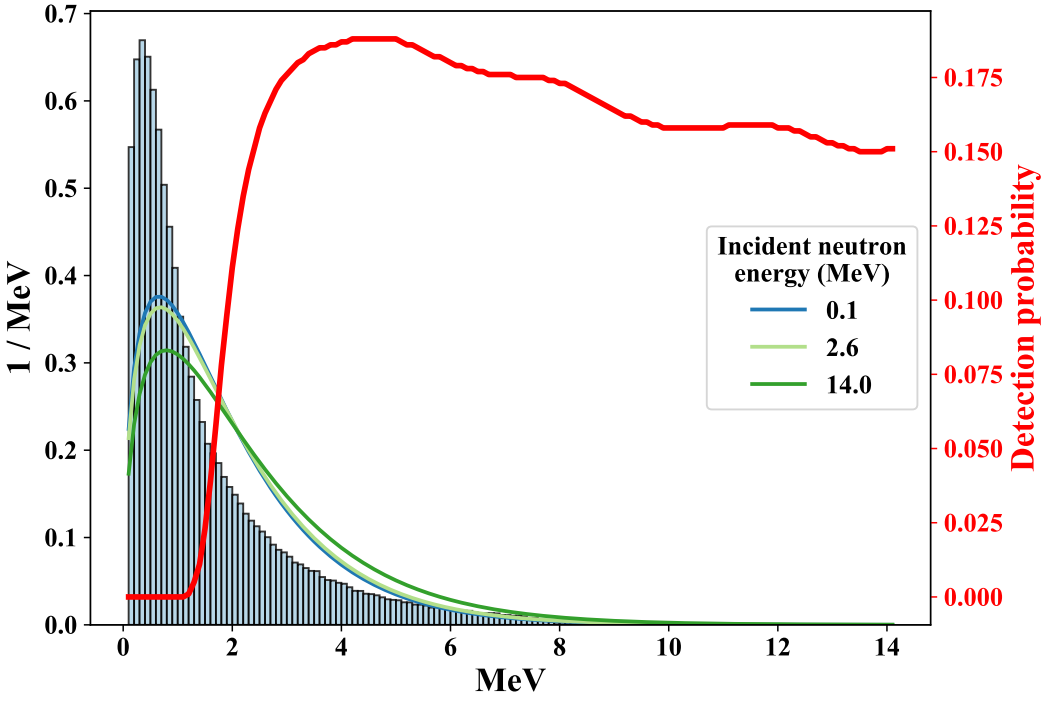

Figure 5.7: Distribution of incident neutron energies versus Watt spectra and detection probability for APNIS Monte Carlo simulations

14.0 MeV, and 27.4 percent are induced by other fission neutrons with an average energy of 2.6 MeV. Watt spectra are calculated based on the induced fission energy for ^{238}U using methods developed for the TART software package described by Cullen in [50]. Using a Watt-sampled energy affects each incident fission neutron's tallied detection contribution to $S_{detected}$ and $D_{detected}$. Because only the energy and not the detection time of the incident fission neutron is corrected, intrinsic efficiencies are estimated assuming no time windowing, and then a time-windowing correction factor is applied afterwards. These correction factors are the fraction of detected fission neutron singles and doubles that are not counted due to the timing window. They are calculated based on the results of the original Monte Carlo simulation. Equations (5.11) and (5.12) are used to estimate the intrinsic efficiencies:

$$\varepsilon_{iS} = 0.837 \, \frac{S_{detected}}{S_{incident}}, \tag{5.11}$$

$$\varepsilon_{iD} = 0.713 \, \frac{D_{detected}}{D_{incident}}. \tag{5.12}$$

Using this downscatter-corrected method, $\varepsilon_{iS} = 0.0716$ and $\varepsilon_{iD} = 0.0052$, which are approximately 71 percent and 132 percent larger than the intrinsic efficiencies estimated without the downscatter corrections.

Uncertainty on the estimate for emitted doubles per single $\sigma_{\Phi 21}$ can be calculated by straightforward propagation of uncertainty of the parameters in eq. (5.10):

$$\sigma_{\Phi 21} = \left| \frac{D_m \varepsilon_{iS}}{S_m \varepsilon_g \varepsilon_{iD}} \right| \sqrt{\left(\frac{\sigma_{DSm}}{\frac{D_m}{S_m}} \right)^2 + \left(\frac{\sigma_{\varepsilon iS}}{\varepsilon_{iS}} \right)^2 + \left(\frac{\sigma_{\varepsilon iD}}{\varepsilon_{iD}} \right)^2 + \left(\frac{\sigma_{\varepsilon g}}{\varepsilon_g} \right)^2}, \tag{5.13}$$

where σ_{DSm} is the uncertainty in the measured doubles per single $\frac{D_m}{S_m}$, $\sigma_{\varepsilon iS}$ is the uncertainty in ε_{iS}, $\sigma_{\varepsilon iD}$ is the uncertainty in ε_{iD}, and $\sigma_{\varepsilon g}$ is the uncertainty in ε_g. The measurement data provided did not include values for uncertainty in the measured doubles or singles. According to Dr. Matthew Blackston, a method for calculating these uncertainties has not been implemented in the APNIS software at the time of this writing [48]. As an alternative, σ_{DSm} can be approximated as the standard deviation of the distribution of measured doubles per single values that are within the pixel boundaries that define the DU casting. When the boundaries shown in fig. 5.5 are used, the relative uncertainty in measured doubles per

single is approximately 20.9 percent. However, the relative uncertainty is highly dependent upon where the boundaries that define the DU casting are drawn. The boundaries shown in fig. 5.5 are 18x32 pixels. If, for example, the boundaries are changed to 27x40 pixels, as shown in fig. 5.8, the relative uncertainty in measured doubles per single increases to approximately 49.1 percent.

While statistical uncertainties for the Monte Carlo estimates of the intrinsic and geometric detection efficiencies can be calculated, there are sources of systematic uncertainty in these estimates that also need to be accounted for. These come from simplifying assumptions made in the Monte Carlo simulation such as omitting room geometry and approximating the neutron detection process within the block detectors. Because of this, a range of total uncertainties on the detection efficiency parameters are examined. Various assumptions about uncertainty in measured doubles per single and uncertainty in the detection efficiencies were used in eq. (5.13) to estimate the relative uncertainty in the emitted doubles per single. The results are shown in table 5.1.

These results show that the uncertainty in the measured doubles per single drives the uncertainty in the emitted doubles per single. However, the uncertainty in the efficiency terms does play a role. Going from 0 to 10 percent relative uncertainty for the efficiencies only increased the relative uncertainty in emitted doubles per single by approximately 6 percent. The method of estimating the uncertainty in measured doubles per single is rather simplistic, but it offers a decent approximation until more sophisticated methods are developed. One weakness of this method of approximating σ_{DSm} is that the choice of the bounding box parameters, which determine what measurement pixels define the casting, plays arguably the largest role in determining the relative uncertainty of the measured doubles per single and consequently the emitted doubles per single. If Monte Carlo simulations are not used to estimate values for geometric and intrinsic detection efficiencies, there may be significant sources of systematic uncertainty such as downscattering effects, self-shielding effects, and finite time windowing. Accounting for these can further increase the relative uncertainty in emitted doubles per single.

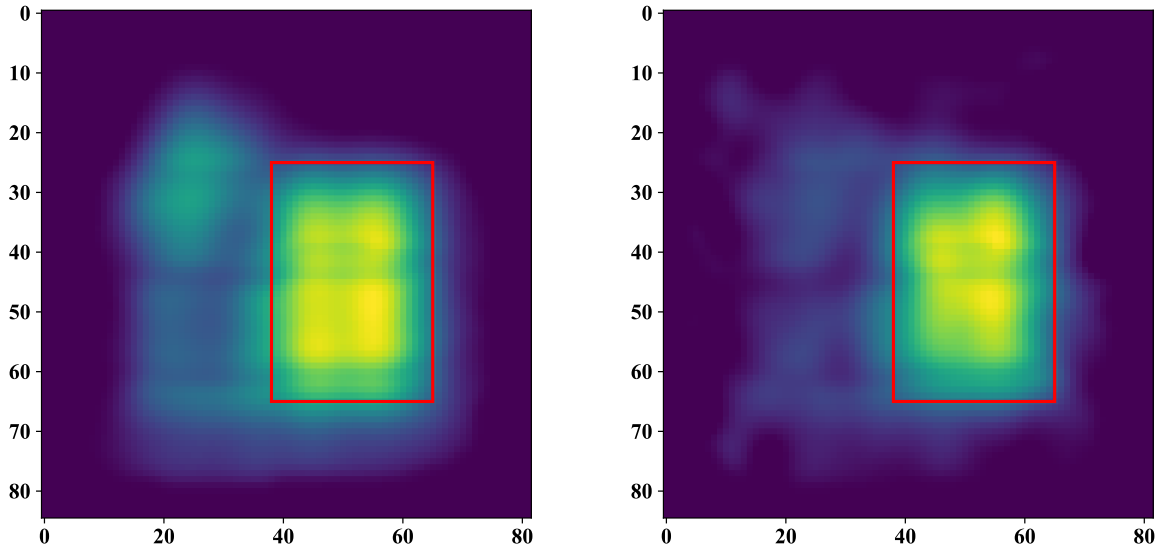

(a) Singles **(b)** Doubles

Figure 5.8: APNIS projection images with an alternative bounding box

Table 5.1: Relative uncertainty in emitted doubles per single for APNIS measurements

$\frac{\sigma_{DSm}}{D_m/S_m}$	$\frac{\sigma_{\varepsilon iS}}{\varepsilon_{iS}}, \frac{\sigma_{\varepsilon iD}}{\varepsilon_{iD}}, \frac{\sigma_{\varepsilon g}}{\varepsilon_g}$	$\frac{\sigma_{\Phi 21}}{\Phi_2/\Phi_{1,f}}$
20.9%	0.0%	20.9%
20.9%	1.0%	21.0%
20.9%	10.0%	27.1%
20.9%	20.0%	40.4%
0.0%	10.0%	17.3%

Chapter 6

Coupling-based Methods

6.1 DT-f method

The DT-f method assumes that the source neutron's only chain-starting interaction is induced fission on either ^{235}U or ^{238}U. Soleilhac, Frehaut and Gauriau measured the multiplicity distributions of induced fission of ^{235}U and ^{238}U by neutrons in the 14 MeV range and found the average multiplicities for the two isotopes to be within less than 1 percent of each other [51]. Thus, it can be assumed that the chain-starting multiplicity terms ν_{s1} and ν_{s2} in the point kinetics equations are constant and independent of enrichment.

By making this assumption, all of the enrichment dependence in the emitted fission chain singles and doubles will be contained in the multiplication term and the source-object coupling. Section 6.1.1 describes how multiplication can be calculated from the emitted fission chain singles and doubles, and section 6.1.2 describes how enrichment can be estimated from either the emitted fission chain singles or doubles after having calculated a value for multiplication. While making this assumption simplifies the enrichment and multiplication

estimation process, it also introduces a source of systematic bias by ignoring the effect of (n,xn) interactions on chain-starting multiplicity. The consequences of this assumption are addressed in further detail in section 6.1.5.

The chain-starting multiplicity distribution, and consequently the ν_{sn} values, for 14.1 MeV induced fission on ^{235}U or ^{238}U is estimated using the Terrell method [52], with the $\bar{\nu}$ taken from ENDF/B-VII.1 [2]. Values for the induced multiplicity terms ν_{in} are calculated from the multiplicity distribution for 2 MeV induced fission on ^{235}U measured by Zucker and Holden [42]. Induced neutron interactions occur at fission neutron energies. At these energies, the multiplicity distribution is largely insensitive to uranium enrichment.

6.1.1 Estimating Multiplication

Taking the ratio of eqs. (3.3) and (3.5), referred to as the emitted fission chain doubles per single ratio, or more simply the emitted doubles per single, the dependence on the source coupling parameter β drops out:

$$\frac{\Phi_2}{\Phi_{1,f}} = \left(M_T - \frac{M_T - 1}{\nu_{i1}}\right) \frac{\nu_{s2} + \nu_{i2}\nu_{s1}\left(\frac{M_T - 1}{\nu_{i1}}\right)}{\nu_{s1}}. \tag{6.1}$$

Using a measured value for the doubles per singles ratio, the resulting second-order polynomial can be solved to estimate M_T:

$$\frac{\Phi_2}{\Phi_{1,f}} = a + bM_T + cM_T^2, \tag{6.2}$$

$$M_T = \frac{-b \pm \sqrt{b^2 - 4c(a - \frac{\Phi_2}{\Phi_{1,f}})}}{2c}, \tag{6.3}$$

where

$$a = \frac{\nu_{i1}\nu_{s2} - \nu_{i2}\nu_{s1}}{\nu_{i1}^2\nu_{s1}},$$

$$b = \frac{\nu_{i1}\nu_{s2}\left(\nu_{i1} - 1\right) - \nu_{i2}\nu_{s1}\left(\nu_{i1} - 2\right)}{\nu_{i1}^2\nu_{s1}},$$

$$c = \frac{\nu_{i2}\left(\nu_{i1} - 1\right)}{\nu_{i1}^2}.$$

When $\Phi_{1,f}$ and Φ_2 are estimated from a Monte Carlo simulation, there is a statistical uncertainty associated the with the estimated value, denoted as σ_1 and σ_2, respectively. These uncertainties are propagated when solving for total multiplication in eq. (6.3). Because it cannot be assumed that σ_1 and σ_2 are uncorrelated, the propagated uncertainty in the ultimate estimate of M_T, σ_M, can be conservatively written as

$$\sigma_M \leq \left|\frac{\delta M_T}{\delta \Phi_{1,f}}\right| \sigma_1 + \left|\frac{\delta M_T}{\delta \Phi_2}\right| \sigma_2. \tag{6.4}$$

The differential terms in eq. (6.4) are found by taking partial derivatives of eq. (6.3):

$$\frac{\delta M_T}{\delta \Phi_{1,f}} = \frac{-\Phi_2}{\Phi_{1,f}^2\sqrt{b^2 - 4c(a - \frac{\Phi_2}{\Phi_{1,f}})}}, \tag{6.5}$$

$$\frac{\delta M_T}{\delta \Phi_2} = \frac{1}{\Phi_{1,f}\sqrt{b^2 - 4c(a - \frac{\Phi_2}{\Phi_{1,f}})}}. \tag{6.6}$$

6.1.2 Estimating Enrichment

For a bare uranium object assumed to contain only ^{235}U and ^{238}U in the DT-f framework, the source coupling β can be expressed using the physics of neutron transmission, source neutron path length through uranium x, and nuclear cross sections:

$$\beta = I\frac{\Sigma_f}{\Sigma_R}\left(1 - e^{-\Sigma_R x}\right), \tag{6.7}$$

where I is the fraction of emitted source neutrons that are incident upon the interrogation object. Using calibration measurements to determine the directional distribution of the D-T neutron source and transmission imaging, I can theoretically be calculated for TNI measurements. The quantity Σ_f is the macroscopic nuclear cross section for induced fission in uranium and Σ_R is the removal cross section and includes all interactions that remove the source neutron from the fission chain. This includes induced fission, (n,xn) interactions, and (n,γ) capture. The macroscopic cross sections can be expressed in terms of ^{235}U weight fraction f_5:

$$\Sigma_i = \frac{N_A \rho}{A_U}\Big(\sigma_{i,5} f_5 + \sigma_{i,8}(1 - f_5)\Big), \tag{6.8}$$

where ρ is uranium metal mass density (assumed to be constant for both uranium isotopes), N_A is Avogadros number, and A_U is the average of ^{235}U and ^{238}U atomic masses. The subscripts 5 and 8 on the σ_i terms denote the microscopic cross section for a 14.1 MeV neutron undergoing interaction i on ^{235}U or ^{238}U, respectively. Because the direction of the interrogation source relative to the imaged object is known, the average path length of the interrogation source through uranium can be estimated. It then follows that if the model parameter β can be estimated by inverting the point kinetics model equations, the enrichment of a bare uranium sample can be estimated.

The definition of the source coupling β given above in eq. (6.7) assumes that all chain-starting interactions are induced fissions by 14.1 MeV neutron on ^{235}U or ^{238}U, which is an assumption made in the DT-f method. While the appropriateness and the effects of this assumption are addressed in section 6.1.5, it is important to note that eq. (6.7) can be modified depending on what types of reactions are considered chain-starting reactions. For example, if all removal interactions [induced fission, (n,xn), and (n,γ) capture] are considered chain-starting interactions,

$$\beta = I\left(1 - e^{-\Sigma_R x}\right). \tag{6.9}$$

The advantage in assuming that only induced fissions initiate fission chains is that the ν_{sn} values in the point kinetics equations will not be enrichment dependent and, aside from the multiplication term which is solved for, all the enrichment dependence will be concentrated

in the source coupling term β. This allows for the straightforward method of enrichment estimation that has been described above.

6.1.3 Results Using Monte Carlo Data

The methods for estimating neutron multiplication and uranium enrichment using the DT-f framework were evaluated using Monte Carlo simulations described in section 4.2. The Monte Carlo estimates for the emitted fission chain singles and doubles were used to estimate M_T using eq. (6.3). These M_T estimates were compared to Monte Carlo simulation estimates of M_T. Two methods of determining the source multiplicity values ν_{s1} and ν_{s2} were considered:

1. "Unknown Isotopics" case: This is the standard assumption made in the DT-f method. Isotopic information is not known a priori and the effect of (n,2n) and (n,3n) on chain-starting multiplicity is ignored. Values for ν_{s1} and ν_{s2} are determined from the multiplicity distribution of 14.1 MeV induced fission on ^{235}U or ^{238}U. Source coupling β is defined to include only 14.1 MeV induced fission as in eq. (6.7).

2. "Known Isotopics" case: Isotopic information is known a priori, allowing ν_{s1} and ν_{s2} parameters to be calculated based on eq. (6.10). Source coupling β is defined to include all removal interactions as in eq. (6.9).

The "Unknown Isotopics" case would apply to a typical enrichment assay situation where one may not know or want to assume the enrichment of a uranium sample. The "Known Isotopics" case is included to evaluate the effect of assuming that all chain-starting interactions are source-neutron-induced fission of ^{235}U or ^{238}U. The results for total multiplication are shown in fig. 6.1.

For the "Known Isotopics" case, a priori isotopic information about a sample is necessary to calculate ν_{s1} and ν_{s2}. If the chain-starting event is defined to include 14.1 MeV induced fission, (n,2n), and (n,3n) interactions, they can be calculated with the following equations:

$$\nu_{sn} = \sum_{\nu=0}^{N_{ind}} \frac{\nu!}{n!(\nu-n)!} \left(\frac{\Sigma_f P_\nu + \Sigma_\gamma \delta_{\nu 0} + \Sigma_{2n} \delta_{\nu 2} + \Sigma_{3n} \delta_{\nu 3}}{\Sigma_f + \Sigma_\gamma + \Sigma_{2n} + \Sigma_{3n}} \right), \tag{6.10}$$

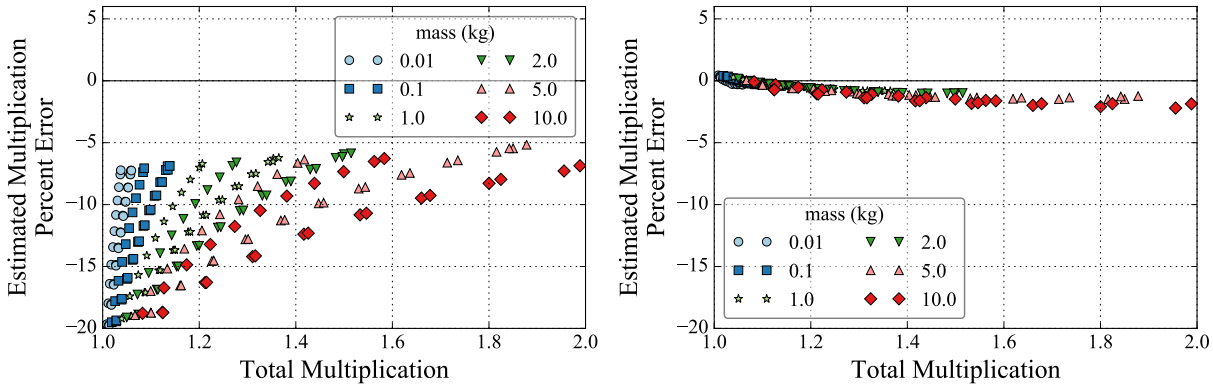

(a) Unknown Isotopics

(b) Known Isotopics

Figure 6.1: Percent error between the total neutron multiplication as calculated by Monte Carlo and estimated from Monte Carlo-simulated emitted fission chain singles and doubles for the two DT-f cases

$$\Sigma_i = N_A \rho \sum_A \frac{f_A \sigma_i^A}{A}, \tag{6.11}$$

where N_{ind} is the highest value of neutron multiplicity ν observed, Σ_i is the macroscopic cross section for a source neutron undergoing interaction i, and P_ν is the probability that a source-neutron-induced fission has multiplicity ν. The parameter f_A is the fraction of isotope A in the uranium, while σ_i^A is the microscopic cross section for a source neutron undergoing interaction i on isotope A. The mass density is represented by ρ and N_A is Avogadro's number. Note that eq. (6.11) is a more general version of eq. (6.8).

Using the DT-f method to estimate enrichment is difficult because β is not sensitive enough to enrichment to accurately differentiate between enrichments. The amount of sensitivity depends on what assumption is made about the chain-starting interactions. The sensitivity of β values to enrichment is shown in fig. 6.2 for both the "Unknown Isotopics" and "Known Isotopics" cases. Results for β and enrichment estimation are shown in fig. 6.3 and fig. 6.4, respectively. It is important to note that β is defined differently depending on the case i.e. what assumptions are used about the chain-starting interactions.

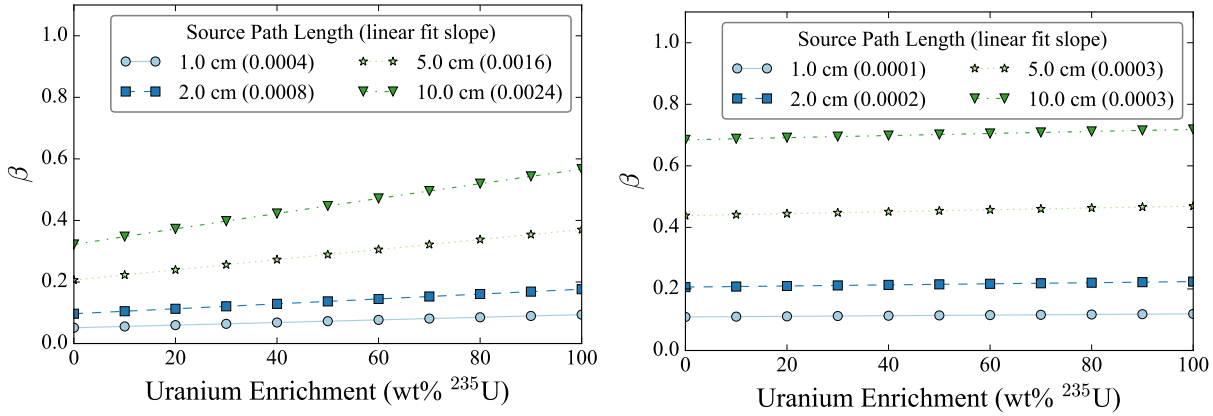

(a) Unknown Isotopics
$\beta = I \frac{\Sigma_f}{\Sigma_R} \left(1 - e^{-\Sigma_R x}\right)$

(b) Known Isotopics
$\beta = I \left(1 - e^{-\Sigma_R x}\right)$

Figure 6.2: Sensitivity of source neutron coupling to uranium enrichment for the two DT-f cases

If all removal interactions are considered chain-starting interactions (the "Known Isotopics" case), β sensitivity to enrichment is nearly nonexistent. This is due to the fact

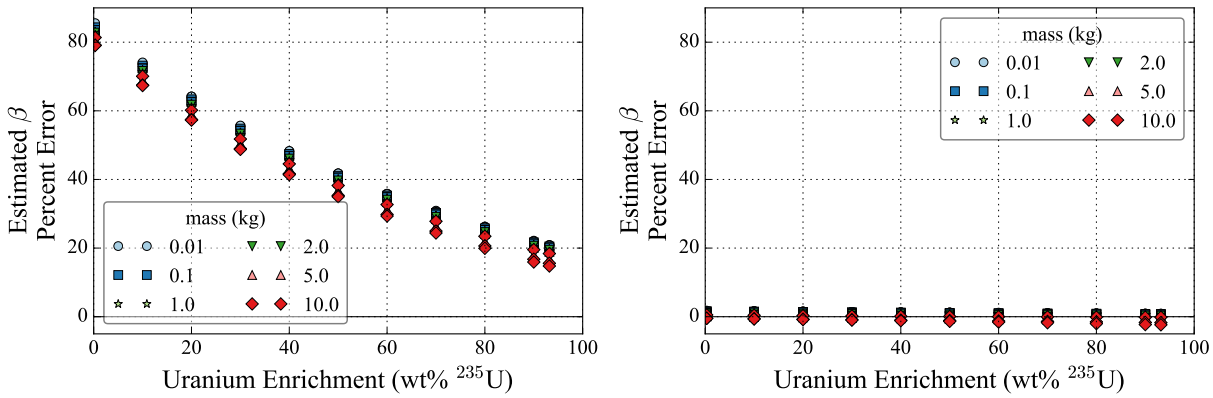

(a) Unknown Isotopics **(b)** Known Isotopics

Figure 6.3: Percent error between the source neutron coupling as calculated by Monte Carlo and estimated from Monte Carlo-simulated emitted fission chain singles and doubles for the two DT-f cases

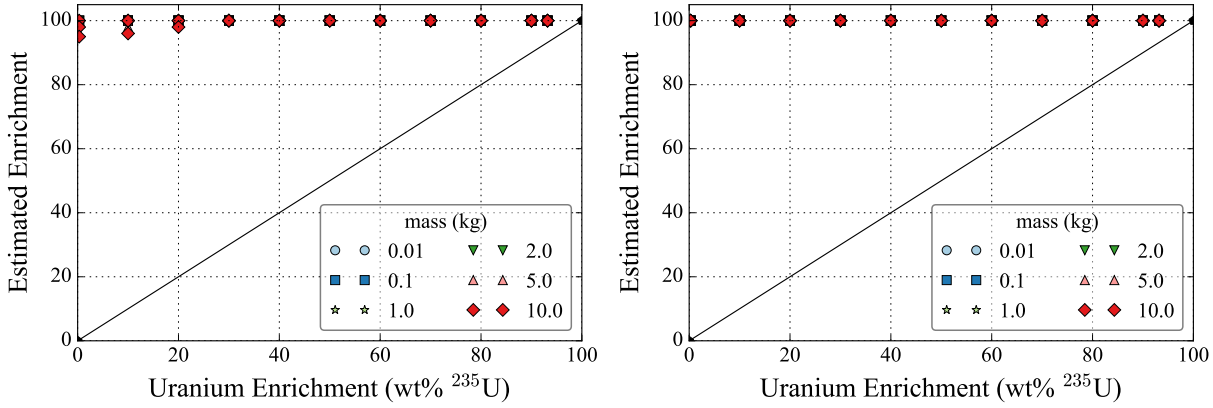

(a) Unknown Isotopics **(b)** Known Isotopics

Figure 6.4: Enrichment estimation of Monte Carlo simulations for the two DT-f cases

that the microscopic (and macroscopic) removal cross sections for ^{235}U or ^{238}U are very similar—2.636 and 2.431 barns, respectively [2]. Values for β can be estimated to within at least 4 percent of their simulated value, but even this small underestimation results in drastic overestimation of enrichment. If it is assumed that only induced fissions initiate fission chains (the "Unknown Isotopics" case), there is slightly improved sensitivity due to the greater difference between 14.1 MeV induced fission microscopic cross sections for ^{235}U and ^{238}U—2.080 and 1.143 barns, respectively [2]. However, The systematic bias associated with ignoring the effect of (n,2n) and (n,3n) interactions on chain-starting multiplicity will bias multiplication estimates (see section 6.1.5) such that estimated β value will always correspond to an enrichment greater than 100 percent.

Figure 6.2 also shows that both definitions of the source coupling β are sensitive to knowing the correct average source neutron path length x. While Monte Carlo estimates for the average neutron path length were used in the above analyses, this parameter would have to be estimated based on geometric and imaging information for a real-life TNI measurement. Future work that investigates the effect that inelastic scatter of source neutrons may have on the uncertainty in average path length could be useful.

6.1.4 Results Using Experimental Data

Using the data from the NMIS measurements of the DU and HEU annular castings described in section 5.1, the emitted fission chain singles and doubles rates of the central pixel measurement were used in eq. (6.3) to estimate M_T for both castings. The uncertainty in the M_T estimate is calculated using eq. (6.4), which propagates the uncertainties of the emitted fission chain singles and doubles rates. A more complete discussion of this error propagation is included in section 6.1.1. The M_T estimates were compared to Monte Carlo simulation estimates of M_T. The results are shown in table 6.1.

Absent all other sources of systematic error, the "Known Isotopics" case, which accounts for the effect of (n,2n) and (n,3n) interactions on the chain-starting multiplicity moments ν_{s1} and ν_{s2}, should provide a M_T estimate closer to the Monte Carlo estimate. This is not the case for the NMIS experiments. The "Unknown Isotopics" case calculated M_T closer to the Monte Carlo estimate than the "Known Isotopics" case. This likely illustrates that

Table 6.1: Total multiplication calculations of uranium casting NMIS measurements © 2017 IEEE

	HEU	DU
MCNPX[1]	1.719	1.094
Known Isotopics	1.812 ± 0.360	1.353 ± 0.271
Unknown Isotopics	1.738 ± 0.360	1.151 ± 0.272

[1] Statistical uncertainties (one standard deviation of the Monte Carlo estimated mean) are less than 0.1 percent.

the systematic error due to estimating emitted fission chain singles and doubles rates from measured singles and doubles rates eclipses the systematic error introduced by assuming that all chain-starting events are 14.1 MeV induced fission on ^{235}U or ^{238}U. However, both cases estimated M_T to within 1σ of the Monte Carlo estimate due to the relatively large measurement uncertainties. This uncertainty is likely driven by the systematic uncertainty of the total detection efficiency for neutrons born inside the interrogated object, which was conservatively estimated to be 10 percent of the value estimated by a ^{252}Cf calibration measurement [5]. Assuming a single detection efficiency is a well-known source of systematic bias in the point kinetics model due to the distribution of energies and locations at which neutrons are born within the sample [31].

The large measurement uncertainty is also evident in the enrichment estimates. As shown in table 6.2, the range of enrichment estimates is so large for all cases that they are not useful. This is a consequence of both the large uncertainty in estimating the emitted fission chain singles and doubles from measured values as well as the fact that the source coupling β is much too sensitive to enrichment, as is shown in fig. 6.2.

Table 6.2: Enrichment estimation ranges of uranium casting NMIS measurements

Enrichment	HEU	DU
True	93%	0.3%
Known Isotopics	0–100%	0–100%
Unknown Isotopics	0–81%	0–62%

6.1.5 Systematic Error Analysis

Using a D-T generator as an external neutron source inserts more systematic bias into the point kinetics equations than using a lower energy source, such an AmLi source in the AWCC [8]. The AmLi source produces neutrons with an average energy of 0.3 MeV, with nearly all source neutrons below the energy region where ^{238}U, the most abundant isotope in most uranium samples, has a significant induced fission cross section [2]. Most of the AmLi neutrons are also below the (n,xn) interaction threshold for both ^{238}U and ^{235}U (approximately 6 and 5 MeV, respectively [2]). These cross sections are shown in fig. 6.5.

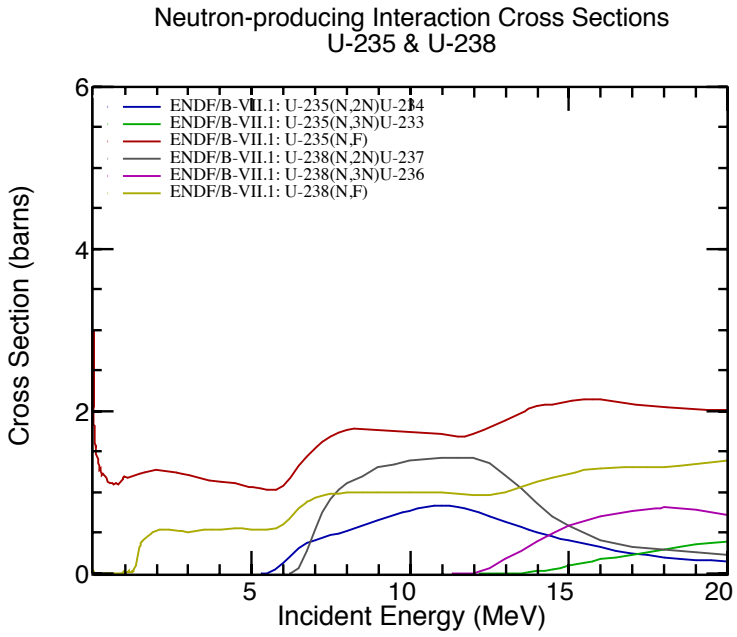

Figure 6.5: Cross section for neutron-producing interactions for ^{235}U and ^{238}U. Plot generated using ENDF/B-VII.1 data [2].

At 14.1 MeV, there are not only contributions from source-neutron-induced fission on ^{238}U, but also from (n,xn) interactions on both ^{235}U and ^{238}U. As shown in table 6.3, the cross sections at 14.1 MeV for (n,2n) and (n,3n) interactions, which are indistinguishable from fission in TNI measurements, are significant compared to the fission cross sections, particularly for ^{238}U.

Table 6.3: Uranium microscopic cross sections for 14.1 MeV neutrons (barns) [2] © 2017 IEEE

	σ_f	σ_{2n}	σ_{3n}
^{235}U	2.080	0.522	0.033
^{238}U	1.143	0.881	0.406

While the nuclear cross sections suggest that the DT-f method assumption that neutron fission chains are only initiated by source neutrons inducing fission on ^{235}U or ^{238}U is not appropriate when using a 14.1 MeV D-T neutron generator as the interrogating source, Monte Carlo simulations were used to assess both the appropriateness and the consequences of the assumption for point kinetics. The results of the "Known Isotopics" case in section 6.1.3 already suggest that this assumption results in significant systematic biases in the estimation of total multiplication and enrichment. This analysis expands upon those results by evaluating the effect on emitted fission chain doubles. In order to prevent any potential systematic error due to the negligible capture assumption made in eq. (3.7), eq. (6.12) is used as the point kinetics equation for the emitted fission chain doubles:

$$\Phi_2 = \beta M_L^2 \left[\nu_{s2} + \nu_{i2}\nu_{s1} p_f M_T\right]. \tag{6.12}$$

The Monte Carlo estimate for doubles is compared to the doubles calculated using the following methods:

1. Doubles as calculated by eq. (6.12) using Monte Carlo-simulated values for M_L, p_f, M_T, ν_{s1}, and ν_{s2}. This serves as a sanity check to ensure the point kinetics model equation in eq. (6.12) faithfully represents the fission chain propagation process and

that the Monte Carlo output interpretation software is working correctly. The results are shown in fig. 6.6.

2. Doubles as calculated by eq. (6.12) using the Monte Carlo simulated value for M_L, p_f, and M_T. The point kinetics values for ν_{s1} and ν_{s2}, which assume a 14.1 MeV neutron inducing fission on ^{235}U or ^{238}U, are used. This quantifies the systematic error introduced by assuming the chain-starting interaction to be a 14.1 MeV neutron inducing fission on either ^{235}U or ^{238}U. Results are shown in fig. 6.7.

The systematic error resulting from assuming that all chain-starting interactions are 14.1 MeV neutron-induced fissions on ^{235}U or ^{238}U is largely a function of uranium enrichment but is insensitive to geometry. This is explained by the fact that ^{238}U has a much higher (n,2n) and (n,3n) cross section relative to its induced fission cross section for 14.1 MeV neutrons (see table 6.3). Even though their multiplicity is below the 14.1 MeV induced fission average of approximately 4.4 neutrons per fission, (n,2n) and (n,3n) events are interpreted as fissions in the DT-f method [51]. This results in emitted fission chain doubles being overestimated when the assumed ν_{s1} and ν_{s2} values, based only on induced fission, are used without taking into account (n,2n) and (n,3n) interactions.

This explanation is supported by Monte Carlo estimations of the multiplicity distribution of the chain-starting event. The neutron multiplicity of all chain-starting events, including (n,xn) and (n,γ) parasitic capture events as well as induced fission was tallied for all simulations and results are shown in fig. 6.8. The values ν_{s1} and ν_{s2} are independent of geometry and independent of uranium mass. It is important to note that these Monte Carlo estimates for ν_{s1} and ν_{s2} are within a few percent of values calculated by eq. (6.10) using a known enrichment, the Terrell estimate for the 14.1 MeV induced fission multiplicity distribution, and the 14.1 MeV cross sections from ENDF/B-VII.1 [2]. This explains why the estimates for total multiplication saw such a significant improvement when isotopic information was used to calculate ν_{s1} and ν_{s2}, as shown in fig. 6.1b in section 6.1.3.

This analysis demonstrates that the DT-f method assumption that all chain-starting interactions are 14.1 MeV induced fission on ^{235}U or ^{238}U results in a significant amount of systematic bias for bare uranium interrogated by 14.1 MeV neutrons. This systematic bias

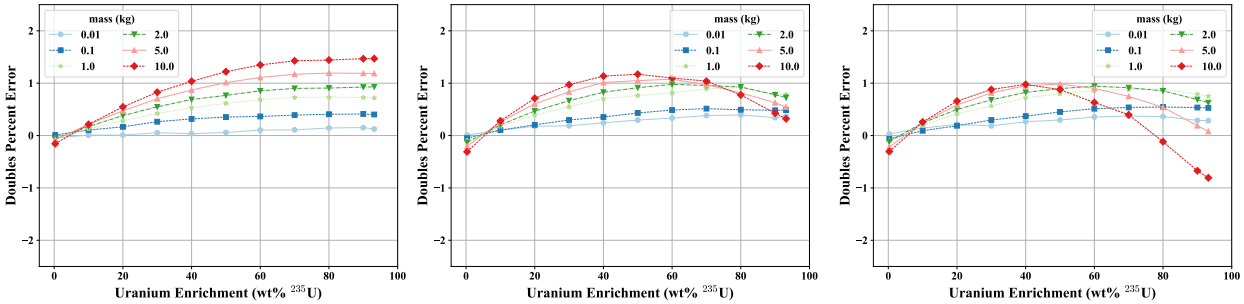

(a) Annular Casting **(b)** Cylinder **(c)** Sphere

Figure 6.6: Case 1 results. Percent error between fission chain doubles as calculated by Monte Carlo and doubles as calculated by eq. (6.12) using all Monte Carlo inputs.

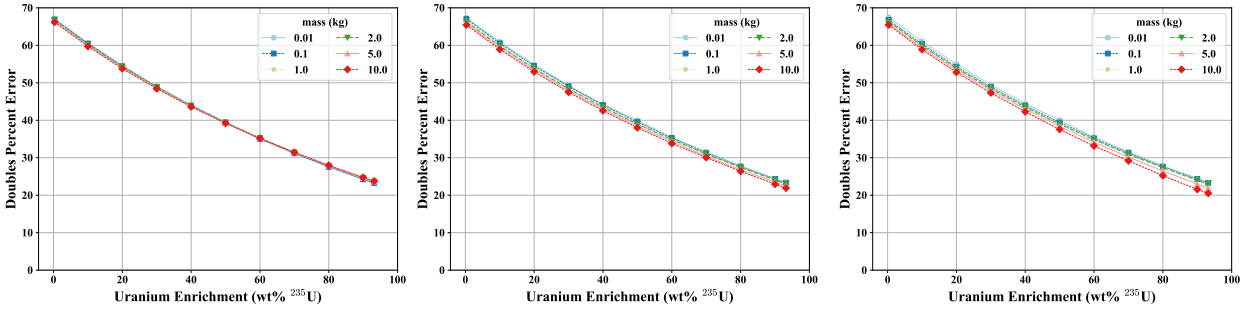

(a) Annular Casting **(b)** Cylinder **(c)** Sphere

Figure 6.7: Case 2 results. Percent error between fission chain doubles as calculated by Monte Carlo and doubles as calculated by eq. (6.12) assuming all chain-starting events are induced fissions. Note the scale difference on the y-axis compared to fig. 6.6.

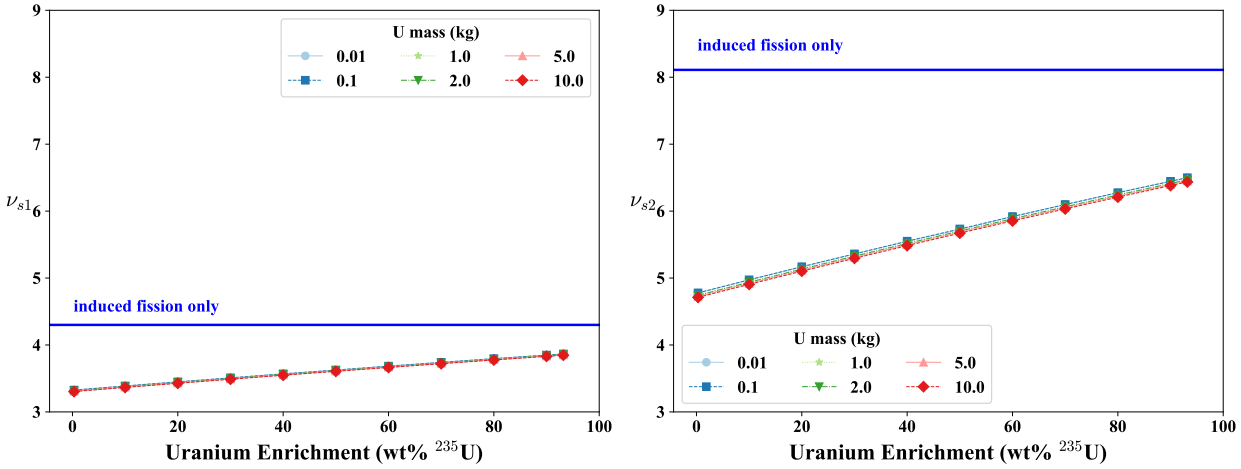

(a) First reduced-factorial moment

(b) Second reduced-factorial moment

Figure 6.8: Values for ν_{s1} (a) and ν_{s2} (b) as estimated by Monte Carlo simulations for 14.1 MeV neutrons incident on uranium. Average values for ν_{s1} and ν_{s2} where only induced fission is considered are shown in blue.

likely explains the systematic underestimation of total multiplication and enrichment by the "Unknown Isotopics" DT-f method. This suggests development of alternative frameworks that could better account for this manifestation of enrichment dependence such as the DT-f-n2n method, which is presented in the following section.

6.2 DT-f-n2n Method

An extension of the DT-f framework was motivated by the study in section 6.1.5 which demonstrated that not accounting for the effect of (n,2n) and (n,3n) interactions on chain-starting multiplicity can introduce a significant source of systematic error in point kinetics equations for TNI. While this can be corrected for by expanding the definition of the chain-starting interaction to include (n,2n) and (n,3n) interactions, this inserts an enrichment dependence into the chain-starting multiplicity terms and enrichment can no longer be estimated from the source coupling term alone. The DT-f-n2n point kinetics method introduces an additional source coupling term. Instead of using a single source coupling β to represent the probability of any chain-starting interaction, the coupling is broken up between (n,2n) interactions and all other interactions, namely induced fission, (n,3n), and (n,γ) capture. The β_{2n} term represents the probability that an incident 14.1 MeV neutron induces an (n,2n) interaction, while β represents the probability that an incident 14.1 MeV neutron induces a different chain-starting interaction. Because the emitted fission chain doubles rate was shown to be insensitive to parasitic neutron capture in section 3.1.1, the emitted fission chain singles, doubles and triples rate equations are formulated in terms of leakage multiplication M_L instead of total multiplication M_T. The point kinetics equations are

$$\Phi_1 = (1 - \beta_{2n} - \beta) + M_L(2\beta_{2n} + \nu_{s1}\beta), \tag{6.13}$$

$$\Phi_2 = M_L^2 \left[\beta_{2n} \left(1 + 2\nu_{i2} \left(\frac{M_L - 1}{\nu_{i1} - 1} \right) \right) + \beta \left(\nu_{s2} + \nu_{s1}\nu_{i2} \left(\frac{M_L - 1}{\nu_{i1} - 1} \right) \right) \right], \tag{6.14}$$

$$\begin{aligned} \Phi_3 = M_L^3 \Bigg[& \beta_{2n} \left(\frac{M_L - 1}{\nu_{i1} - 1} \right) \left[2\nu_{i2} + 2\nu_{i3} + 4\left(\nu_{i2}\right)^2 \left(\frac{M_L - 1}{\nu_{i1} - 1} \right) \right] \\ & + \beta \left[\nu_{s3} + \left(\frac{M_L - 1}{\nu_{i1} - 1} \right) \left(2\nu_{i2}\nu_{s2} + \nu_{i3}\nu_{s1} \right) + 2 \left(\frac{M_L - 1}{\nu_{i1} - 1} \right)^2 \left(\nu_{i2}\right)^2 \nu_{s1} \right] \Bigg]. \end{aligned} \tag{6.15}$$

As with the DT-f framework, the emitted singles rate Φ_1 can be broken down into the singles due to transmitted source neutrons $\Phi_{1,t}$ and the singles due to fission chain multiplication within the uranium object $\Phi_{1,f}$:

$$\Phi_{1,t} = 1 - \beta_{2n} - \beta, \tag{6.16}$$

$$\Phi_{1,f} = M_L \left(2\beta_{2n} + \nu_{s1}\beta \right). \tag{6.17}$$

It is important to note that any (n,3n) interactions by source neutrons are still considered to be induced fissions in the DT-f-n2n method. However, the bias introduced by this assumption is significantly smaller than if (n,2n) and (n,3n) interactions are lumped in with induced fissions, as is the case in the DT-f method. This is due to the lower incidence of (n,3n) compared to fission and is shown in fig. 6.9. In the DT-f-n2n method, the constant values for ν_{s1}, ν_{s3}, and ν_{s3} are based on the multiplicity distribution for 14.1 MeV induced fission on ^{235}U or ^{238}U. In reality, there is some enrichment dependence when the chain-starting multiplicity distribution is defined to include induced fission, (n,3n), and (n,γ) capture. Thus, the issue of what interactions to include in the source event, as was encountered in the DT-f method, is not gone. However, there is less systematic bias because (n,2n) chain-starting interactions are separated from all other chain-starting interactions in the DT-f-n2n method.

Separating the effect of (n,2n) from fission and other interactions on the source coupling term reduces the enrichment sensitivity of chain-starting multiplicity parameters ν_{s1}, ν_{s2}, and

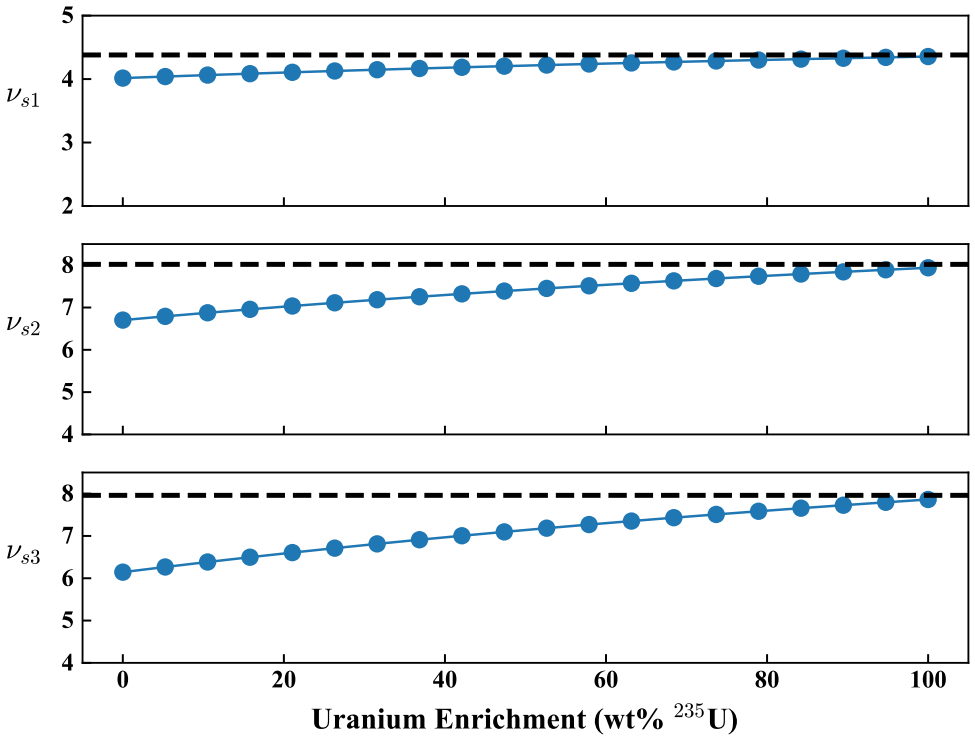

Figure 6.9: The first, second, and third reduced-factorial moments for the prompt-neutron multiplicity distributions for 14.1 MeV neutrons incident on uranium when the source event includes only induced fission, (n,3n), and (n,γ) capture. The values for 14.1 MeV induced fission on ^{235}U or ^{238}U are shown as the dotted lines.

ν_{s3}. This results in less systematic error when using a constant value for these parameters, allowing the enrichment dependence to be contained in other parameters that can be solved for. The disadvantage of the DT-f-n2n method is that introducing an additional coupling term is introducing an additional independent unknown variable which requires an additional observable such as the emitted fission chain triples rate or the transmitted singles rate. Assuming that the emitted fission chain singles, and doubles rates, and either the emitted fission chain triples rate or transmitted singles rate can be estimated, the unknowns β_{2n}, β and M_L should be able to be solved for. This would theoretically allow for enrichment to be solved for using what is defined as the "beta ratio". This is covered in more detail in section 6.2.1.

In the situation where the average source-neutron path length through the uranium object x is known, the dimensionality of the system can be reduced from three unknowns (β_{2n}, β, and M_L) to two (M_L and enrichment). Both β_{2n} and β can be calculated using eqs. (6.18) and (6.19), which are generalized versions of eqs. (6.7) and (6.8) for a given enrichment.

$$\beta = \sum_i \beta_i, \tag{6.18}$$

$$\beta_i = I \frac{\Sigma_i}{\Sigma_R} \left(1 - e^{-\Sigma_R x}\right), \tag{6.19}$$

where Σ_R is the removal macroscopic cross section, I is the fraction of emitted source neutrons that are incident upon the interrogation object, and the subscript i represents a given interaction such as induced fission or (n,3n). Depending on what interactions are assumed to be chain-starting interactions, β is calculated as a sum of the couplings for each individual interaction. For example, if only induced fissions are considered chain-starting interactions, $\beta = \beta_f$. If induced fissions and (n,3n) interactions are considered chain-starting interactions, $\beta = \beta_f + \beta_{3n}$. The unknown variables that determine the emitted fission chain multiplicity rates are then enrichment and M_L. It is important to note, however, that these two unknown variables are not independent of each other.

6.2.1 Estimating Enrichment Using the Beta Ratio

The beta ratio is advantageous in that it is only a function of enrichment, as the dependence on source neutron path length falls out. Using eqs. (6.7) and (6.8), the beta ratio can be written using eq. (6.20):

$$\beta/\beta_{2n} = \beta_f/\beta_{2n} = \frac{\sigma_{f,8} + f_5\left(\sigma_{f,5} - \sigma_{f,8}\right)}{\sigma_{2n,8} + f_5\left(\sigma_{2n,5} - \sigma_{2n,8}\right)}, \tag{6.20}$$

where the subscripts 5 and 8 on the terms σ_i denote the microscopic cross section for a 14.1 MeV neutron undergoing interaction i on ^{235}U or ^{238}U, respectively. The quantity f_5 denotes the mass fraction of ^{235}U i.e. the enrichment.

The beta ratio definition in eq. (6.20) assumes that all chain-starting events are either 14.1 MeV induced fission or (n,2n) and ignores the effects of (n,3n) and (n,γ) capture. While the latter interactions have a much smaller effect on source-event multiplicity than the former, they can still introduce systematic bias. One method that was used in an attempt to account for this bias was to lump the (n,3n) and (n,γ) capture events in with the induced fission probability β. The beta ratio is then

$$\begin{aligned}\beta/\beta_{2n} &= \frac{\beta_f + \beta_{3n} + \beta_\gamma}{\beta_{2n}} \\ &= \frac{\sigma_{f,8} + \sigma_{3n,8} + \sigma_{\gamma,8} + f_5\left(\sigma_{f,5} - \sigma_{f,8} + \sigma_{3n,5} - \sigma_{3n,8} + \sigma_{\gamma,5} - \sigma_{\gamma,8}\right)}{\sigma_{2n,8} + f_5\left(\sigma_{2n,5} - \sigma_{2n,8}\right)}.\end{aligned} \tag{6.21}$$

Both of the beta ratios as described in eqs. (6.20) and (6.21) can be used to solve for enrichment. Given an input of the beta ratio, traditional quadratic solving methods and cross sections for 14.1 MeV neutrons taken from ENDF/B-VII.1 [2] can be used to solve for enrichment. Figure 6.10 shows the relationship between the two beta ratio definitions. Because (n,3n) and (n,γ) are a larger portion of the removal cross section for 14.1 MeV neutrons on ^{238}U compared to ^{235}U, there is larger difference between the two definitions at lower enrichment.

Before the beta ratio is used to estimate enrichment, values for β_{2n} and β must be calculated from emitted fission chain singles and doubles rates, and either the emitted fission

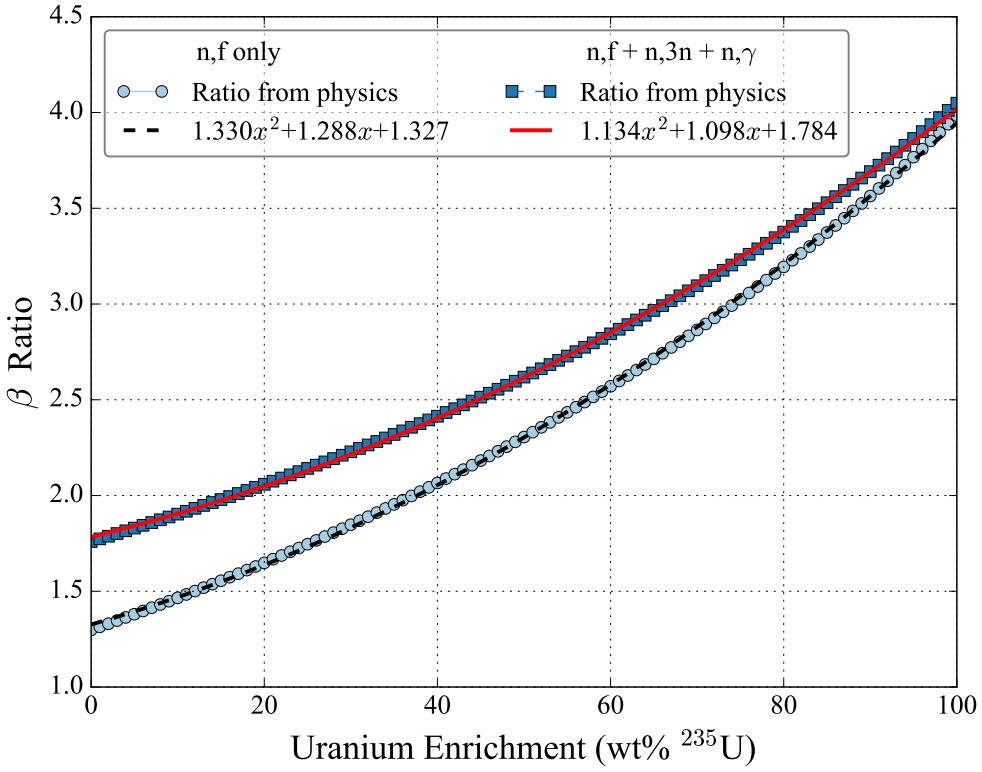

Figure 6.10: Beta ratio versus uranium enrichment for the beta ratio definitions in eqs. (6.20) and (6.21). Quadratic fits are plotted on top of the calculated values.

chain triples rate or the transmitted singles rate using the DT-f-n2n equations. Sections 6.2.2 and 6.2.3 address different methods of accomplishing this.

6.2.2 Lookup Table Method

This method generated a series of lookup tables (LUTs) over the domain of the unknown variables in the system described by eqs. (6.13) to (6.15), whether it be β_{2n}, β, and M_L or enrichment and M_L in the situation where average source-neutron path length is known. The point kinetics model parameter p_f, which is the probability of a fission neutron inducing further fission, was used in place of leakage multiplication M_L. Equations (6.22) and (6.23) below show the relevant conversions between these two interchangeable parameters using the negligible parasitic capture assumption described in eq. (3.7).

$$M_L = \frac{1 - p_f}{1 - p_f \nu_{i1}} \tag{6.22}$$

$$\frac{M_L - 1}{\nu_{i1} - 1} = \frac{p_f}{1 - p_f \nu_{i1}} \tag{6.23}$$

Because β_{2n} and β are so correlated, all of the attempted LUTs that treated them as independent variables performed significantly worse than those methods that correlated them via eqs. (6.7) and (6.8). Therefore, these more simplistic methods are not described here.

Several methods of generating and searching LUTs were attempted. The strategy described here was finally decided upon as the most direct and efficient method of generating the LUTs. The methods allow for a set of emitted fission chain singles, doubles, and triples rates, either from a theoretical measurement or a Monte Carlo simulation, to be used to look up corresponding values for uranium enrichment and p_f. Assuming that TNI measurements can give geometric information about the uranium object and that the directional distribution of the interrogation source relative to the uranium object is known, the average source neutron path length through the uranium object should be able to be estimated. The lookup methods calculated values for β_{2n} and β using uranium enrichment, average source neutron path length (assumed to be known) and eqs. (6.7) and (6.8). Only 14.1 MeV induced fissions were included in the definition of β. Values for emitted fission

chain singles, doubles, and triples rates can be calculated using eqs. (6.13) to (6.15). These emitted fission chain rates correspond to the values of enrichment and p_f in the LUT. The pseudocode of this LUT generation scheme is described in algorithm 6.1.

Algorithm 6.1 Lookup table generation for singles, doubles, & triples

for $0 \leq p_f \leq$ MAX p_f **do**
  for $0 \leq$ enrichment ≤ 1.0 **do**
    for $0 \leq$ path length $\leq$ MAX PATH LENGTH **do**
      Calculate β_{2n}, β using enrichment and path length in eqs. (6.7) and (6.8)
      Calculate $\Phi_{1,f}, \Phi_2, \Phi_3$ using β_{2n}, β, p_f and DT-f-n2n eqs. (6.13) to (6.15)
      LUT[path length][$(\Phi_{1,f}, \Phi_2, \Phi_3)$] = (enrichment, p_f)
    end for
  end for
end for

Because triple neutron coincidences can often be difficult to detect with any degree of statistical confidence during TNI measurements, a LUT that returns uranium enrichment and p_f based on inputs of only emitted fission chain singles and doubles rates was also developed. This is described in algorithm 6.2.

Algorithm 6.2 Lookup table generation for singles & doubles

for $0 \leq p_f \leq$ MAX p_f **do**
  for $0 \leq$ enrichment ≤ 1.0 **do**
    for $0 \leq$ path length $\leq$ MAX PATH LENGTH **do**
      Calculate β_{2n}, β using enrichment and path length in eqs. (6.7) and (6.8)
      Calculate $\Phi_{1,f}, \Phi_2$ using β_{2n}, β, p_f and DT-f-n2n eqs. (6.13) to (6.15)
      LUT[path length][$(\Phi_{1,f}, \Phi_2)$] = (enrichment, p_f)
    end for
  end for
end for

Because querying these lookup tables requires matching an input set of emitted fission chain singles, doubles, and sometimes triples rates to a key set in the table, it was necessary to implement a minimization function to match an input set to its closest reference set. This was performed in two ways—Cartesian distance minimization and relative error minimization. Cartesian distance minimization matches a reference set to an input based on eq. (6.24):

$$\sqrt{\left(\Phi_{1,f} - \Phi'_{1,f}\right)^2 + \left(\Phi_2 - \Phi'_2\right)^2 + \left(\Phi_3 - \Phi'_3\right)^2}, \tag{6.24}$$

where the primed variables represent the reference values stored in the LUT. Relative error minimization matches a reference set to an input based on eq. (6.25):

$$\frac{\Phi_{1,f} - \Phi'_{1,f}}{\Phi_{1,f}} + \frac{\Phi_2 - \Phi'_2}{\Phi_2} + \frac{\Phi_3 - \Phi'_3}{\Phi_3}. \tag{6.25}$$

In all cases, the relative error minimization method outperformed the Cartesian distance minimization method when estimating p_f and enrichment.

Both algorithms were used to estimate M_L [via p_f and eq. (6.22)] and enrichment for a series of Monte Carlo simulations of TNI of bare uranium samples of varying mass and geometry described in section 4.2. Figures 6.11 and 6.12 show these results. The largest percent errors in leakage multiplication estimation were seen at lower multiplications. However, even the singles and doubles only LUT described in algorithm 6.2 was able to estimate multiplication to within 5 percent for all simulations. Both algorithms performed similarly when estimating enrichment. There appears to be an almost linear systematic overestimation of enrichment. Mass and geometry also play a role in the estimation error. Since the two variables being "solved for", enrichment and p_f, are not independent, this systematic bias is not surprising.

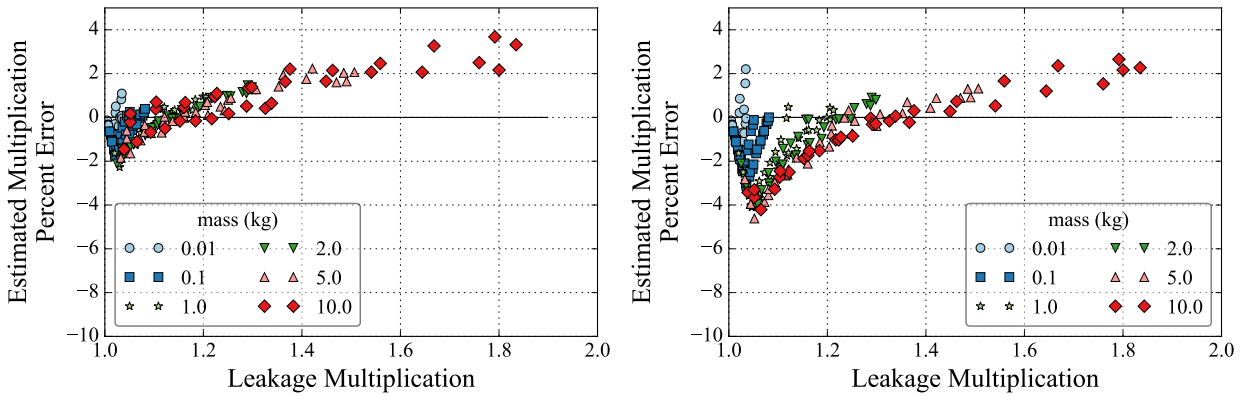

(a) Singles, doubles, & triples **(b)** Singles & doubles only

Figure 6.11: Percent error in estimating leakage multiplication using LUTs in the DT-f-n2n method. The solid black line represents a true estimate.

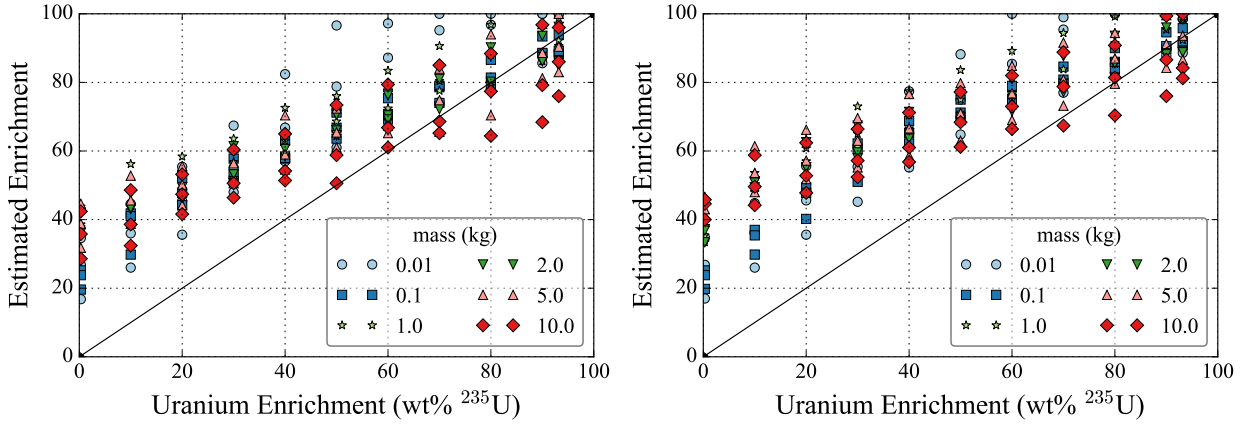

(a) Singles, doubles, & triples **(b)** Singles & doubles only

Figure 6.12: Uranium enrichment estimation using LUTs in the DT-f-n2n method. The solid black line represents a true estimate.

6.2.3 Newton-Raphson Root-Finding Methods

In addition to the LUT method of solving the two or three-dimensional system of nonlinear equations to estimate multiplication and enrichment from emitted fission chain singles, doubles, and triples rates, a root-finding approach based on the Newton-Raphson method was also used [53]. The Newton-Raphson method is a simple yet effective iterative method for solving roots of a series of nonlinear equations. Solving multidimensional systems of nonlinear equations is traditionally difficult. While there are three equations and three unknowns, this does not guarantee that a real solution for β, β_{2n}, and M_L exists. The accuracy of the Newton-Raphson method is highly dependent upon the quality of the initial guess of the solution.

Two different methods using this approach were developed. The first method, referred to as SDTML, used the emitted fission chain singles, doubles, and triples rates to solve for β, β_{2n}, and M_L. Enrichment was then estimated using both of the beta ratio methods described in section 6.2.1 [eqs. (6.20) and (6.21)]. Equations (6.14), (6.15) and (6.17) were rearranged to give the equations fed into the root-finding algorithm:

$$0 = M_L\left(2\beta_{2n} + \nu_{s1}\beta\right) - \Phi_{1,f}, \tag{6.26}$$

$$0 = M_L^2\left[\beta_{2n}\left(1 + 2\nu_{i2}\left(\frac{M_L - 1}{\nu_{i1} - 1}\right)\right) + \beta\left(\nu_{s2} + \nu_{s1}\nu_{i2}\left(\frac{M_L - 1}{\nu_{i1} - 1}\right)\right)\right] - \Phi_2, \tag{6.27}$$

$$\begin{aligned} 0 = M_L^3\Bigg[&\beta_{2n}\left(\frac{M_L - 1}{\nu_{i1} - 1}\right)\left[2\nu_{i2} + 2\nu_{i3} + 4\left(\nu_{i2}\right)^2\left(\frac{M_L - 1}{\nu_{i1} - 1}\right)\right] \\ &+ \beta\left[\nu_{s3} + \left(\frac{M_L - 1}{\nu_{i1} - 1}\right)\left(2\nu_{i2}\nu_{s2} + \nu_{i3}\nu_{s1}\right) + 2\left(\frac{M_L - 1}{\nu_{i1} - 1}\right)^2\left(\nu_{i2}\right)^2\nu_{s1}\right]\Bigg] - \Phi_3. \end{aligned} \tag{6.28}$$

The second method using the Newton-Raphson root-finding approach, referred to as SSDML, used the transmitted singles, emitted fission chain singles, and emitted fission chain doubles rates to solve for β, β_{2n}, and M_L. Again, both methods of estimating enrichment from the beta ratio were used. In this case, eqs. (6.14), (6.16) and (6.17) were rearranged to

give the equations fed into the root-finding algorithm:

$$0 = 1 - \beta_{2n} - \beta - \Phi_{1,t}, \tag{6.29}$$

$$0 = M_L \left(2\beta_{2n} + \nu_{s1}\beta\right) - \Phi_{1,f}, \tag{6.30}$$

$$0 = M_L^2 \left[\beta_{2n}\left(1 + 2\nu_{i2}\left(\frac{M_L - 1}{\nu_{i1} - 1}\right)\right) + \beta\left(\nu_{s2} + \nu_{s1}\nu_{i2}\left(\frac{M_L - 1}{\nu_{i1} - 1}\right)\right)\right] - \Phi_2. \tag{6.31}$$

Because the ability of the root-finding algorithm to converge on an answer is highly dependent on the quality of the initial guesses, the relationship between enrichment, average source neutron path length, and β_i values as expressed in eq. (6.19) are used to generate the initial guesses. Using a known path length, this resulted in convergence for nearly all calculations.

As shown in fig. 6.13, both the SDTML and SSDML Newton-Raphson root-finding methods accurately predicted leakage multiplication to within at most 4 percent error. The largest errors occurred with larger masses i.e. larger multiplication. This is likely explained by the point kinetics model assumptions being violated for large, high-multiplication objects. Leakage multiplication is the most influential term by far in the emitted multiplicity rate equations, particularly in the doubles and triples. There is a third-order dependence in the doubles equation and a fifth-order dependence in the triples equation. Thus, solving for leakage multiplication is highly sensitive to small differences in emitted multiplicity rate inputs.

As shown in figs. 6.14 and 6.15, both the SDTML and SSDML Newton-Raphson root-finding methods underestimate enrichment by at least 10 percent. This is a result of underestimating the beta ratio, however it may be calculated. Using the "(n,f) only" definition of the beta ratio in eq. (6.20) performed better than the "(n,f) + (n,3n) + (n,γ)" definition in eq. (6.21). This is due to the fact that a given beta ratio corresponds to a higher enrichment in the "(n,f) only" definition versus the "(n,f) + (n,3n) + (n,γ)" definition (see fig. 6.10), so the systematic effect of underestimating the true beta ratio was not as significant.

The SDTML method performed marginally better than the SSDML method when estimating enrichment for most simulations. One feature of note is the larger variance in

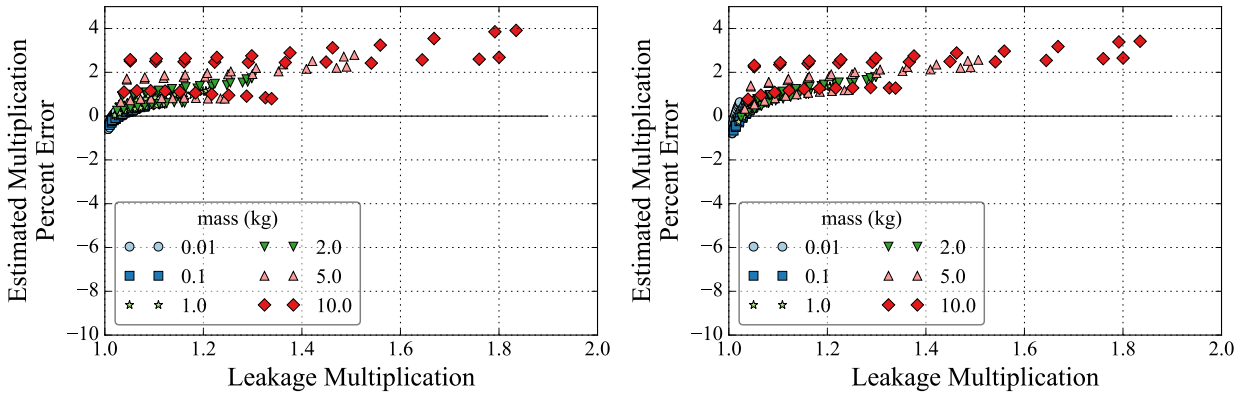

(a) SDTML Method

(b) SSDML Method

Figure 6.13: Percent error in estimating leakage multiplication using Newton-Raphson root-finding methods in the DT-f-n2n framework. The solid black line represents a true estimate.

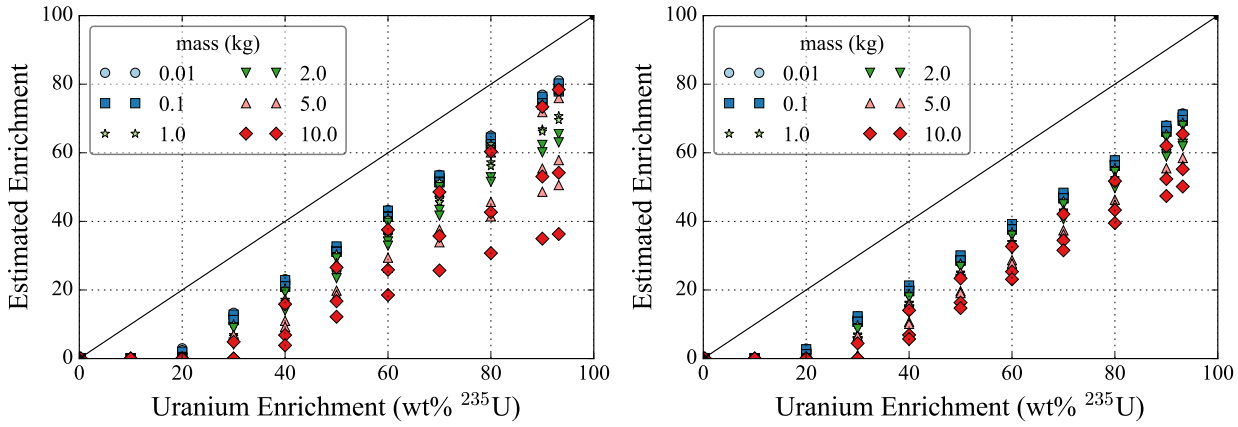

(a) SDTML Method **(b)** SSDML Method

Figure 6.14: Uranium enrichment estimation using Newton-Raphson root-finding methods in the DT-f-n2n framework and the "(n,f) only" beta ratio method described in eq. (6.20). The solid black line represents a true estimate.

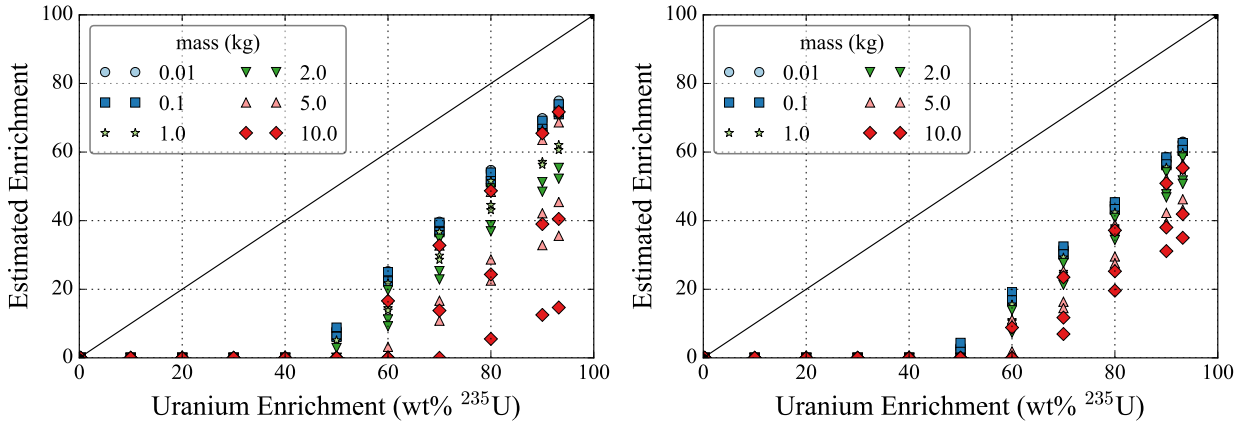

(a) SDTML Method **(b)** SSDML Method

Figure 6.15: Uranium enrichment estimation using Newton-Raphson root-finding methods in the DT-f-n2n framework and the "(n,f) + (n,3n) + (n,γ)" beta ratio method described in eq. (6.21). The solid black line represents a true estimate.

enrichment estimation for a given set of simulations with the same mass and enrichment, but different geometry for the SDTML method. This is likely indicative of the fact that multiplication has some dependence upon geometry, and this dependence increases as mass increases. The SDTML method is more sensitive to changes in multiplication versus the SSDML method because it considers the emitted fission chain triples rate which has a fifth-order dependence on leakage multiplication.

The ability of the SDTML and SSDML methods to estimate leakage multiplication and enrichment are comparable. However, both have their drawbacks if they are to be implemented in a real-life measurement scenario. While singles and doubles emission rates have been successfully measured using TNI of uranium [7], accurately measuring triple coincidences (actually quadruple coincidences with the tagged alpha particle) has not yet been done and may prove difficult given the small solid angle of the detector arrays in existing TNI systems. The ability to accurately measure triples rates is a prerequisite for implementing the SDTML method. Instead of requiring emitted fission chain triples rates, the SSDML method requires an accurate measurement of transmitted source neutron singles rates. In practice, there are several sources of false coincidences between the alpha particle detector inside the API neutron generator and the neutron detectors that can bias the transmitted singles rate. Inelastically scattered source neutrons can often register in neutron detectors as false coincidences with a different alpha detection event within the API neutron generator [7]. Accounting for inelastic neutron scatter in TNI measurements is an area of active research [4], but it is not possible, at the time of this writing, to accurately estimate the number of fission chains initiated from a transmission measurement. Using the SSDML method in a TNI measurement is contingent upon the ability to perform an adequate scatter correction so that estimating transmitted neutron singles from eq. (6.16) is accurate.

Chapter 7

Chain-starting Multiplicity-based Method

The chain-starting multiplicity-based method leverages the TOF capabilities of TNI systems to estimate values for the transmitted source neutron singles and emitted fission chain singles rates. This method is advantageous in that it does not require a triples estimate nor does it require limiting assumptions that exclude certain chain-starting interactions from chain-starting multiplicity terms ν_{sn}, as was the case for the coupling-based methods. Instead, it uses the enrichment dependence in the chain-starting multiplicity terms in order to estimate enrichment. The point kinetics model equations used are

$$\Phi_{1,t} = (1-\beta)\,, \tag{7.1}$$

$$\Phi_{1,f} = \beta\nu_{s1}M_L, \tag{7.2}$$

$$\Phi_2 = \beta M_L^2\left[\nu_{s2} + \nu_{s1}\nu_{i1}\left(\frac{M_L-1}{\nu_{i1}-1}\right)\right], \tag{7.3}$$

where ν_{s1} and ν_{s2} include all chain-starting interactions by 14.1 MeV source neutrons and can be calculated using eqs. (6.10) and (6.11). Consequently, the enrichment dependence is present in the ν_{s1} and ν_{s2} terms as well as the M_L term. The three unknown variables in the system of the equations are the probability of a 14.1 MeV source neutron inducing any chain starting reaction β (the coupling), leakage multiplication M_L, and enrichment. The coupling β can be directly calculated from the transmitted singles $\Phi_{1,t}$ using eq. (7.1).

Both the transmitted and fission chain singles are used to estimate a relationship between M_L and enrichment. In the system of equations defined by eqs. (7.2) and (7.3), the two unknowns are enrichment (contained in the ν_{s1} and ν_{s2} terms) and M_L. A simple substitution yields an equation which can be solved for enrichment:

$$\Phi_2 = \frac{\Phi_{1,f}^2}{\nu_{s1}^2\left(1-\Phi_{1,t}\right)}\left[\nu_{s2} + \frac{\nu_{s1}\nu_{i2}}{\left(\nu_{i1}-1\right)}\left(\frac{\Phi_{1,f}}{\nu_{s1}\left(1-\Phi_{1,t}\right)}\right)\right]. \tag{7.4}$$

Making this substitution in the equation is equivalent to using eqs. (7.1) and (7.2) to express M_L in terms of enrichment (via ν_{s1}) using eq. (7.5):

$$M_L = \frac{\Phi_{1,f}}{\nu_{s1}\left(1-\Phi_{1,t}\right)}. \tag{7.5}$$

7.1 Results Using Monte Carlo Data

Using eq. (7.4) to solve for the enrichment using values of $\Phi_{1,t}$, $\Phi_{1,f}$, and Φ_2 from MCNPX-PoliMi simulations described in chapter 4 resulted in a significant systematic underestimation compared to the true enrichment used for the simulation, as can be seen in fig. 7.1a.

The systematic underestimation that is observed is largely due to the high sensitivity that the enrichment estimation algorithm has to M_L. This can be observed when performing the same analysis but instead of substituting for M_L using eq. (7.5), the Monte Carlo estimate for M_L is used. These results are shown in fig. 7.1b. While there is still some evidence of systematic bias that appears to be correlated to mass, the enrichment estimates are all within 10 percent ^{235}U by weight. This suggests that the systematic underestimation observed in fig. 7.1a is due to the systematic underestimation of M_L when it is calculated using transmitted and fission chain singles in eq. (7.5). However, these errors are less than 3 percent, as is shown in fig. 7.2. If a 1.5–3.0 percent bias in estimating M_L results in a 20–40 percent bias in estimating enrichment, one can conclude that this method is too sensitive to leakage multiplication to be viable.

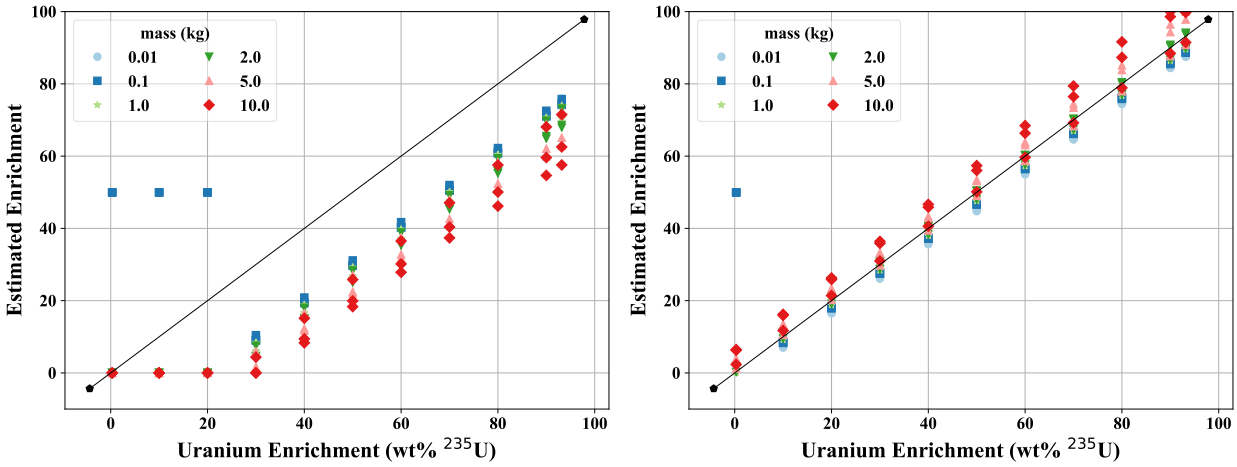

(a) M_L from eq. (7.5) **(b)** M_L from Monte Carlo

Figure 7.1: Uranium enrichment estimation using eq. (7.4) and different methods of estimating M_L. The solid black line represents a true estimate.

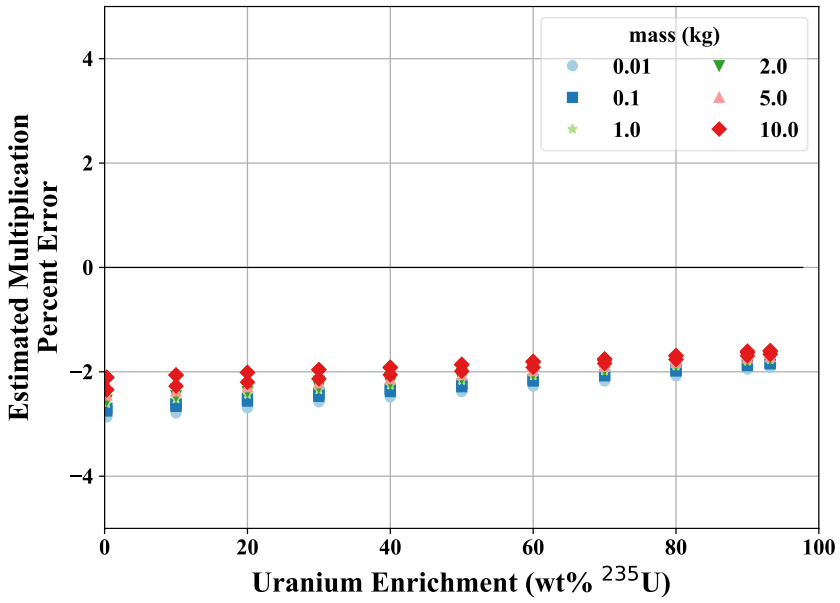

Figure 7.2: Percent errors in estimating M_L using eq. (7.5)

Chapter 8

Parametric Monte Carlo Study

The focus of this work is to back out physical characteristics, particularly enrichment, from observables in a coincidence measurement, namely emitted fission chain singles and doubles. Methods developed in chapters 6 and 7 exhibit significant systematic biases due to either too much or too little sensitivity to various physical characteristics such as enrichment and total uranium mass or physically-based parameters such as multiplication. This chapter examines the quantitative relationship between the coincidence observables and physical characteristics. This study used the results of more than 49 000 MCNPX-PoliMi simulations which are described in greater detail in section 4.2.

8.1 Determinants of Emitted Doubles per Single

The emitted doubles per single ratio is a good observable to use when attempting to invert point kinetics equations because it, depending on how the equations are formulated, allows for some efficiency correction terms, source-object coupling terms, and some leakage multiplication terms to cancel out. This results in an observable that is independent of, or at least less sensitive to, uncertainties in these terms, which is useful when values for these terms can be difficult to estimate, as is the case with the source-object coupling, or when uncertainties for these terms are difficult to estimate, as is the case with the efficiency correction terms. In the point kinetics equations for emitted fission chain singles and doubles [eqs. (7.2) and (7.3), respectively], taking the emitted doubles per single allows for the

source-object coupling β to drop out, resulting in only a second-order dependence on leakage multiplication M_L instead of third-order dependence as in the doubles equation. Because the source-object coupling drops out in the point kinetics equations, enrichment affects emitted doubles per single in two separate ways. The first is the M_L term. The second is the chain-starting multiplicity i.e. the ν_{s1} and ν_{s2} terms. The sensitivity of these chain-starting multiplicity parameters to enrichment is shown in fig. 6.8.

Figure 8.1 shows the relationship between emitted doubles per single, enrichment, and M_L using Monte Carlo estimates for emitted doubles per single and M_L. These results demonstrate that the majority of the enrichment sensitivity for the emitted multiplicity response lies within the leakage multiplication term as opposed the chain-starting multiplicity terms. It is also important to note that enrichment may have some effect on source-object coupling, but emitted doubles per single is independent of this effect and thus is not a factor in this analysis.

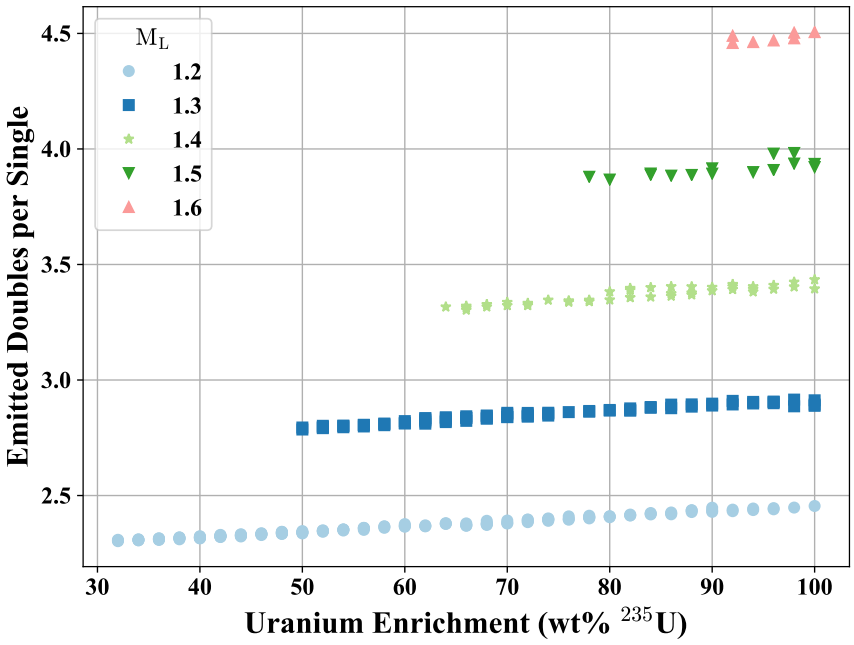

Figure 8.1: Emitted doubles per single versus enrichment and leakage multiplication for Monte Carlo simulations

This highlights how difficult it is to estimate enrichment if the relationship between leakage multiplication and enrichment is not understood. Even if a value of M_L is calculated from other observables, as in the methods described in chapters 6 and 7, the little sensitivity that emitted doubles per single has to enrichment would likely be dwarfed by any uncertainty in the M_L estimate.

While this analysis shows how influential the M_L term is in determining emitted doubles per single, leakage multiplication itself is determined by a combination of physical characteristics—enrichment, mass, sphericity, and the geometry of source-object-detector system. The following analyses examines how these physical properties affect the emitted doubles per single.

To examine the sensitivity of emitted doubles per single to the geometry of source-object-detector system, the directional distribution of the simulated D-T neutron source was varied in Monte Carlo simulations. One set of simulations used a directional profile based on the central alpha pixel of NMIS, denoted as pixel 8. The other set used a completely straight source that was incident on the center of the uranium object. The results are shown in fig. 8.2.

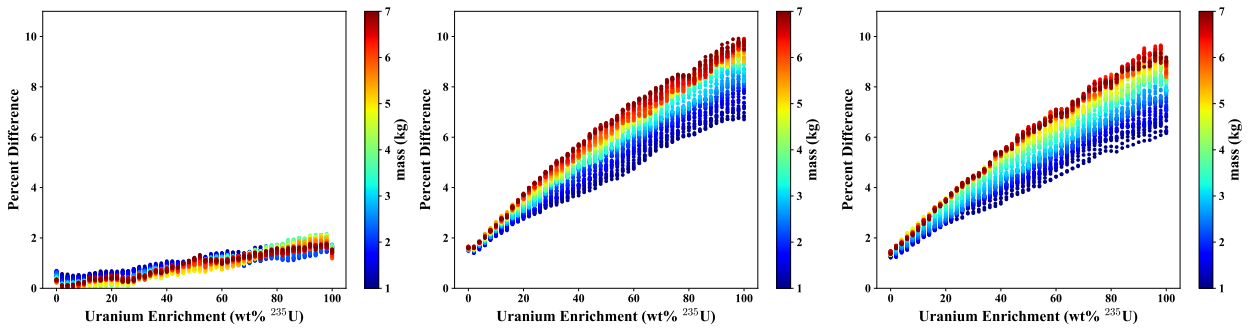

(a) Casting **(b)** Cylinder **(c)** Sphere

Figure 8.2: Percent difference between emitted doubles per single for a pixel 8 source and a straight source

The percent difference between emitted doubles per single for the pixel 8 source and the straight source is small at low enrichments, but can increase up to around 10 percent for highly multiplying items. While the analysis of the effect of source direction suggests that an understanding of the source-object-detector system geometry can be important, the effect on emitted doubles per single is small compared to that of the physical characteristics of the

uranium object such as enrichment, uranium mass, and geometry. This is demonstrated in figs. 8.3 and 8.4, which show the emitted doubles per single's relationships to uranium mass and enrichment, respectively.

While this analysis certainly suggests that emitted doubles per single is sensitive to uncertainties in geometry, uranium mass, and enrichment, it is also important to quantify this sensitivity. This was done by expressing a relationship between emitted doubles per single DPS and enrichment e, uranium mass m, and sphericity s, and then fitting a curve to this relationship. As the above analysis demonstrates, directional distribution was a less important parameter and is thus excluded from the set of independent variables. Several different functions were evaluated but eq. (8.1) below fit the large set of Monte Carlo simulations the best, based on an R^2 value of 0.974.

$$DPS = a_1 + a_2 e + a_3 ems \tag{8.1}$$

The fitting coefficient $a_1 = 1.4683 \pm 0.0013$ DPS, $a_2 = 0.0066 \pm 0.0001$ DPS per percent ^{235}U, and $a_3 = 0.0038 \pm 0.0001$ DPS per percent ^{235}U-kg uranium-sphericity. Quantitative values for the dependency of emitted doubles per single on each of the input parameters (enrichment, uranium mass, and sphericity) can be calculated by taking separate partial derivatives of eq. (8.1) with respect to the independent variables e, m, and s. These partial derivatives are referred to as sensitivity coefficients. The equations are

$$\frac{\partial DPS}{\partial e} = a_2 + a_3 ms, \tag{8.2}$$

$$\frac{\partial DPS}{\partial m} = a_3 es, \tag{8.3}$$

$$\frac{\partial DPS}{\partial s} = a_3 em. \tag{8.4}$$

It is important to note the nonlinearity of this relationship between the emitted doubles per single and all three of the input parameters. This results in a nonconstant sensitivity coefficient that is a function of other input parameters. Figure 8.5 shows these relationships for each sensitivity coefficient. To put it more plainly, a 10 percent increase in enrichment

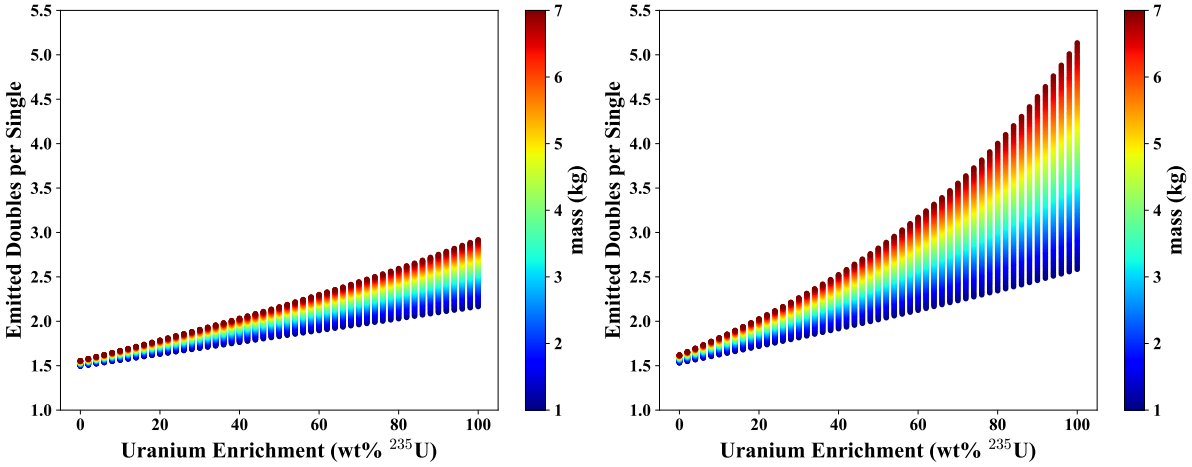

(a) Casting **(b)** Sphere

Figure 8.3: Emitted doubles per single as a function of enrichment and uranium mass for a pixel 8 source

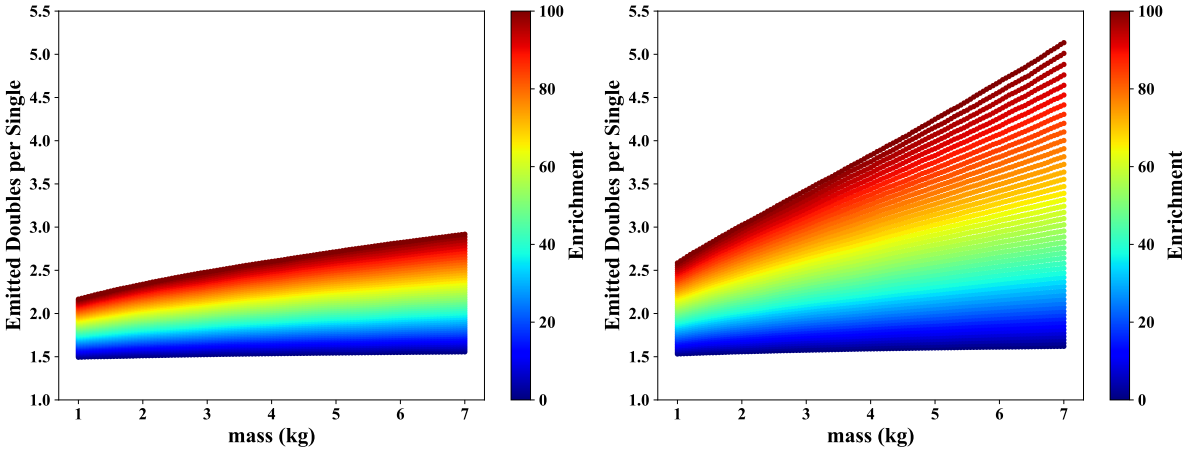

(a) Casting **(b)** Sphere

Figure 8.4: Emitted doubles per single as a function of uranium mass and enrichment for a pixel 8 source

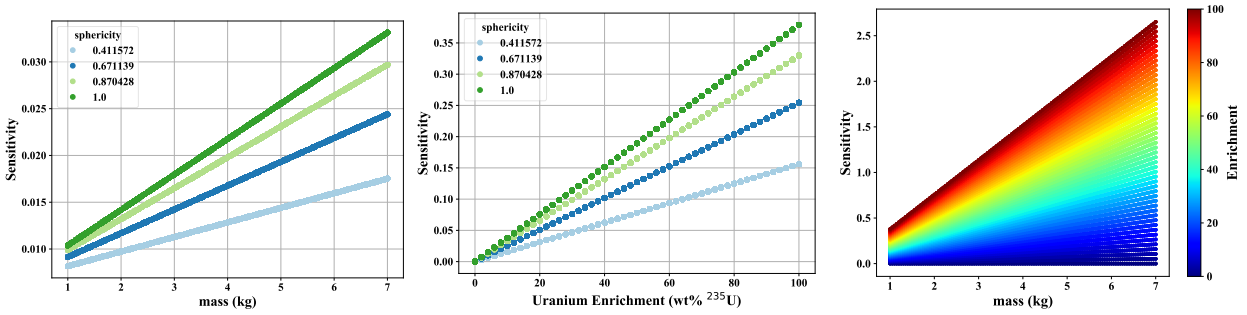

(a) $\frac{\partial DPS}{\partial e}$ **(b)** $\frac{\partial DPS}{\partial m}$ **(c)** $\frac{\partial DPS}{\partial s}$

Figure 8.5: Sensitivity coefficients for emitted doubles per single to physical parameters

can increase emitted doubles per single by anywhere from 0.08 to 0.33 depending on uranium mass and sphericity. A 1 kg increase in total uranium mass can increase emitted doubles per single by anywhere from 0.0 to 0.38 depending on enrichment and sphericity. If an object originally in an annular casting geometry ($s = 0.411572$) were to be transformed into a spherical geometry ($s = 1.0$), emitted doubles per single would increase anywhere from 0.0 to 1.56 depending on uranium mass and enrichment. For context, values of emitted doubles per single for the data set used range from 1.49 for a 1 kg casting at 0 percent enrichment to 5.13 for a 7 kg sphere at 100 percent enrichment.

In a theoretical TNI measurement, uranium mass and sphericity could be estimated from a combination of transmission and fission imaging. With this knowledge, a simple relationship between enrichment and emitted doubles per single could be determined for a given measurement. The method described in chapter 9 attempts to take advantage of this.

8.2 Determinants of Leakage Multiplication

Because leakage multiplication is often the largest determining factor in emitted multiplicities for the large uranium metal samples that are considered in this research, it is also interesting to quantify how leakage multiplication is affected by its underlying physical characteristics enrichment, geometry, and uranium mass. A similar analysis to that performed in section 8.1 was performed and results are shown in figs. 8.6 and 8.7.

A curve fit was again performed to express the relationship between leakage multiplication M_L and enrichment e, mass m, and sphericity s. The best-fit curve is shown in eq. (8.5), based on an R^2 value of 0.981.

$$M_L = a_1 + a_2 es + a_3 ems \tag{8.5}$$

The fitting coefficient $a_1 = 1.0303 \pm 0.0002\ M_L$, $a_2 = 0.0016 \pm 0.0001\ M_L$ per percent ^{235}U-sphericity, and $a_3 = 0.0007 \pm 0.0001\ M_L$ per percent ^{235}U-kg uranium-sphericity. Similar to the analysis of the emitted doubles per single, quantitative values of leakage multiplication's sensitivity to enrichment, mass, and sphericity can be calculated by taking partial derivatives

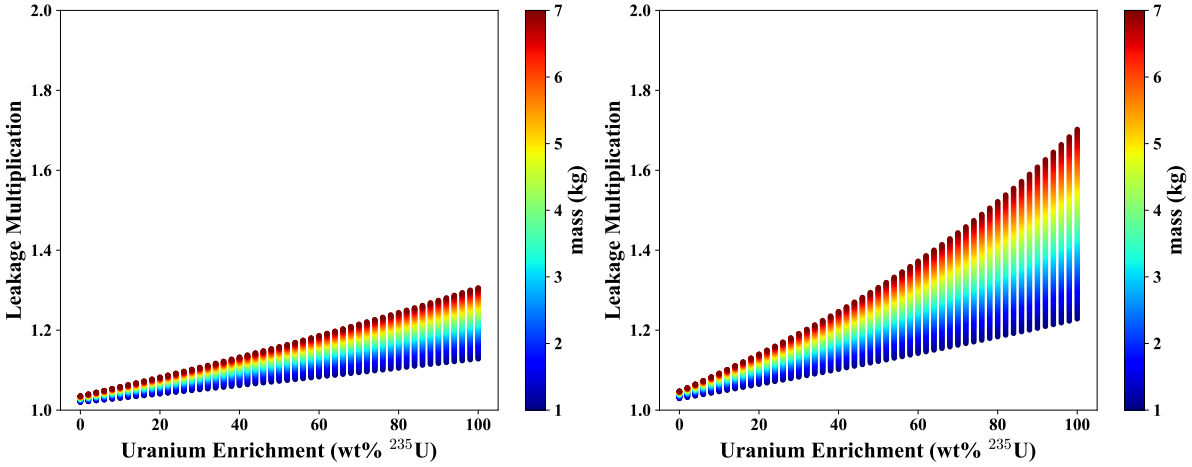

(a) Casting **(b)** Sphere

Figure 8.6: Leakage multiplication as a function of enrichment and mass for a pixel 8 source

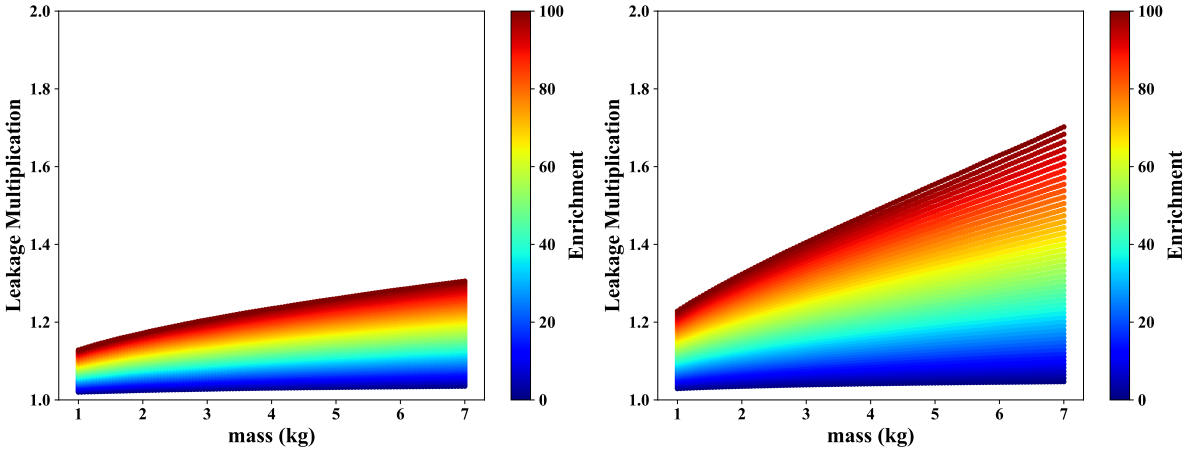

(a) Casting **(b)** Sphere

Figure 8.7: Leakage multiplication as a function of mass and enrichment for a pixel 8 source

of eq. (8.5), referred to as sensitivity coefficients.

$$\frac{\partial M_L}{\partial e} = a_2 s + a_3 m s \tag{8.6}$$

$$\frac{\partial M_L}{\partial m} = a_3 e s \tag{8.7}$$

$$\frac{\partial M_L}{\partial s} = a_2 e + a_3 e m \tag{8.8}$$

As with the sensitivity analysis for the emitted doubles per single, the sensitivity coefficients for leakage multiplication are similarly dependent on other input parameters. Figure 8.8 shows these relationships for each input parameter.

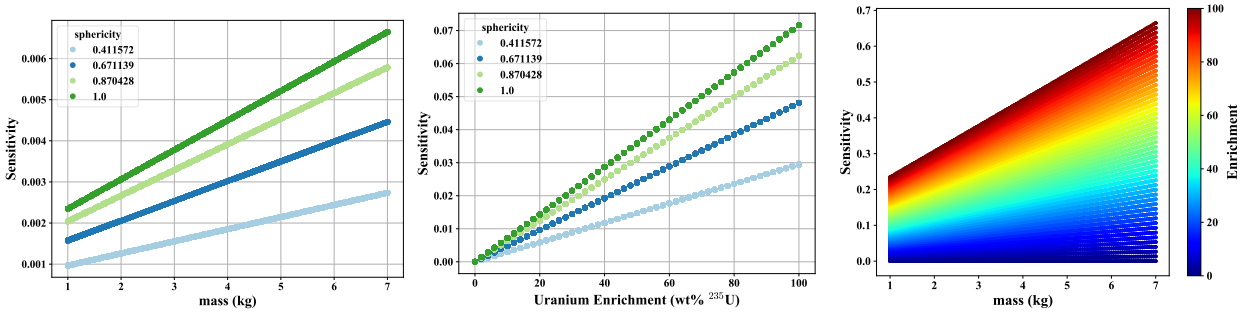

(a) $\frac{\partial M_L}{\partial e}$ **(b)** $\frac{\partial M_L}{\partial m}$ **(c)** $\frac{\partial M_L}{\partial s}$

Figure 8.8: Sensitivity coefficients for leakage multiplication to physical parameters

To put it more plainly, a 10 percent increase in enrichment can increase leakage multiplication by anywhere from 0.001 to 0.066 depending on mass and sphericity. A 1 kg increase in total uranium mass can increase leakage multiplication by anywhere from 0.0 to 0.072 depending on enrichment and sphericity. If an object originally in an annular casting geometry ($s = 0.411572$) were to be transformed into a spherical geometry ($s = 1.0$), leakage multiplication would increase anywhere from 0.0 to 0.391 depending on mass and enrichment. For context, values of leakage multiplication for this data set range from 1.02 for a 1 kg casting at 0 percent enrichment to 1.70 for a 7 kg sphere at 100 percent enrichment.

Chapter 9

Hybrid Method

After performing the parametric study on how emitted doubles per single $\frac{\Phi_2}{\Phi_{1,f}}$ is affected by different physical characteristics in section 8.1, it was determined that the majority of the enrichment sensitivity for the emitted multiplicity response lies within the leakage multiplication term as opposed to the source-coupling term or chain-starting multiplicity terms. Thus, a method of inverting the point kinetics model equations to assay enrichment would benefit from incorporating the physical relationships between the quasi-physical leakage multiplication term and its underlying physical characteristics such as enrichment, uranium mass, and geometry.

While it is not possible to express leakage multiplication in terms of these physical parameters using purely first principles, the hybrid method accomplishes this by using the large amount of Monte Carlo simulations described in section 4.2 to generate a precomputed lookup table. The hybrid method first looks up the object by uranium mass and geometry, which are assumed to be assayed by a combination of transmission and fission imaging measurements, and then returns a list of relevant mappings between emitted doubles per single and (M_L, enrichment) combinations. If measured or simulated values for emitted doubles per single, total uranium mass, and geometry is input, the method will return the top n (M_L, enrichment) pairs that, when used to calculated emitted doubles per single in the point kinetics equations, yield the closest match to the input emitted doubles per single. The point kinetics equation used for these calculations, shown in eq. (9.1), is a ratio of eqs. (7.2) and (7.3), which consider all chain-starting interactions. The chain-starting multiplicity

terms ν_{s1} and ν_{s2} are calculated using eqs. (6.10) and (6.11).

$$\frac{\Phi_2}{\Phi_{1,f}} = \frac{M_L}{\nu_{s1}} \left(\nu_{s2} + \nu_{s1}\nu_{i2} \left(\frac{M_L - 1}{\nu_{i1} - 1} \right) \right) \tag{9.1}$$

Because these lookup tables, also referred to as mappings, are generated by Monte Carlo simulations, they are a good estimate of physically valid relationships between emitted doubles per single, leakage multiplication, and the underlying physical parameters (enrichment, total uranium mass, and geometry).

9.1 Verification Using Monte Carlo Data

The hybrid method was verified by using the Monte Carlo simulations described in section 4.2. The data that generated the lookup table mapping was also used as input data. The results for the annular casting, solid cylinder and solid sphere geometries with a central NMIS pixel source distribution are shown in figs. 9.1 and 9.2. There is a slight systematic overestimation in both enrichment and leakage multiplication. This suggests some small amount of systematic error inherent in the D-T point kinetics model. Possible options are using slightly lower than true values of ν_{i1} and ν_{i2} due to the point kinetics model ignoring variance in fission neutron energy or the inappropriateness of assuming that $\langle M_L \rangle^2 \neq \langle M_L^2 \rangle$ as is discussed in section 2.3.1. Given how sensitive the D-T point kinetics equations are to leakage multiplication, these small systematic biases are not troubling as far as the verification of the hybrid method is concerned.

9.2 Sensitivity Analysis with Monte Carlo Data

The following analyses utilize the Monte Carlo data described in section 4.2 that was generated over a wide range of enrichments, uranium masses, geometries, and source profiles. They evaluate how sensitive the hybrid method is to differences between the input data and the data used to generate the lookup tables.

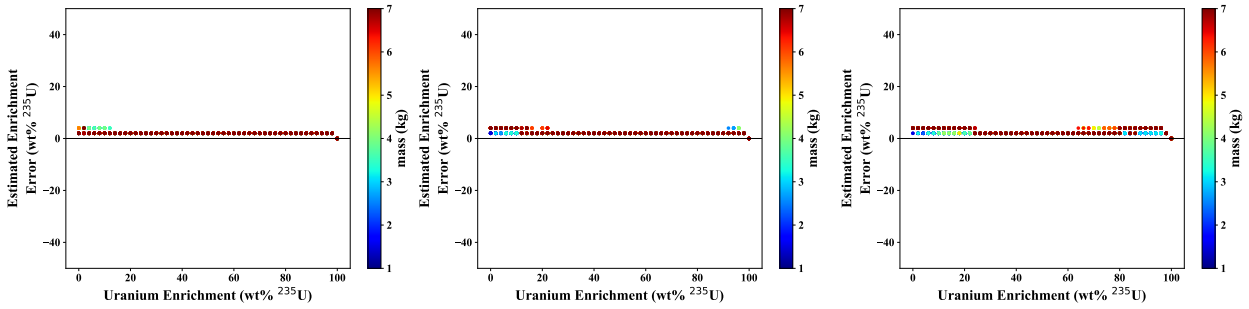

(a) Annular Casting **(b)** Cylinder **(c)** Sphere

Figure 9.1: Verification of hybrid method enrichment estimation using Monte Carlo data

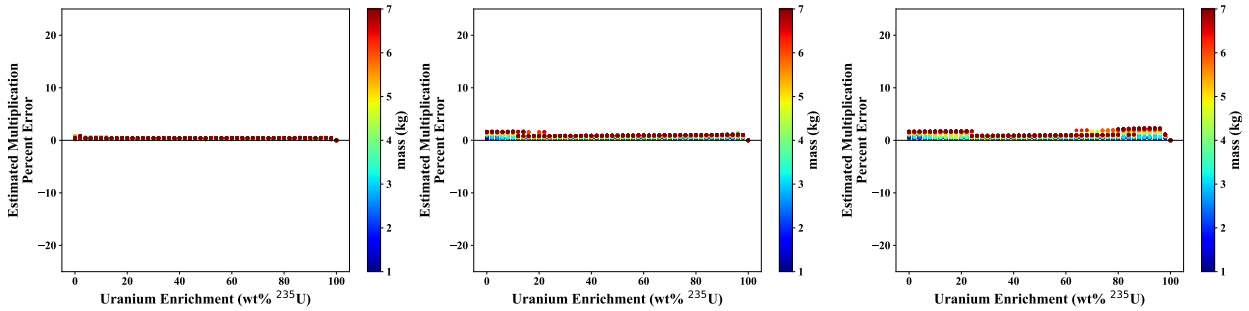

(a) Annular Casting **(b)** Cylinder **(c)** Sphere

Figure 9.2: Verification of hybrid method leakage multiplication estimation using Monte Carlo data

9.2.1 Sensitivity to Geometry

If a mapping corresponding to a geometry different than that of the input data is used, there is potential for significant systematic bias. The extent of this systematic bias was estimated by using a lookup table that was generated by one geometry to estimate enrichment and leakage multiplication from the emitted doubles per single of a different geometry. The results are shown in figs. 9.3 to 9.6. Because the solid cylinder and solid sphere are geometrically similar (sphericity of 0.87 and 1.0, respectively), there was barely any systematic bias introduced by using a solid cylinder mapping for solid sphere data or vice versa, as can be seen in figs. 9.3 and 9.4. However, when data from the annular casting geometry (sphericity = 0.41) is used with a mapping from the solid sphere or vice versa, the systematic bias introduced by using a different mapping becomes very noticeable.

For a uranium metal sample geometry with a lower sphericity such as the annular casting, leakage multiplication will be lower compared to a geometry with higher sphericity at a given enrichment and mass. In the case where annular casting input data is used with a solid sphere mapping (fig. 9.5), enrichment is significantly underestimated, up near 50 percent ^{235}U by weight error, while leakage multiplication is only slightly overestimated, around 3 percent error. This implies that the method places significantly more weight on estimating a correct leakage multiplication than a correct enrichment. This is likely due to the fact that in the D-T point kinetics model, the leakage multiplication term is the most influential in determining the emitted multiplicities, particularly for uranium metal samples larger than 1 kg. This is consistent with the results of the analysis in section 8.1.

In the case where solid sphere input data is used with an annular casting mapping (fig. 9.6), enrichment is significantly overestimated, with the inflection point due to the fact that the algorithm cannot return higher than 100 percent enrichment. This limitation also manifests itself in the leakage multiplication estimation, where an inflection point can be seen in the leakage multiplication estimation percent error due to the annular casting mapping not having leakage multiplication higher than 1.306.

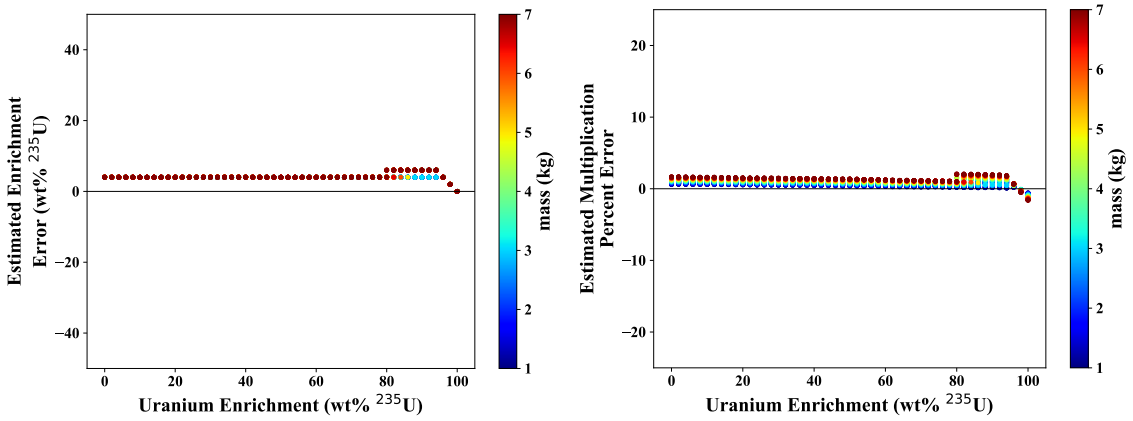

(a) Enrichment Estimate **(b)** Leakage Multiplication Estimate

Figure 9.3: Hybrid method estimation of spherical Monte Carlo data using cylindrical mappings

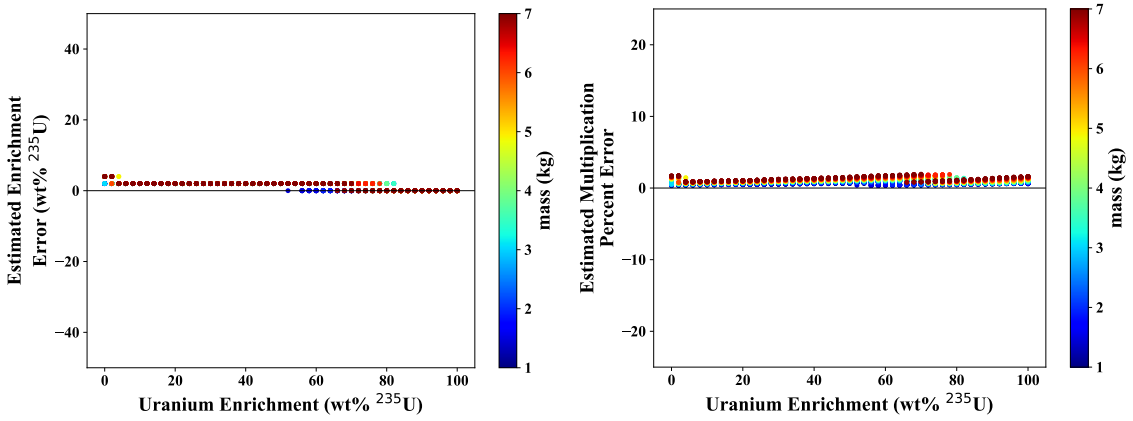

(a) Enrichment Estimate **(b)** Leakage Multiplication Estimate

Figure 9.4: Hybrid method estimation of cylindrical Monte Carlo data using spherical mappings

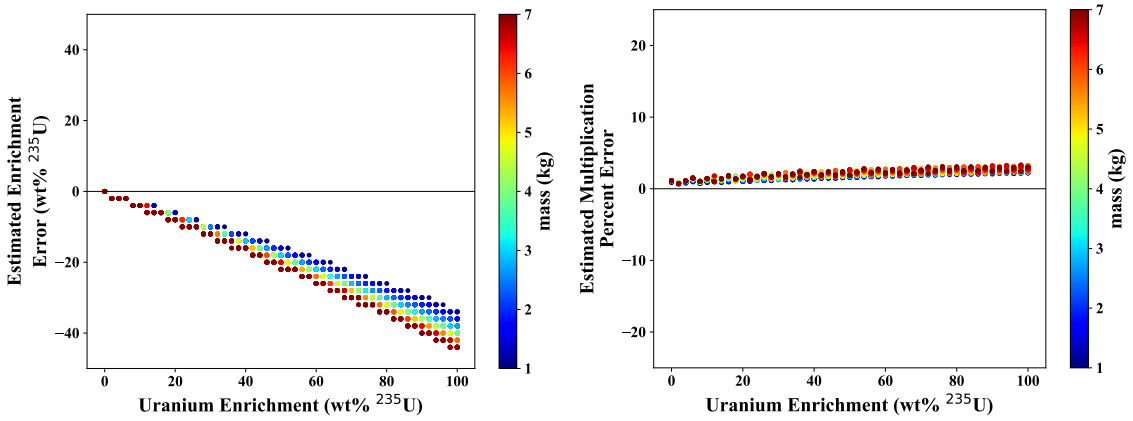

(a) Enrichment Estimate **(b)** Leakage Multiplication Estimate

Figure 9.5: Hybrid method estimation of annular casting Monte Carlo data using spherical mappings

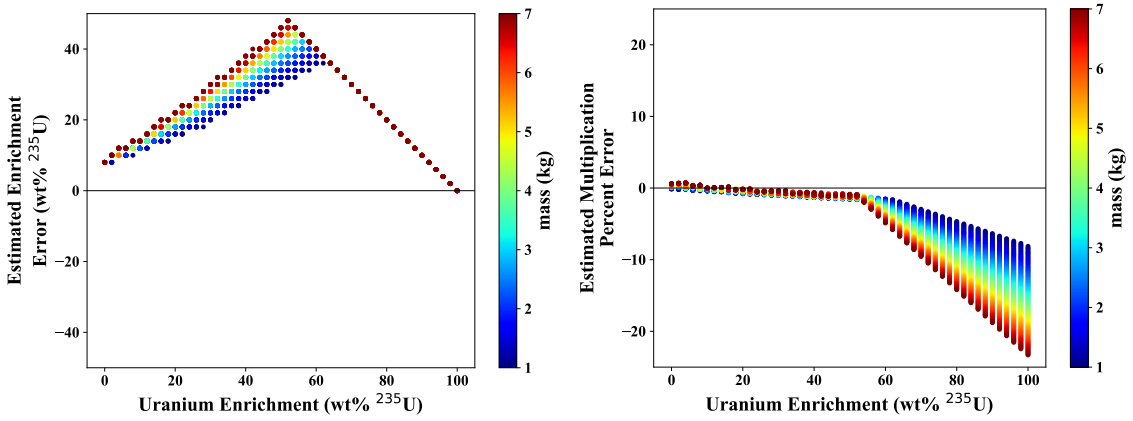

(a) Enrichment Estimate **(b)** Leakage Multiplication Estimate

Figure 9.6: Hybrid method estimation of spherical Monte Carlo data using annular casting mappings

9.2.2 Sensitivity to Total Uranium Mass

The hybrid method relies on accurate knowledge of the total uranium mass from a TNI measurement. Estimating the total uranium mass would likely involve both transmission and fission site imaging. While the mechanics of this mass estimation process are not within the scope of this research, there will undoubtedly be a degree of uncertainty in the mass estimate. A study was performed to quantify the effect of the enrichment estimate by the hybrid method if there is uncertainty in the total uranium mass input. The Monte Carlo mapping for an annular casting and solid spherical geometry under the pixel 8 interrogation source was used for this study. For each geometry, a separate mapping was used. The same data was used as an input but the uranium mass was increased or decreased by 10, 20, or 30 percent before being entered into the algorithm. Because the mapping data set ranged from 1.0 to 7.0 kg of uranium, the input data set was constricted to 1.45–5.35 kg so that increases and decreases by 30 percent would lie within the mapping mass range. The results for enrichment estimation are shown in figs. 9.7 and 9.8, while the results for leakage multiplication are shown in figs. 9.9 and 9.10.

Most of the results show a 10 percent ^{235}U by weight or less bias in the enrichment estimate as a result of systematically biasing the input uranium mass values. For some larger multiplication objects where the uranium mass is biased by -30 percent, enrichment biases can exceed 17 percent ^{235}U by weight. This is consistent with other sensitivity analyses of the hybrid method that higher multiplication objects are more sensitive to changes in input values. Leakage multiplication estimation errors are typically within 2 percent. The largest errors occur when the uranium mass is reduced by 30 percent, as shown in fig. 9.10c. This highlights a weakness of the hybrid method estimation algorithm where the input value for the emitted doubles per single is outside of the solution space corresponding to a given input (uranium mass, geometry) pair.

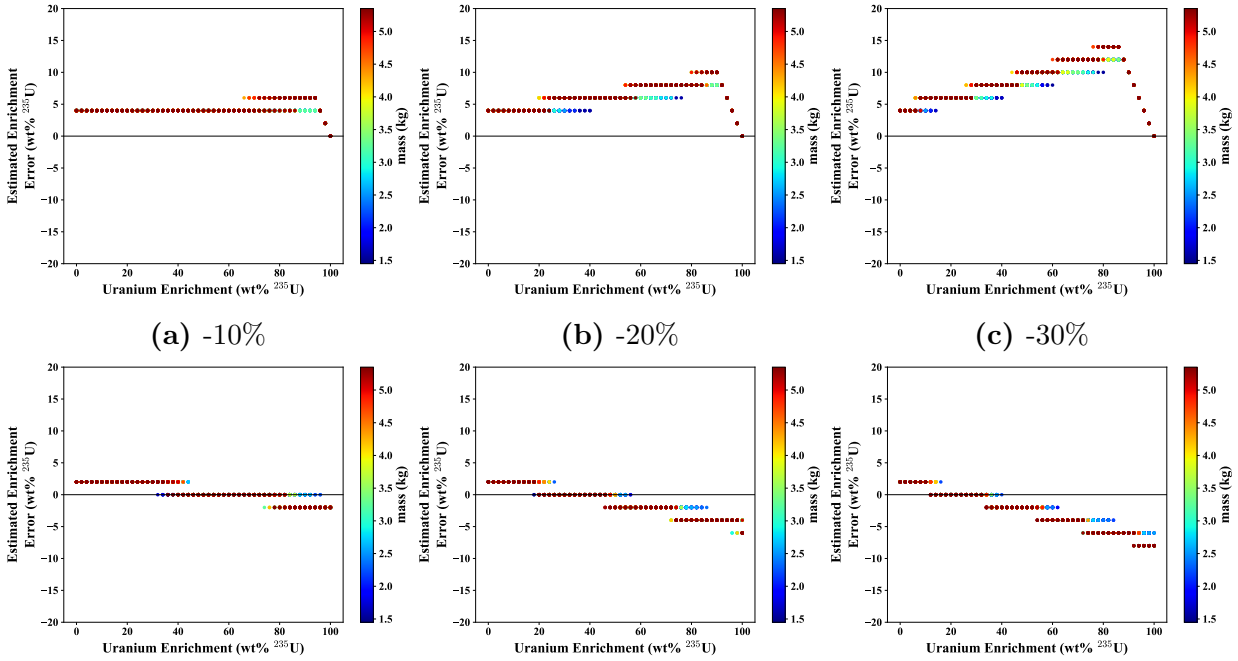

(a) -10% **(b)** -20% **(c)** -30%

(d) +10% **(e)** +20% **(f)** +30%

Figure 9.7: Hybrid method enrichment estimation error for biased uranium mass inputs of Monte Carlo data of pixel 8 source and annular casting geometries

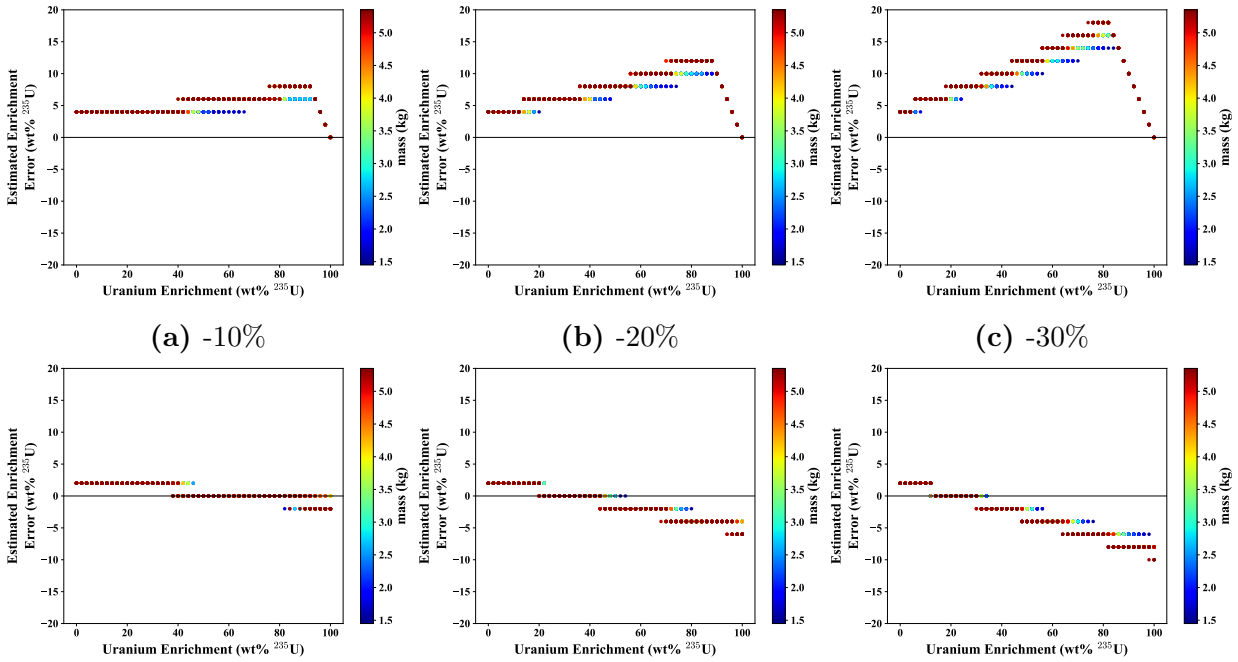

(a) -10% **(b)** -20% **(c)** -30%

(d) +10% **(e)** +20% **(f)** +30%

Figure 9.8: Hybrid method enrichment estimation error for biased uranium mass inputs of Monte Carlo data of pixel 8 source and spherical geometries

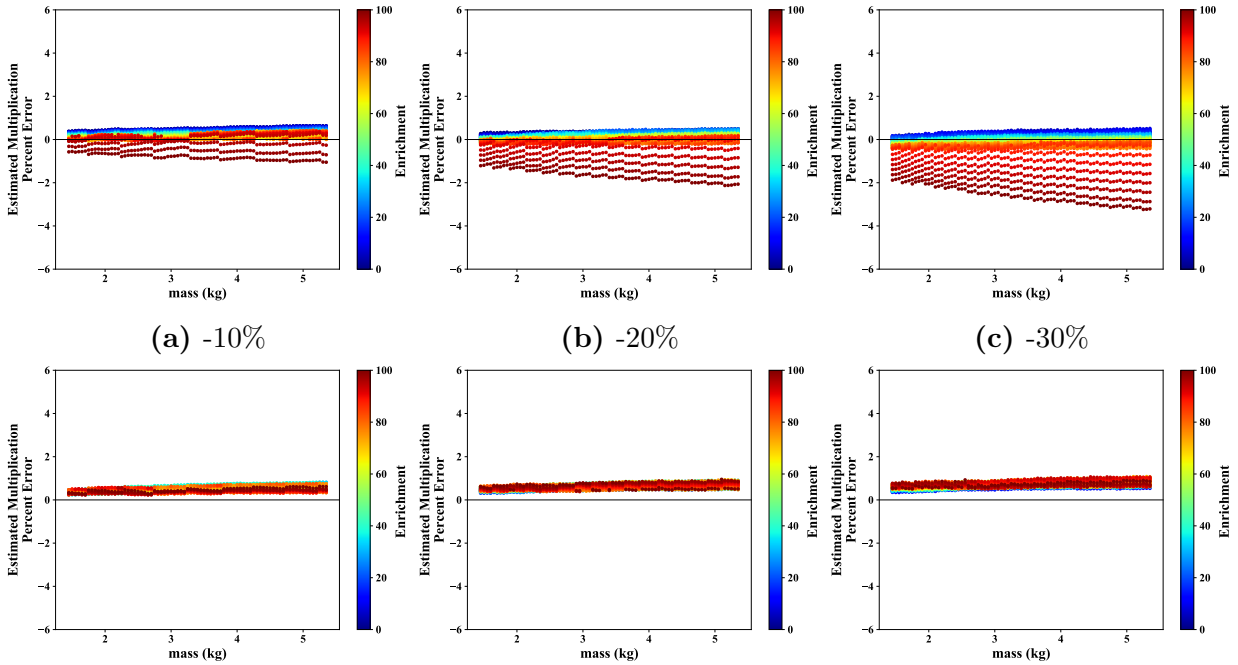

(a) -10% **(b)** -20% **(c)** -30%

(d) +10% **(e)** +20% **(f)** +30%

Figure 9.9: Hybrid method leakage multiplication estimation error for biased uranium mass inputs of Monte Carlo data of pixel 8 source and annular casting geometries

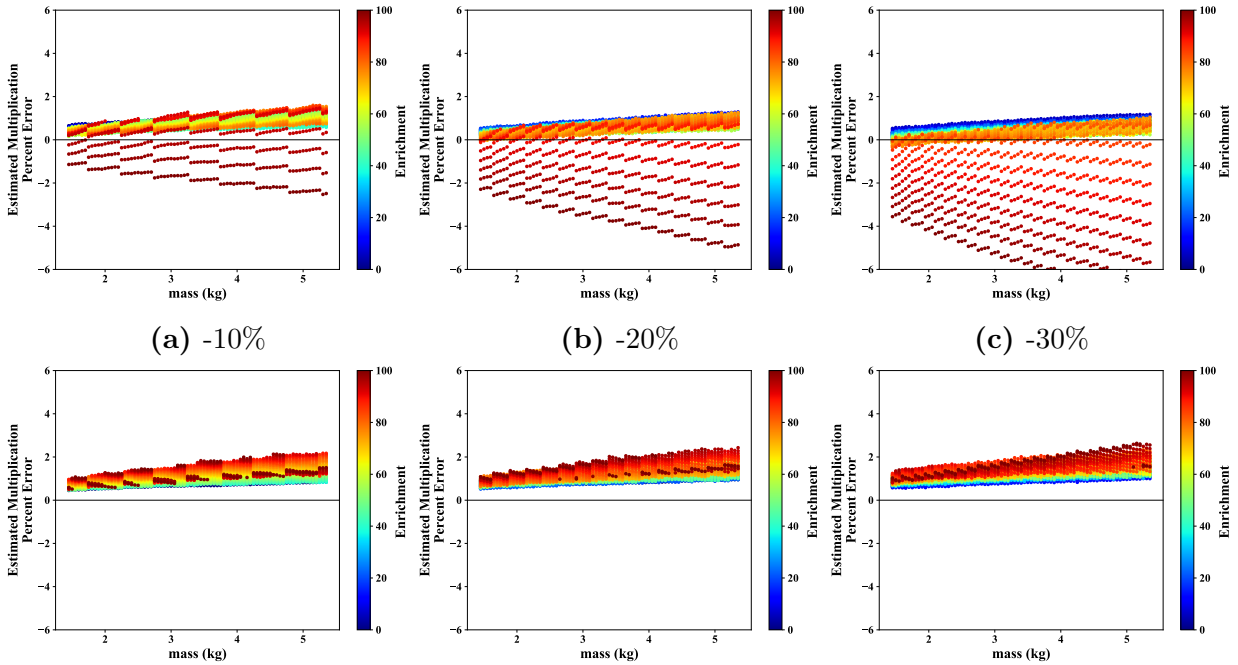

(a) -10% **(b)** -20% **(c)** -30%

(d) +10% **(e)** +20% **(f)** +30%

Figure 9.10: Hybrid method leakage multiplication estimation error for biased uranium mass inputs of Monte Carlo data of pixel 8 source and spherical geometries

9.2.3 Sensitivity to Source Directional Distributions

A study was also performed to determine if the directional distribution of the D-T neutron source used in the Monte Carlo simulation that generates the mapping can introduce any systematic bias when using the hybrid method. In order to evaluate this, two mappings were generated—one with the central NMIS pixel source distribution, which is referred to as pixel 8, and one with a purely straight distribution that is pointed at the middle of the bare uranium metal object. The data from the pixel 8 simulations was evaluated using a mapping from the straight source simulations and vice versa. The results are shown in figs. 9.11 and 9.12.

When annular casting data from the pixel 8 simulations are evaluated using a mapping from the straight source simulations (fig. 9.11), there is a slight shift downwards of 2–6 percent ^{235}U by weight in the enrichment estimate compared to when a pixel 8 mapping is used, as shown in fig. 9.1. For a more highly multiplying geometry such as a sphere, this systematic bias is increased a bit to between 2 and 10 percent ^{235}U by weight. This trend has been observed in other systematic evaluations of the hybrid method, where enrichment estimates can be more biased for higher multiplication objects due to the leakage multiplication value having such a large amount of influence in the emitted fission chain singles and doubles in the point kinetics model.

There is a similar trend in the opposite direction for the opposite case when straight source data is evaluated using a pixel 8 mapping, as shown in fig. 9.12. Using a mapping that employs a different source direction profile resulted in less than 3 percent difference in the leakage multiplication estimates for all cases. Based on this analysis, it can be concluded that the directional distribution that is used to generate the mapping used in the hybrid method is not a significant source of systematic error when compared to the method's sensitivity to other parameters such as uranium mass and geometry. This is consistent with the results of the analysis performed in section 8.1 that examined how source direction profiles affect emitted doubles per single and leakage multiplication.

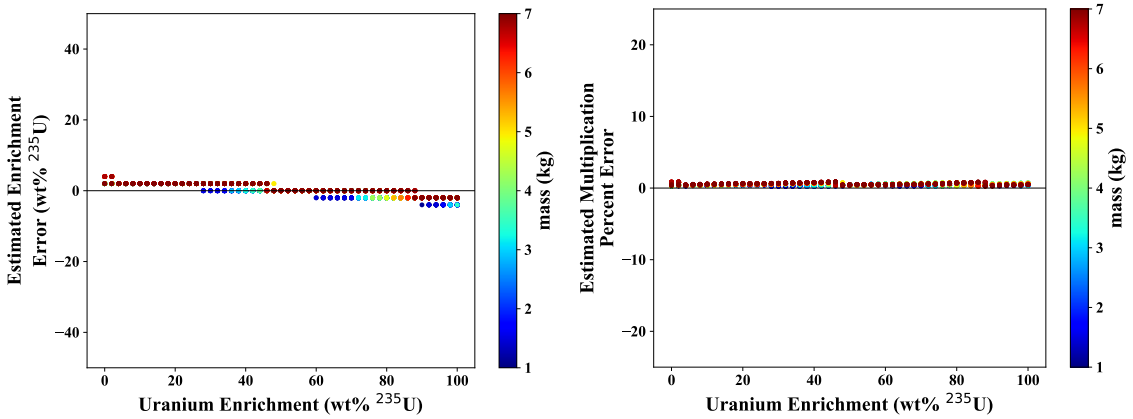

(a) Enrichment Estimate Annular Casting

(b) Leakage Multiplication Estimate Annular Casting

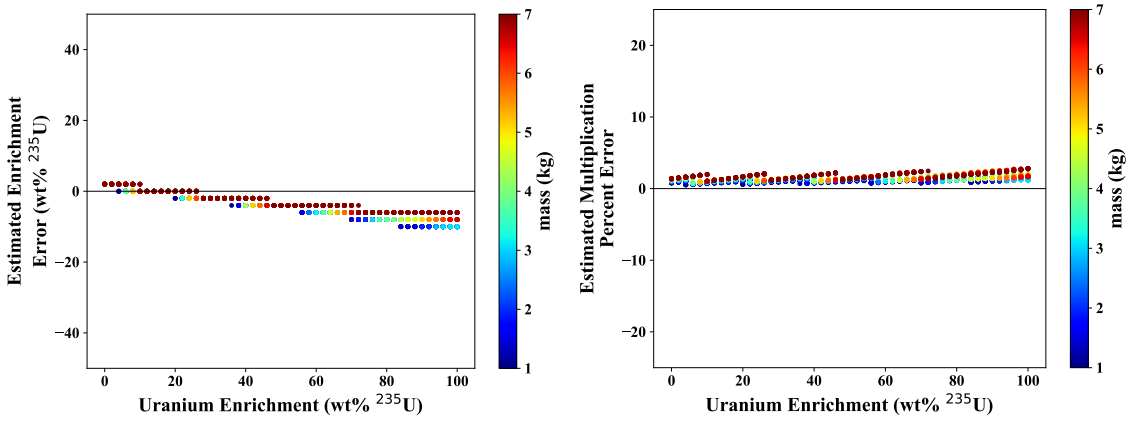

(c) Enrichment Estimate Sphere

(d) Leakage Multiplication Estimate Sphere

Figure 9.11: Hybrid method estimation of pixel 8 Monte Carlo data using straight source mappings

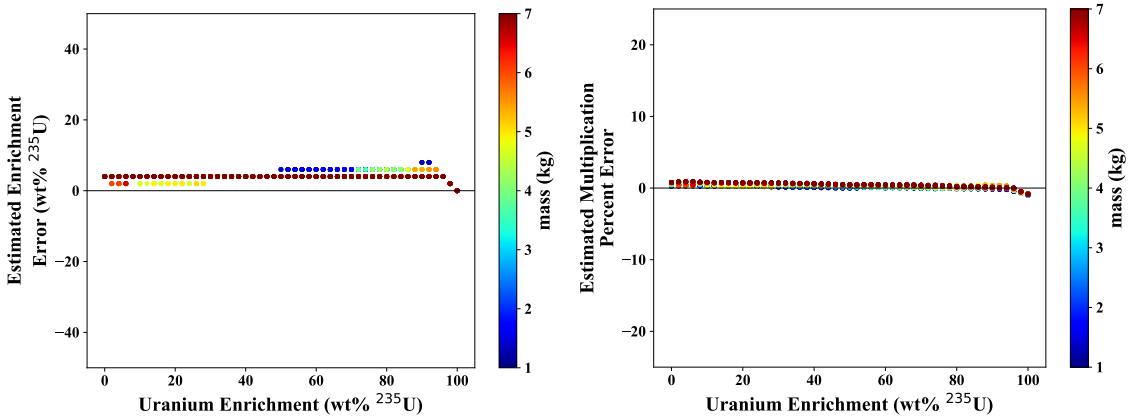

(a) Enrichment Estimate Annular Casting

(b) Leakage Multiplication Estimate Annular Casting

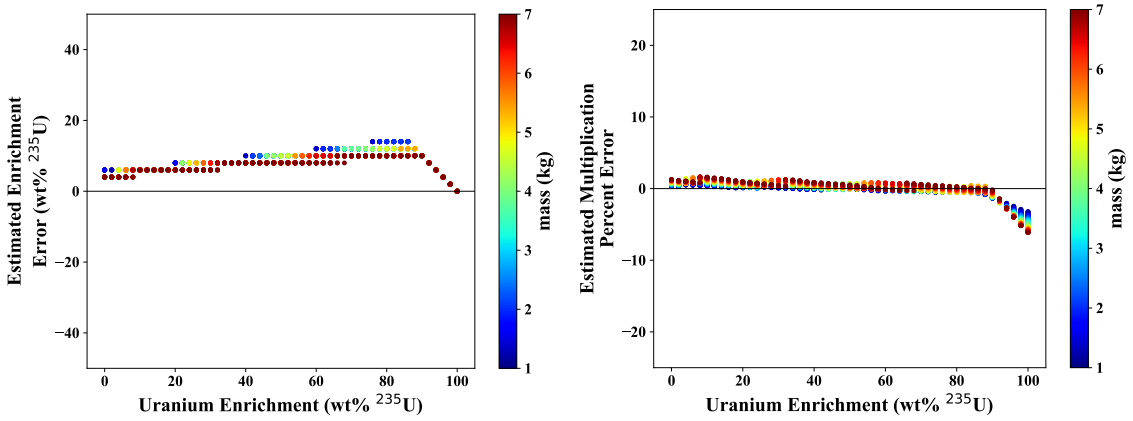

(c) Enrichment Estimate Sphere

(d) Leakage Multiplication Estimate Sphere

Figure 9.12: Hybrid method estimation of straight source Monte Carlo data using pixel 8 mappings

9.2.4 Sensitivity to Emitted Doubles per Single

When estimating the emitted fission chain singles and doubles from a TNI measurement, there will always be some amount of measurement uncertainty, whether statistical or systematic. Therefore, it is important to study how sensitive the hybrid method is to variation in the emitted doubles per single input value. The Monte Carlo mapping for a solid sphere under the pixel 8 interrogation source was used for this study. The same data was used as an input but the emitted doubles per single was increased or decreased by 10, 20, or 30 percent before being entered into the algorithm. The results are shown in fig. 9.13. These results suggest that larger masses are less sensitive to relative changes in emitted doubles per single. Nevertheless, the sensitivity of the hybrid method to large uncertainties in emitted doubles per single is quite high, and it is not uncommon for a TNI measurement to have a 20 or 30 percent uncertainty in emitted doubles per single due to large systematic uncertainties in estimating emitted singles and doubles from measured singles and doubles. This process is discussed further in sections 5.1 and 5.2.

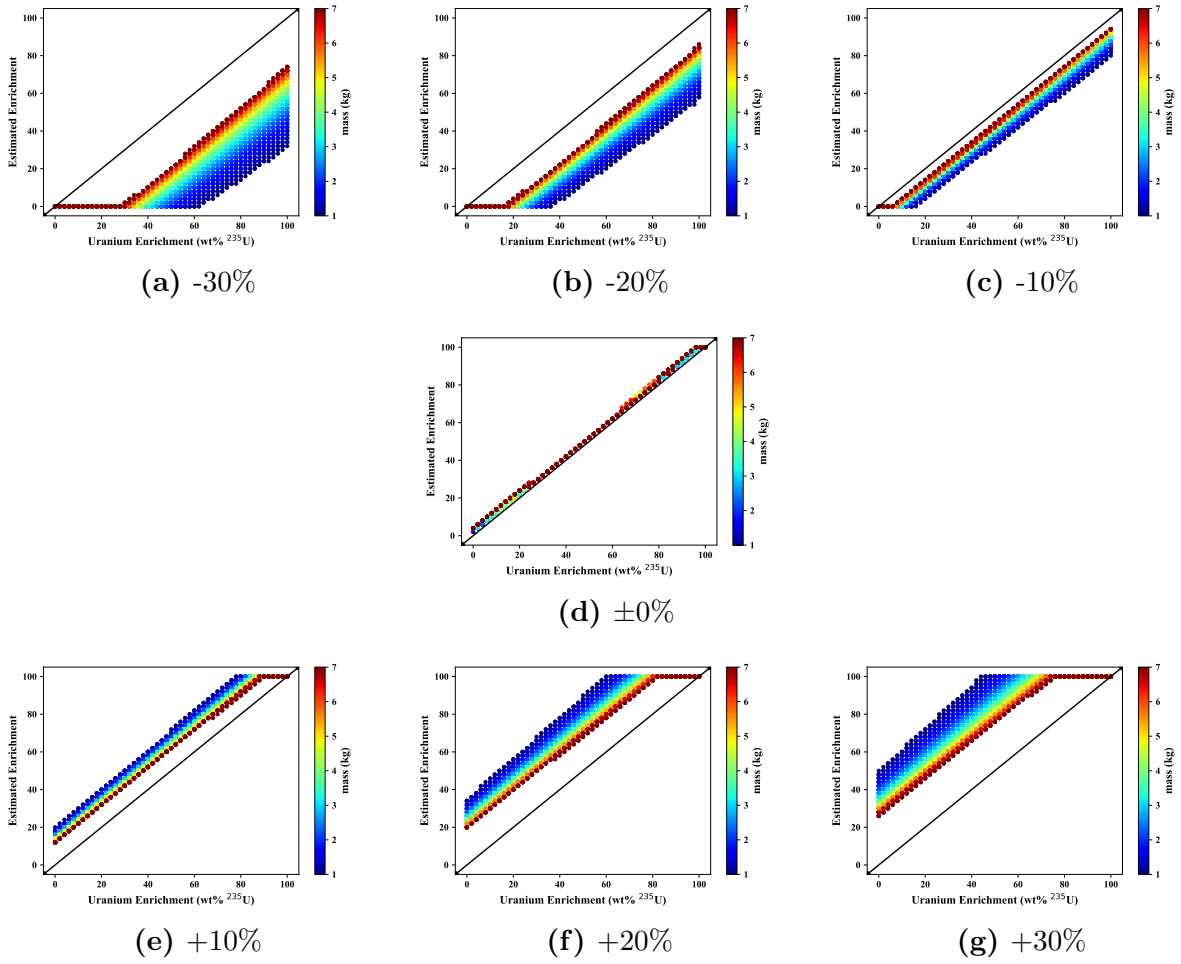

(a) -30% **(b)** -20% **(c)** -10%

(d) ±0%

(e) +10% **(f)** +20% **(g)** +30%

Figure 9.13: Hybrid enrichment estimation for varying percent change in emitted doubles per single

9.3 Results Using Experimental Data

9.3.1 NMIS Measurements

Data from the NMIS measurements of DU and HEU castings performed by Crye [5] and described in section 5.1 were used with the hybrid method to evaluate the hybrid method's ability to estimate the enrichment from a real-life TNI measurement. Additional Monte Carlo simulations of annular castings, spheres, and cylinders of masses ranging from 17.0 to 18.0 kg of uranium were performed in order to generate a mapping for the 17.915 kg castings that were measured. The results are shown in table 9.1 when mappings generated by Monte Carlo simulations of a 17.9 kg uranium object of varying geometry are used to estimate the enrichment and leakage multiplication from the emitted doubles per single for the central pixel. Because the effect of measurement uncertainty addressed later, the enrichment estimates are shown without uncertainties.

Table 9.1: Hybrid method enrichment estimates by mapping geometry (wt. % ^{235}U)

True Enrichment	Annular Casting	Cylinder	Sphere
DU (0.3%)	38%	18%	18%
HEU (93%)	100%	50%	50%

When the correct mapping geometry (annular casting) is used, the results show a significant systematic overestimation of both the DU and HEU measurements. This overestimation is suspected to be a result of a systematic error in estimating the total detection efficiency of emitted fission chain neutrons in the NMIS measurement. Based on work performed by Crye [5] and Canion [54] that suggests that MCNPX-PoliMi simulates the fission chain propagation process and NMIS detection process to an acceptable degree of accuracy, it is believed that the rudimentary efficiency correction is largely responsible for this source of systematic bias.

These results also suggest that using the incorrect geometry in generating the lookup table can result in large systematic biases. While the systematic effects of an uncertain detection efficiency correction and a varying geometry for the mapping cannot be easily deconvolved, these results agree with what previous analyses and parametric studies have

suggested—that geometry is an important determinant of leakage multiplication and emitted doubles per single. When the input mass was varied between 18.0 and 19.0 kg, the estimates did not change, suggesting that results are consistent within at least a 1 kg window.

As is discussed in section 5.1, the uncertainty in the total detection efficiency is the main driver in the total uncertainty of the emitted doubles per single. Figure 9.14 shows how sensitive the hybrid method enrichment estimation algorithm is to the uncertainty in the total detection efficiency, with even a 10 percent detection efficiency uncertainty resulting in up to ±30 percent ^{235}U by weight uncertainty.

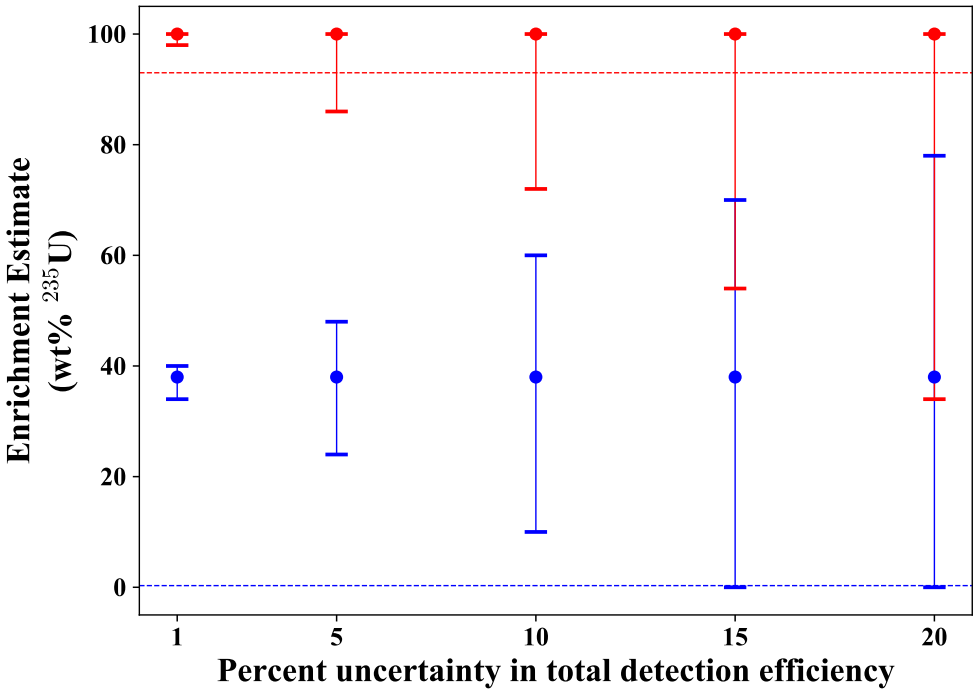

Figure 9.14: Hybrid method enrichment estimates for NMIS measurement data for varying uncertainty in total detection efficiency

9.3.2 APNIS Measurements

Data from the APNIS measurement described in section 5.2 of a 17.1 kg DU casting were also used to evaluate the hybrid method. It is assumed that total uranium mass is known perfectly and a mapping based only on the annular casting geometry is used. Recall that in section 5.2, two different sets of intrinsic efficiencies were estimated from Monte Carlo simulations—one with a downscatter correction and one without. Both are considered in

this analysis. The results for enrichment estimation by the hybrid method are shown in fig. 9.15.

While there appears to be a significant systematic overestimation in the enrichment estimate, it is important to remember that relative uncertainties for the emitted doubles per single calculated in section 5.2 range from 20.9 to 40.4 percent, and are driven mostly by the uncertainty in measured doubles per single, although uncertainty in efficiency values does play a role. In this uncertainty range, the hybrid method has large enrichment uncertainties ranging from 20 to 56 percent ^{235}U by weight. This suggests that while the hybrid method may be an accurate method of estimating uranium enrichment from APNIS measurements, the uncertainty in emitted doubles per single is too large to make a determination. The sources of this uncertainty are discussed in more detail in section 5.2, but generally arise from the fact that estimating absolute values for singles and doubles in TNI is a very approximate process.

Despite the large uncertainties, it is evident that there is a significant systematic overestimation of the true enrichment. The downscatter correction provides some improvement and gives estimates within the correct range for the large emitted doubles per single uncertainties that were calculated for this measurement. While the methods of estimating the uncertainty in both the measured doubles per single and the emitted doubles per single are quite approximate, this analysis instructs how accurate uncertainty quantification in TNI coincidence counting needs to be in order for the hybrid method to be feasible.

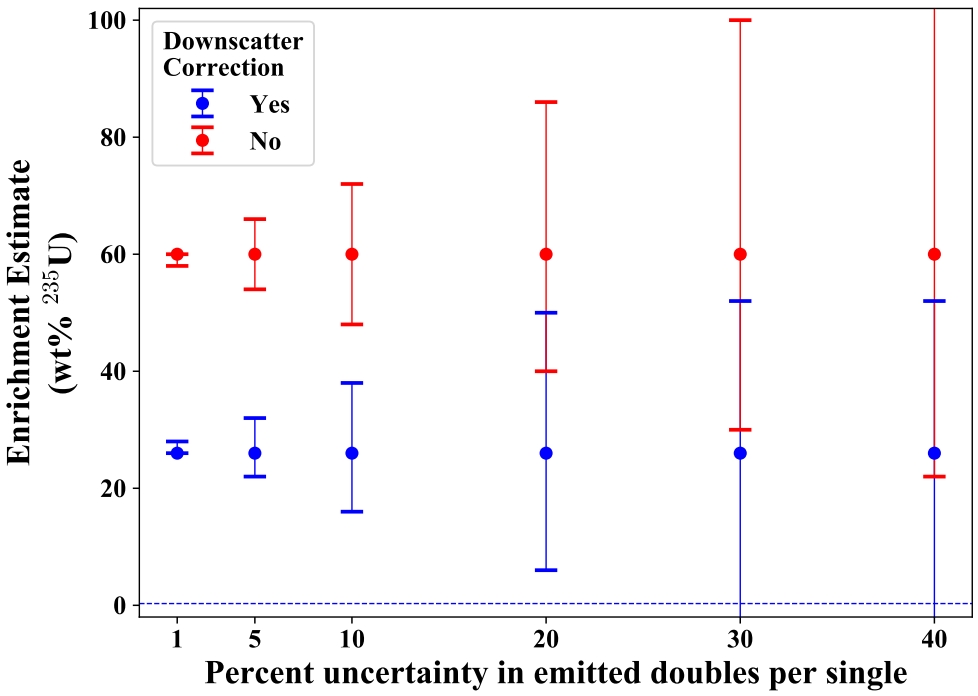

Figure 9.15: Hybrid method enrichment estimates for APNIS measurement data for varying uncertainty in emitted doubles per single

Chapter 10

Conclusions and Future Work

This research has developed several point kinetics-based methods of estimating enrichment and neutron multiplication of a bare uranium metal sample under TNI. A combination of Monte Carlo and measurement data were used to assess the accuracy and sensitivities of these methods. Enrichment affects emitted multiplicities via three pathways in the point kinetics model: source-object coupling (fission-chain initiation rate), chain-starting multiplicity, and leakage multiplication. Four methods for estimating enrichment and neutron multiplication based on inputs that would theoretically be available from a TNI measurements have been developed and evaluated. These inputs include emitted fission chain neutron singles, doubles, and triples, transmitted neutron singles, geometric data about the dimensions, total uranium mass, and source-neutron path length through the uranium object. Each method attempts to solve for one of these pathways using these inputs and then use physics-based relationships to back out the enrichment. In the case of the hybrid method described in chapter 9, Monte Carlo-based relationships are used to estimate leakage multiplication and enrichment.

Coupling-based methods described in chapter 6 are required to make limiting assumptions about chain-starting multiplicity in order to remove the enrichment dependence in the chain-starting multiplicity terms, resulting in one less unknown to solve for. The DT-f method assumed that all chain-starting interactions had the multiplicity of 14.1 MeV induced fission and was then able to solve for multiplication and the source-object coupling. It required inputs of the emitted fission chain singles and doubles as well as the source neutron mean free path through the object. The source-object coupling was used to back out enrichment

based on transmission physics. The assumption about chain-starting interactions was found to introduce enough systematic bias that estimating enrichment was not viable. The DT-f-n2n method attempted to correct for this limiting assumption by expanding the DT-f method and introducing a separate coupling term for fission chains initiated by (n,2n). This additional unknown required an additional input term, either emitted fission chain triples or transmitted neutron singles along with emitted fission chain singles and doubles. Both lookup tables and root-finding methods were used to solve the nonlinear system of three equations, and a ratio of the two coupling parameters was used to estimate enrichment. Enrichment estimation accuracy was improved, but a systematic bias of 20–60 percent ^{235}U by weight was still present when using Monte Carlo simulated input values. This was determined to be a result of the very large sensitivity in the coupling ratio to enrichment. Due to the fact that (n,2n) and (n,3n) chain-starting interactions cannot be differentiated from fission in TNI, there is very little sensitivity to enrichment within the source-object coupling. Based on cross section data, a 14.1 MeV neutron has a nearly equal probability of initiating a fission chain on ^{235}U and ^{238}U so methods that isolate the fission chain initiation rate to estimate enrichment do not fare well.

Instead of assuming away the enrichment dependence in the chain-starting multiplicity as the coupling-based methods did, the aptly named chain-starting multiplicity-based method described in chapter 7 utilized this dependence to estimate enrichment. Using three inputs, emitted fission chain singles and doubles and transmitted singles, the method used algebraic substitution to arrive at an equation which related chain-starting multiplicity terms to known input values. A physics-based equation that relied on cross section data and accounted for (n,xn) as well as induced-fission-initiated fission chains was used to estimate enrichment from chain-starting multiplicity terms. Small biases in estimating leakage multiplication from transmitted and emitted fission chain singles resulted in 20–40 percent biases in enrichment estimates, highlighting just how influential leakage multiplication is in determining values of emitted fission chain singles and doubles.

This finding motivated the parametric study described in chapter 8 which used Monte Carlo simulation data to evaluate just how important leakage multiplication, as well as its underlying physical characteristics (enrichment, uranium mass, and geometry), is in

determining emitted doubles per single for a bare uranium object under TNI. This showed that nearly all of the effect that enrichment has on emitted doubles per single is manifested through its effect on leakage multiplication and not chain-starting multiplicity, hence the systematic bias that was observed by the chain-starting multiplicity-based method. The study quantified the sensitivity of emitted doubles per single and leakage multiplication to enrichment, uranium mass, and geometry. It was found that the relationship between leakage multiplication and all of these physical characteristics was nonlinear—the effect of a unit change in one characteristic on leakage multiplication was highly dependent on the value of the other characteristics. While these sensitivities were quantified, the results highlighted the unfortunate reality that leakage multiplication is the only parameter in the point kinetics equations that has enough sensitivity to enrichment to perform an assay, while also being a quasi-physical concept that cannot be estimated using a physics-based approach even if other physical characteristics (uranium mass and geometry) of the uranium object are known.

The findings of the parametric study in chapter 8 motivated the development of the hybrid method described in chapter 9. While a closed-form physics-based relationship between leakage multiplication and enrichment is not feasible, the hybrid method related leakage multiplication to enrichment using results from Monte Carlo simulations. Using input values for emitted doubles per single, total uranium mass, and object geometry, the hybrid method was shown to estimate uranium enrichment to within 5–10 percent ^{235}U in ideal situations where the input values were known with little uncertainty. However, uncertainties as small as 10 percent in emitted doubles per single or uranium mass or using the incorrect geometry could result in enrichment uncertainties over 20 percent ^{235}U by weight. When the hybrid method was applied to measurement data from NMIS and APNIS measurements, results were not precise due to the significant uncertainties associated with efficiency corrections of TNI measurement data.

Despite having Monte Carlo simulation data to relate leakage multiplication to uranium mass and enrichment, the hybrid method, like the other point kinetics-based methods developed in this work, is simply too sensitive to the relatively large amount of systematic and statistical uncertainty in emitted doubles per single calculated from measured doubles per single. These methods rely on accurate inputs for singles and doubles that are emitted

from the interrogation object, not just the coincidences that are measured by the detector. If point kinetics-based methods are to be used effectively ($\pm$10 percent ^{235}U by weight) to estimate uranium enrichment from TNI measurements, this uncertainty needs to be kept below 5 percent. Improvements in APNIS processing of uncertainty on measured singles and doubles is planned [48], and can hopefully bring the measurement uncertainty in line with what is necessary to use point kinetics-based methods.

Unless calibration standards of similar geometry and chemical composition are used, as is typically done for passive plutonium assay, the ability to perform accurate and precise efficiency corrections is the most important component to using point-kinetics based methods for uranium enrichment assay in TNI measurements. As TNI systems continue to develop and mature, focus should also be directed towards improving methods of calculating geometric and intrinsic detection efficiencies using imaging data.

Even if future work improves the accuracy and precision of estimating emitted fission chain singles and doubles, this work found that enrichment sensitivity within point kinetics models is nearly all contained within the leakage multiplication. Because leakage multiplication is a quasi-physical combination of several different physical characteristics, inferring enrichment from leakage multiplication is difficult if Monte Carlo or physical calibration information is not incorporated. This work serves as a first step for understanding the relationship between enrichment and leakage multiplication for bare uranium metal under TNI, but a better understanding could lead to more precise enrichment assay capabilities.

While the focus of this work was to develop point kinetics-based methods for assay of bare uranium enrichment in TNI measurements, this work found that these point kinetics-based methods do a considerably better job of estimating leakage multiplication than enrichment. While leakage multiplication is not as useful of a physical assay characteristic, it may be suitable for some applications. In certain situations, detecting any multiplication at all is significant, and using point kinetics-based methods to quantify a range of how much multiplication is present could be considerably useful.

Bibliography

[1] T. R. Douglas, "Useful Nuclear Data for NDA," in *Passiv. Nondestruct. Assay Man. Add. 2007*, 2007, ch. 11. [Online]. Available: http://www.lanl.gov/orgs/n/n1/panda/11.NuclearDataforNDA.pdf viii, 10, 11

[2] M. B. Chadwick *et al.*, "ENDF/B-VII.1 nuclear data for science and technology: Cross sections, covariances, fission product yields and decay data," *Nucl. Data Sheets*, vol. 112, no. 12, pp. 2887–2996, 2011. [Online]. Available: http://www.sciencedirect.com/science/article/pii/S009037521100113X viii, x, 32, 57, 64, 66, 67, 68, 69, 76

[3] D. K. Hauck and V. Henzl, "Spatial Multiplication Model as an Alternative to the Point Model in Neutron Multiplicity Counting," Los Alamos National Laboratory, Tech. Rep., 2014. [Online]. Available: http://permalink.lanl.gov/object/tr?what=info:lanl-repo/lareport/LA-UR-14-21991 ix, 15, 16, 18, 34

[4] J. T. Mihalczo, P. R. Bingham, M. A. Blackston, J. M. Crye, B. R. Grogran, P. A. Hausladen, S. McConchie, and J. A. Mullens, "Fast-Neutron Imaging With API DT Neutron Generators," in *Proc. 2012 Int. Sci. Tech. Conf.* Moscow: All-Russia Research Institute of Automatics-VNIIA, 2012, pp. 198–212. [Online]. Available: https://ntrl.ntis.gov/NTRL/dashboard/searchResults/titleDetail/DE20131079274.xhtml ix, 20, 21, 42, 86

[5] J. M. Crye, "Enrichment Determination of Uranium Metal in Shielded Configurations Without Calibration Standards," Ph.D. dissertation, University of Tennessee, 2013. [Online]. Available: http://trace.tennessee.edu/utk_graddiss/1711/ x, 24, 39, 43, 44, 45, 46, 66, 113

[6] J. A. Mullens, S. McConchie, P. A. Hausladen, J. T. Mihalczo, B. R. Grogran, and E. Sword, "Neutron Radiography And Fission Mapping Measurements Of Nuclear Materials With Varying Composition And Shielding," in *Proc. 52nd INMM Annu. Meet.*, Desert Palm, 2011, pp. 1–10. [Online]. Available: https://www.nti.org/media/pdfs/Mullens_et_al_Neutron_RadiogFissio_MapMeasNMvarying_comp-shield.pdf?_=1439478747 1, 20

[7] P. A. Hausladen, M. A. Blackston, J. A. Mullens, S. McConchie, J. T. Mihalczo, P. R. Bingham, M. N. Ericson, and L. Fabris, "Induced-Fission Imaging of Nuclear Material," in *Proc. 51st INMM Annu. Meet.*, Baltimore, 2010, pp. 1–10. [Online]. Available: https://www.researchgate.net/publication/255220437_Induced-Fission_Imaging_of_Nuclear_Material 1, 22, 39, 42, 47, 86

[8] N. Ensslin, W. H. Geist, M. S. Krick, and M. M. Pickrell, "Active Neutron Multiplicity Counting," in *Passiv. Nondestruct. Assay Man. Add. 2007*. Los Alamos National Laboratory, 2007, ch. 7, pp. 1–23. [Online]. Available: http://www.lanl.gov/orgs/n/n1/panda/7.ActiveNeutronMultiplicityLAUR.pdf 1, 12, 20, 66

[9] M. C. Tweardy, S. McConchie, and J. P. Hayward, "A Point Kinetics Model for Estimating Neutron Multiplication of Bare Uranium Metal in Tagged Neutron Measurements," *IEEE Trans. Nucl. Sci.*, vol. 64, no. 7, pp. 1963–1969, jul 2017. [Online]. Available: http://ieeexplore.ieee.org/document/7947180/ 5, 42, 56

[10] D. M. Cifarelli and W. Hage, "Models for a three-parameter analysis of neutron signal correlation measurements for fissile material assay," *Nucl. Instr. and Meth. A*, vol. 251, no. 3, pp. 550–563, nov 1986. [Online]. Available: http://www.sciencedirect.com/science/article/pii/0168900286906510 5

[11] K. Böhnel, "The Effect of Multiplication on the Quantitative Determination of Spontaneously Fissioning Isotopes by Neutron Correlation Analysis," *Nucl. Sci. Eng.*, vol. 90, pp. 75–82, 1985. [Online]. Available: https://doi.org/10.13182/NSE85-2 6, 10

[12] N. Ensslin, W. C. Harker, M. S. Krick, D. G. Langner, M. M. Pickrell, and J. E. Stewart, "Application Guide to Neutron Multiplicity Counting," Los Alamos National Laboratory, Tech. Rep., 1998. [Online]. Available: http://permalink.lanl.gov/object/tr?what=info:lanl-repo/lareport/LA-13422-M 6, 10, 32

[13] W. Hage and D. M. Cifarelli, "Correlation Analysis with Neutron Count Distributions in Randomly or Signal Triggered Time Intervals for Assay of Special Fissile Materials," *Nucl. Sci. Eng.*, vol. 176, pp. 159–176, 1985. [Online]. Available: https://doi.org/10.13182/NSE85-8 6, 10

[14] M. M. Stephens, J. E. Swansen, and L. V. East, "Shift Register Coincidence Module," Los Alamos National Laboratory, Tech. Rep., 1975. [Online]. Available: http://www.osti.gov/scitech/servlets/purl/4120745-1Tavun/ 7

[15] S. Croft, A. Favalli, D. K. Hauck, D. Henzlova, and P. A. Santi, "Feynman variance-to-mean in the context of passive neutron coincidence counting," *Nucl. Instr. and Meth. A*, vol. 686, pp. 136–144, sep 2012. [Online]. Available: http://www.sciencedirect.com/science/article/pii/S0168900212005426 9, 30

[16] P. Peerani, V. Canadell, J. Garijo, K. Jackson, R. Jaime, M. Looman, A. Ravazzani, P. Schwalbach, and M. T. Swinhoe, "Development of high-efficiency passive counters (HEPC) for the verification of large LEU samples," *Nucl. Instr. and Meth. A*, vol. 601, no. 3, pp. 326–332, apr 2009. [Online]. Available: http://linkinghub.elsevier.com/retrieve/pii/S0168900208019232 10

[17] N. Ensslin, M. S. Krick, D. G. Langner, and M. C. Miller, "Active neutron multiplicity counting of bulk uranium," in *Proc. 32nd INMM Annu. Meet.*, New Orleans, jul 1991. [Online]. Available: http://www.osti.gov/scitech/biblio/5528176-YMKA3H/ 12

[18] N. Ensslin, "The Origins of Neutron Radiation," in *Passiv. Nondestruct. Assay Man.*, 1991, ch. 11, pp. 337–356. [Online]. Available: http://www.lanl.gov/orgs/n/n1/panda/00326406.pdf 12

[19] M. S. Krick, N. Ensslin, R. N. Ceo, and P. K. May, "Analysis of active neutron multiplicity data for Y-12 skull oxide samples," Los Alamos National Laboratory (LANL), Los Alamos, NM, Tech. Rep., sep 1996. [Online]. Available: http://www.osti.gov/scitech/biblio/373900-LtM4bY/webviewable/ 13

[20] B. Goddard, W. Charlton, and P. Peerani, "First principle active neutron coincidence counting measurements of uranium oxide," *Nucl. Instr. and Meth. A*, vol. 739, pp. 1–5, mar 2014. [Online]. Available: http://www.sciencedirect.com/science/article/pii/S0168900213016665 13, 14

[21] C. L. Hollas, C. A. Goulding, and W. L. Myers, "Determination of neutron multiplication of subcritical HEU systems using delayed neutrons," *Nucl. Instr. and Meth. A*, vol. 543, no. 2-3, pp. 559–569, may 2005. [Online]. Available: https://www.sciencedirect.com/science/article/pii/S0168900205000331 14, 25

[22] R. Feynman, F. De Hoffmann, and R. Serber, "Dispersion of the neutron emission in U-235 fission," *J. Nucl. Energy*, vol. 3, no. 1-2, pp. 64–IN10, aug 1956. [Online]. Available: http://linkinghub.elsevier.com/retrieve/pii/0891391956900420 14

[23] D. G. Langner and P. A. Russo, "Geometry-based Multiplication Correction for Passive Neutron Coincidence Assay of Materials with Variable and Unknown (α,n) Neutron Rates," Los Alamos National Laboratory, Tech. Rep., 1993. [Online]. Available: https://inis.iaea.org/search/search.aspx?orig_q=RN:24039513 15, 16, 32

[24] M. S. Krick, W. H. Geist, and D. R. Mayo, "A Weighted Point Model for the Thermal Neutron Multiplicity Assay of High-Mass Plutonium Samples," Los Alamos National Lab, Tech. Rep., 2005. [Online]. Available: http://www.osti.gov/energycitations/product.biblio.jsp?osti_id=876505 15, 16, 17, 32

[25] S. Croft, E. Alvarez, P. M. J. Chard, R. D. McElroy, and S. Philips, "An Alternative Perspective on the Weighted Point Model for Passive Neutron Multiplicity Counting," in *Proc. 48th INMM Annu. Meet.*, Tuscon, 2007. [Online]. Available: http://www.canberra.com/fr/literature/waste_special_systems/tech_papers/INMM48_2007-Weighted-Point-Model_Abstr-130.pdf 17, 34

[26] M. Göttsche and G. Kirchner, "Improving neutron multiplicity counting for the spatial dependence of multiplication: Results for spherical plutonium samples," *Nucl. Instr. and Meth. A*, vol. 798, pp. 99–106, 2015. [Online]. Available: http://linkinghub.elsevier.com/retrieve/pii/S0168900215008360 15

[27] W. H. Geist, M. S. Krick, and D. R. Mayo, "Reduction of Bias in Neutron Multiplicity Assay using a Weighted Point Model," in *7th Int. Conf. Facil. Oper. - Safeguards Interface*, Charleston, 2004. [Online]. Available: http://permalink.lanl.gov/object/tr?what=info:lanl-repo/lareport/LA-UR-04-1149 16

[28] J. J. Duderstadt and L. J. Hamilton, *Nuclear Reactor Analysis*. New York: Wiley, 1976. 18

[29] P. A. Santi, T. E. Cutler, A. Favalli, K. E. Koehler, V. Henzl, D. Henzlova, R. F. Parker, and S. Croft, "Implementation and Initial Testing of Advanced Processing and Analysis Algorithms for Correlated Neutron Counting," Los Alamos National Laboratory, Tech. Rep., 2015. [Online]. Available: http://permalink.lanl.gov/object/tr?what=info:lanl-repo/lareport/LA-UR-15-29225 18, 19

[30] M. S. Krick, D. G. Langner, and J. E. Stewart, "Energy-Dependent Bias in Plutonium Verification Measurements Using Thermal Neutron Multiplicity Counters," Los Alamos National Laboratory, Tech. Rep., 1997. [Online]. Available: http://permalink.lanl.gov/object/tr?what=info:lanl-repo/lareport/LA-UR-97-3427 19

[31] P. A. Santi and W. H. Geist, "Energy Dependent Bias in the Weighted Point Model," in *Proc. 46th INMM Annu. Meet.*, 2005. [Online]. Available: https://inis.iaea.org/search/search.aspx?orig_q=RN:41092977 19, 66

[32] H. A. Smith Jr., "The Measurement of Uranium Enrichment," in *Passiv. Nondestruct. Assay Man.*, 1991, ch. 7, pp. 195–220. [Online]. Available: http://www.lanl.gov/orgs/n/n1/panda/00326402.pdf 23

[33] Canberra, "In Situ Object Counting Systems (ISOCS)." [Online]. Available: http://www.canberra.com/products/insitu_systems/isocs.asp 23

[34] J. K. Mattingly, T. E. Valentine, J. T. Mihalczo, L. G. Chiang, and R. B. Perez, "Enrichment and Uranium Mass From NMIS for HEU Metal," in *Proc. 41st INMM Annu. Meet.*, New Orleans, 2000. [Online]. Available: https://www.ipndv.org/wp-content/uploads/2017/10/Mattingly_et_al_Enrichment_and_Uranium_Mass_from_NMIS_for_HEU_metal.pdf 23

[35] A. L. Swift, "Materials and Configuration from NMIS Type Neutron Imaging and Gamma Spectroscopy," Ph.D. dissertation, University of Tennessee, Knoxville, 2012. [Online]. Available: http://trace.tennessee.edu/utk_gradthes/1210/ 24

[36] S. A. Pozzi, E. Padovani, and M. Marseguerra, "MCNP-PoliMi: a Monte-Carlo code for correlation measurements," *Nucl. Instr. and Meth. A*, vol. 513, no. 3, pp. 550–558, nov 2003. [Online]. Available: http://linkinghub.elsevier.com/retrieve/pii/S0168900203023027 24

[37] W. L. Myers, C. A. Goulding, and C. L. Hollas, "Determination of the ^{235}U Enrichment of Bulk Uranium Samples Using Delayed Neutrons," Los Alamos National Laboratory, Tech. Rep., 2006. [Online]. Available: http://permalink.lanl.gov/object/tr?what=info:lanl-repo/lareport/LA-UR-06-3984 25

[38] X. Li, R. Henkelmann, and F. Baumgärtner, "Rapid determination of uranium and plutonium content in mixtures through measurement of the intensitytime curve of delayed neutrons," *Nucl. Instruments Methods Phys. Res. Sect. B Beam Interact. with Mater. Atoms*, vol. 215, no. 1-2, pp. 246–251, jan 2004. [Online]. Available: http://linkinghub.elsevier.com/retrieve/pii/S0168583X03018226 25

[39] P. Campbell, E. M. Gardy, and D. G. Boase, "Assay of Fissionable Isotopes in Aqueous Solution by Pulsed Neutron Interrogation," Atomic Energy of Canada Limited, Tech. Rep., 1978. [Online]. Available: https://inis.iaea.org/search/search.aspx?orig_q=RN:9410498 25

[40] C. L. Hollas, C. A. Goulding, and W. L. Myers, "Subcritical Neutron Multiplication Measurements of HEU Using Delayed Neutrons as the Driving Source," Los Alamos National Laboratory, Tech. Rep., 1999. [Online]. Available: https://www.osti.gov/servlets/purl/761233 25

[41] G. R. Keepin, *Physics of Nuclear Kinetics*. Reading, Mass.: Addison-Wesley Publishing Company, Inc., 1965. 25

[42] M. S. Zucker and N. E. Holden, "Energy dependence of the Neutron Multiplicity P_{nu} in fast neutron induced fission of ^{235,238}U and ^{239}Pu," Brookhaven National Laboratory, Tech. Rep., 1986. [Online]. Available: http://www.iaea.org/inis/collection/NCLCollectionStore/_Public/18/063/18063960.pdf 29, 57

[43] J. K. Mattingly, "Computation of Neutron Multiplicity Statistics Using Deterministic Transport," *IEEE Trans. Nucl. Sci.*, vol. 59, no. 2, pp. 314–322, apr 2012. [Online]. Available: http://ieeexplore.ieee.org/document/6153406/ 30

[44] Nuclear Energy Agency, "Table of Simple Integral Neutron Cross Section Data From JEF-2.2, ENDF/B-VI, JENDL-3.2, BROND2 and CENDL-2," Nuclear Energy Agency, Tech. Rep., 1994. [Online]. Available: https://www.oecd-nea.org/dbdata/nds_jefreports/jefreport-14.pdf 30

[45] S. A. Pozzi *et al.*, "MCNPX-PoliMi for nuclear nonproliferation applications," *Nucl. Instr. and Meth. A*, vol. 694, pp. 119–125, dec 2012. [Online]. Available: http://linkinghub.elsevier.com/retrieve/pii/S0168900212008224 37

[46] H. Wadell, "Volume, Shape, and Roundness of Quartz Particles," *J. Geol.*, vol. 43, no. 3, pp. 250–280, 1935. [Online]. Available: http://dx.doi.org/10.1086/624298 38

[47] J. W. Cates, "Investigation of Time and Position Resolved Alpha Transducers for Multi-Modal Imaging with a D-T Neutron Generator," Ph.D. dissertation, University of Tennessee, Knoxville, 2013. [Online]. Available: http://trace.tennessee.edu/utk_graddiss/2406/ 47

[48] M. A. Blackston, "Private Communication," 2017. 51, 53, 120

[49] J. M. Verbeke, C. Hagmann, and D. Wright, "Simulation of Neutron and Gamma Ray Emission from Fission and Photofission. LLNL Fission Library 2.0.2." Lawrence Livermore National Laboratory, Tech. Rep., 2016. [Online]. Available: https://nuclear.llnl.gov/simulation/fission.pdf 51

[50] D. E. Cullen, "Sampling ENDL Watt Fission Spectra," Lawrence Livermore National Laboratory, Tech. Rep., 2004. [Online]. Available: https://wci.llnl.gov/codes/tart/media/pdf/UCRL-TR-203351.pdf 51, 53

[51] M. Soleilhac, J. Frehaut, and J. Gauriau, "Energy dependence of for neutron-induced fission of ^{235}U, ^{238}U and ^{239}Pu from 1.3 to 15 MeV," *J. Nucl. Energy*, vol. 23, no. 5, pp.

257–282, may 1969. [Online]. Available: http://www.sciencedirect.com/science/article/pii/0022310769900604 56, 69

[52] J. Terrell, "Distribution of Fission Neutron Numbers," *Phys. Rev.*, vol. 108, no. 3, pp. 783–789, 1957. [Online]. Available: https://link.aps.org/doi/10.1103/PhysRev.108.783 57

[53] W. H. Press, S. A. Teukolsky, W. T. Vetterling, and B. P. Flannery, *Numerical Recipes 3rd Edition: The Art of Scientific Computing, vol. 3*, 3rd ed. New York, NY, USA: Cambridge University Press, 2007. 82

[54] B. E. Canion, "Incorporation of Photon Analysis into an Active Interrogation System for Shielded Uranium Characterization," Ph.D. dissertation, University of Texas at Austin, 2015. [Online]. Available: https://repositories.lib.utexas.edu/handle/2152/39687 113

Vita

Matthew Christopher Tweardy grew up west of Chicago with three younger siblings and two loving parents. In 2013 he graduated from American University with a Bachelor's of Science in Physics and a Bachelor's of Arts in International Studies. Following his undergraduate studies, he combined his two areas of interest and joined the nuclear engineering department at the University of Tennessee, Knoxville as a graduate student under the guidance of Professor Jason P. Hayward. While in Knoxville, he earned a Master's of Science in Nuclear Engineering in 2015 and a graduate certificate in Nuclear Security Science and Analysis in 2016. His research on applying point kinetics models to tagged neutron interrogation systems was conducted in collaboration with the Nuclear Materials Detection and Characterization group at Oak Ridge National Laboratory.